Antibacterial activity and cytotoxicity *in vitro* of green-synthesized silver nanoparticles using *Brassica rapa* var. *japonica* leaf

（ミズナの葉を用いてグリーン合成された銀ナノ粒子の抗菌活性および試験管内細胞毒性

Mahmuda Akter

Course of Environmental Adaptation Science

Division of Environmental Science Development

Graduate School of Environmental Science

Hokkaido University

February 2019

Acknowledgement

At the very beginning, I humbly acknowledge my heartfelt gratitude to the almighty, the most gracious, benevolent and merciful Allah for his infinite mercy bestowed on me in carrying out the research work presented in the dissertation. It's a great pleasure for me to acknowledge my deepest sense of gratitude, sincere appreciation, heartfelt indebtedness and solemn regards to my reverend teacher and supervisor Dr. Masaaki Kurasaki for his kind supervision, indispensable guidance, valuable and constructive suggestions, generous help and continuous encouragement during the whole period. It is obvious that his attributive contribution and efforts have greatly shaped me into what I am today. In fact, I am quite lucky to be a part of his ambitious research team.

It's my great honor to convey my sincere gratitude to my respected professors, Professor Takeshi Saito, Professor Tatsufumi Okino, Professor Shin-ichiro Noro, Professor Hideki Kuramitz and Professor Ram Avtar, for giving me their wonderful support to move through the academic processes during this degree program. I would like to convey my deepest gratitude to Professor Shunitz Tanaka, Professor Umezawa and Professor Kamya for their valuable instrumental support in experimental works. I am thankful to Professor Yoshinori Kuboki, Professor Seiichi Tokura and Professor Toshiyuki Hosokawa for their cordial support. I am highly grateful to Dr. Parvin Sultana for her suggestions and guidance during the research period. I am ever thankful to Ms. Miyako Komori for her nice and cordial support in all situations. Her generous behavior and expert cooperation helped me to overcome obstacle from various situations.

I would like to acknowledge the MEXT for supporting me by providing scholarship in conducting my study in Hokkaido University. I would also like to remember the Hokkaido University Frontier Research Foundation for selecting me as a fellow to complete Nitobe School advanced study program with a supporting scholarship.

My sincere gratitude goes to Dr. Tajuddin Sikder for his significant suggestions, intellectual help, solutions of abstruse matters and continuous inspiration throughout my research work. I would also like to thank Dr. Mostafizur Rahman and Dr. Habiba for their support during my research period. I am especially thankful to Subrata Banik and also want to show my appreciation to Ms. Kaniz Fatima Rumana an Md. Shiblur Rahman for their generous help in my research work. I would like to extend my cordial thanks to Mr. Senoo, Ms. Hirase, Ms. Kita, Mr. Yamazaki and all other lab mates to whom I met in Kurasaki laboratory.

I would like to express my earnest gratitude to Mr. A.K.M. Atique Ullah for his cordial and indispensable support in this long journey. His inspiration, support, care and suggestion made this critical journey quite smooth. My gratitude goes to my better half Mr. Md. Rashedul Alam for his cooperation and immense sacrifice. My appreciation goes to Ms. Nahid Akter and Ms. Mou Banik for their hospitality. I would like to remember my friends Ms. Nahmina Begum and Amatur Rahman Urmi for their inspiration during my research period. I would like to thank Dr. Nusrat Kabir Nisuka, Ms. Maksuda Akter, Mr. Touhid Md. Ekram, Dr. Habib Mohammad Sazzad and Ms. Mahmuda Hakim Silvi. Finally, I would like to express my heartfelt indebtedness and profound gratitude to my beloved father, Mr. Md. Mir Hossain, mother, Ms. Saleha Akter, all of my family members and relatives for their continuous inspiration.

Abstract

In recent era versatile applications of silver nanoparticles (Ag-NPs) have been elevated by various requirements from the consumers and researchers. According to these requirements, tremendous amounts of Ag-NPs have been synthesized using conventional method. Unfortunately, conventional method for synthesis of Ag-NP has been pointed out a matter of concern in respect of environmental toxicity and human health. Already cytotoxic effects of Ag-NPs have been reported in several cell lines. Therefore, the green synthesis of Ag-NPs is considered to be a safer synthesis method, even though it is an alternative to the conventional synthesis method. On the other hand, Ag-NPs are reported to have potential antitumor and anticancer properties in both *in vitro* and *in vivo* experiments. From above viewpoints, the present study aimed to be green synthesis of Ag-NPs and evaluation their biomedical applications with underlying mechanisms. To achieve the purpose actual objectives were set. First, Ag-NPs were successfully synthesized from the reduction of Ag^+ using $AgNO_3$ solution as a precursor and *Brassica rapa var. nipposinica/japonica* leaf extract as a reducing and capping agents. In the synthesis procedure no additional chemical reductant and stabilizing agents were used. The characterization of Ag-NPs was carried out using UV-vis spectrometry, energy dispersive X-ray (EDX) spectrometry, fourier transform infrared (FT-IR) spectrometry, field emission scanning electron microscopy (FESEM), X-ray diffraction (XRD), atomic absorption spectrometry (AAS), and transmission electron microscopy (TEM). The analyses data revealed the successful synthesis of nano-crystalline Ag possessing more stability than commercial Ag-NPs. To confirm synthesis of Ag-NPs exhibiting less toxicity with high antibacterial activity, following experiments have been done. The cytotoxicity of Brassica Ag-NPs was compared with commercial Ag-NPs using PC12 cell system. Three ppm of commercial Ag-NPs reduced cell viability to 23% (control 97%) and increased lactate dehydrogenase activity, whereas, Brassica Ag-NPs did not show any cytotoxicity on both parameters up to a concentration level of 10 ppm in PC12 cells. Moreover, Brassica Ag-NPs exhibited inhibition zone of against growth of *Escherichia coli* (11.1 ± 0.5 mm) and *Enterobacter sp.* (15 ± 0.5 mm) which was higher than other green-synthesized Ag-NPs reported previously. The less cytotoxicity and high antibacterial activity of green synthesized Ag-NPs will be great benefits for the safe use of Ag-NPs in consumer products. On the basis of results in this study it could be concluded that cytotoxicity of Ag-NPs is depended on the stability of the particles and the stability depends on the encapsulation or coating of the surface of the particles. Therefore, it was considered that reaction temperature during synthesis could play a vital role in coating of the particles. From the results, it was tried to synthesize optimal

Ag-NPs using *Brassica rapa var. nipposinika/japonica* leaf extract with various temperatures. The synthesis of Ag-NPs was done at four different temperatures such as 25 °C (room temperature), 60 °C, 80 °C and 100 °C in order to evaluate the extent of encapsulation of Ag-NPs. The synthesized Ag-NPs were again characterized using UV-vis. spectrophotometer, EDX spectrometer, XRD spectrometer, TEM, and dynamic light scattering techniques. The adopted characterization techniques clearly demonstrate that at 100 °C almost all particles were found to be encapsulated which was the primary objective of the present study.

Furthermore, in this study, the behavior of various concentrations of green synthesized Ag-NPs in cancer cells was clarified. Brassica Ag-NPs exposed to Caco-2 cells showed significant decrease of the cell viability, increase of the LDH activity in the medium, and decrease of intracellular GSH amounts. Subsequent western blotting analyses revealed that Brassica Ag-NPs induced Beclin 1 mediated autophagic cell death in Caco-2 cells where LC3-II plays a key role. This autophagic process was further accelerated via upregulation of p53. Hence, downregulation of Akt suppressed mTOR activation. Moreover, upregulation of IkB and downregulation of NFkB inhibit DNA transcription which might also promote autophagy and subsequent cell death. Involvement of apoptosis or necrosis behind cell death mechanism in Caco-2 cells was not detected from any of the results in current study. Thus, these results indicated the possibility of anticancer ability of Brassica Ag-NPs to Colorectal cancer cells, Caco-2.

In conclusion, this study clearly reveals the potentiality of Brassica leaf extract for the environment friendly green synthesis of Ag-NPs which can be encapsulated with optimal temperature. In addition, Brassica Ag-NPs are less toxic in comparison of commercial Ag-NPs with high antibacterial activity, and also have a possibility of anticancer ability.

Chapter 1 General introduction

1.1 Background

Nanomaterials have been reported to be the "materials of the 21st century" because of their unique designs and property combinations compared with conventional materials (Camargo et al., 2009). There is a wide range of applications of nanoparticles (NPs) such as in human health appliances, industrial fields, medical applications, biomedical fields, engineering, electronics, and environmental studies (Hamzeh et al., 2013). Recently, enormous attention has been focused on the use of NPs such as nanotubes, nanowires, fullerene derivatives, and quantum dots to create new types of analytical tools in the fields of life science and biotechnology (Bruchez et al., 1988). Among all of the nanomaterials, silver nanoparticles (Ag-NPs) are the most widely used and may be considered as one of the most important materials. They have become a high-demand material for consumer products (Edwards et al., 2009). Ag-NPs are used in medicine, medicinal devices, pharmacology, biotechnology, electronics, engineering, energy, magnetic fields, and also in environmental remediation (Yu et al., 2013). Moreover, because of their highly effective antibacterial activity both in solution and in components, Ag-NPs have gained popularity in industrial sectors including textiles, food, consumer products, medicine, etc. (Naidu et al., 2015). Currently, Ag-NPs are extensively used in healthcare products, women's hygiene products, the food industry, paints, cosmetics, medical devices, sunscreen, bio-sensors, clothing, and electronics (Edwards et al., 2009).

The unique physical and chemical characteristics of Ag-NPs along with their antimicrobial ability, differing largely from bulk materials, make them a high-demand material in different sectors. For example, the high surface area-to-volume ratio enhances the surface properties of Ag-NPs, thereby increasing the interaction with serum, saliva, mucus, and fluid components of the lung lining compared with bulk particles (Beer et al., 2012). However, the strong oxidative activity of Ag-NPs releases silver ions, which results in several negative effects on biological systems by inducing cytotoxicity, genotoxicity, immunological responses, and even cell death (Chernousova et al., 2013). Unfortunately, the use of Ag-NPs carries a series of unpredictable concerns regarding their interaction with biological systems (Beer et al., 2012). Therefore, the enormous applications of Ag-NPs raise concerns about human exposure, because they can easily pass through the blood brain barrier (BBB) by transcytosis of capillary endothelial cells or into other critical areas or tissues (Tang et al., 2010).

According to Aueviriyavit et al. (2014), Ag products in colloidal form for medicinal or other purposes have activated Ag^{+}, which might have a direct effect on human health (Aueviriyavit et al., 2014). In addition, because of the increased use of Ag-NPs, concentrations of Ag^{+} are increasing in soil and water, which were measured to be 22.7 ppm and 0.76 ppm, respectively (Aueviriyavit et al., 2014). Moreover, it is hypothesized that Ag^{+} possesses an enhanced toxicity potential than elemental Ag and Ag-NPs (Cho et al., 2013). However, an increasing number of recent occurrences of diseases due to microbial infections has been prevented by the noble metal, with Ag-NPs having a well-documented antimicrobial and disinfectant activity. Very recently, antibacterial activity of green-synthesized Ag-NPs against *Bacillus subtilis* and *Escherichia coli* has been revealed (Roe et al., 2008). Therefore, safe synthesis of Ag-NPs is areas that remain to be explored. In this point of view, we will be discussing significance of the green synthesis instead of conventional commercial synthesis of Ag-NPs, how physiological properties of Ag-NPs contribute in cytotoxicity, and possible mechanism of Ag-NPs induces cytotoxicity. Moreover, potentiality of *Brassica rapa* var *nipposinica/ japonica* as a reducing or capping agent for the synthesis of Ag-NPs will also be explained in brief. In addition, an explanation of motivation of further research in the light of green synthesis of Ag-NPs and their biomedical applications, and finally outline of the current thesis will be included in this chapter.

1.2 Green synthesis of Ag-NPs

Large amounts of Ag-NPs can be produced using silver nitrate as a precursor and ethylene glycol along with polyvinylpyrolidone (PVP) as a reducing and stabilizing agent (Yugang et al., 2002). However, the oleylamine-liquid paraffin system has been used to prepare almost monodisperse Ag-NPs from silver nitrate (Chen et al., 2007). The reduction in different silver salts also results in a colloidal solution of Ag particles, which is followed by both nucleation and subsequent growth. Usually, through the optimization of different parameters such as temperature, pH, precursors, reducing agents, and other experimental conditions, the silver nanocube can be given a definite size (Chen et al., 2012). Using atmospheric pressure, Ag-NPs can be synthesized by evaporation-condensation, thermal decomposition, the arc discharge method, and the metal sputtering method into the powder form (Siegel et al., 2012). The Ag-NPs can also be synthesized by photo-induced synthetic strategies, which involve photo-reduction of $AgNO_3$ using sodium citrate (NaCit) and light sources such as UV, white, blue, cyan, green, and orange light at room temperature (Sato et al., 2009).

A recent discovery of a methodology for synthesizing green Ag-NPs involves the utilization of bacteria, fungi, yeasts (Hamzeh et al., 2013), algae, or plant extracts (Nel et al., 2006) as reducing and/or stabilizing compounds to work on silver salts, which addresses the draw backs of physico-chemical methods (Daima et al., 2015). *Shewanella oneidensis*, *Trichoderma viride* (*T. viride*), *Bacillus* species, *Lactobacillus* species, and some vegetative parts of plants are now being used to produce environmentally friendly Ag-NPs. The association of nanotechnology with green chemistry is thus allowing for the emergence of biologically and cytologically compatible metallic NPs (Maynard et al., 2011). Table 1.1 shows the size variability of the green-synthesized Ag-NPs from plant and microbial origins. It is evidenced from Table 1.1 that the size of synthesized Ag-NPs ranges from 50–100 nm in most of the listed studies. In general, Ag-NPs synthesized using biological reducing and capping agents have shown wide variations in shape and size. The researchers also reported low toxicity levels of these green-synthesized Ag-NPs in comparison to chemically synthesized Ag-NPs.

Table 1.1 Some examples of successful green synthesis of Ag-NPs

Sl. No.	**Author**	**Reducing Agent**	**Particle Characteristics**	**Remarks**
1	Kathiraven et al., 2014	Filtered aqueous extract of *Caulerpa racemosa* marine algae	Size—5 - 25 nm Shape—sph, tri. Structure—FCC	Antibacterial action against *P. mirabilis* and *S. aureus*
2	Britto et al., 2014	Aqueous filtrate of *Pteris argyreae, Pteris confuse* and *Pteris blaurita*	-	Antibacterial action against *Shigella boydii, Shigella dysenteriae, S. aureus, Klebsiella vulgaris* and *Salmonalla typhi*
3	Sant et al., 2013	Aqueous filtrate of *Adiantum philippense* L	Size—10 - 18 nm Shape—anisotropic Structure—FCC Nature—MD	Ag-NPs from medicinally important plants opens spectrum of medical applications.
4	Bhor et al., 2014	Aqueous filtrate of *Nephrolepis sexaltata* L. fern	Size—avg 24.76 nm Shape—sph. Structure—FCC	Antibacterial against many human and plant pathogens

5	Ajitha et al., 2014	Filtered aqueous extract of Tephrosia purpurea leaf powder	Size— 20 nm Shape—sph. Structure—FCC	Antimicrobial agents against Pseudomonas spp. and Penicillium spp.
6	Rahimi etal., 2014	Methanol extract and essential oil of Eucalyptus leucoxylon leaf	Size— 50 nm Shape—sph. Structure—FCC	Ag-NPs with biomedical potential
7	Bagherzade et al., 2017	Aqueous extract of saffron (Crocus sativus L.)	Size—12–20 nm	Inhibiting activity against Escherichia coli, Pseudomonas aeruginosa, Klebsiella pneumonia, Shigella flexneri and Bacillus subtilis.
8	Ashokkumar et al., 2015	Filtered aqueous extract of Abutilon indicum leaf	Size—7 - 17 nm Shape—sph. Structure—FCC	Antimicrobial action against S. typhi, E. coli, S. aureus, B. subtilis
9	Tagad et al., 2013	Locust bean gum polysaccharide.	Size—18 - 51 nm	Stability: 7 months, Ag-NPs served in development of H2O2 sensor
10	Yasin et al., 2013	Filtered aqueous extract of Bamboo leaf	Size—13 ± 3.5 nm Shape— nearly sph. Structure—cryst.	Antibacterial to E. coli and S. aureus
11	Sadeghi et al., 2015	Methanol extracted aqueous filtrate of Ziziphora tenuior leaf	Size—8 - 40 nm. Shape—sph. Structure—FCC	Stability: 6 - 12 pH range

12	Chen et al., 2014	Chitosan biopolymer	Size—~218.4 nm Shape—oval and sph. Nature—Ag/ chitosan nano hybrids	Antimicrobial to E. coli, S. choleraesuis, S. aureus and B. subtilis
13	Mondal et al., 2014	Saline washed, filtered aqueous extract of Parthenium hysterophorous root	Shape—spherical	Potential larvacidal for Culex quinquefasciatus
14	Nalwade et al., 2013	Aqueous filtrate of Cheilanthes forinosa Forsk leaf	Size—~26.58 nm Shape—sph. Structure—FCC	Antibacterial action against S. aureus and Proteus morgani
15	Singh et al., 2015	Lantana camara	48.1 nm	Anti microbial to E coli and S. aureus. Leakage due to cell wall rupturing
16	Vimala et al., 2015	Leaf and fruit of Couroupita guianensis	Cubic size 10-45 nm 5—15 nm	water soluble phenolic compounds as reducing and stabilizing agent larvicidal to A. aegypti extensive mortality rate (LC90~5.65 ppm)
17	Cheng et al., 2014	Chondrotin sulfate	Size— 20 nm Shape—sph.	Stable for 2 months, Served as nano carrier for drug delivery
18	Sadeghi et al., 2014	Filtered aqueous-methanol extract of Pistacia atlantica seed powder.	Size—10 - 50 nm Shape—sph. Structure—FCC	Stability: 7 - 11 pH range. Antibacterial affect against S. aureus.

19	Zhang et al., 2014	Lactobacillus fermentum. LMG 8900 cells	Size—~6 nm Shape—sph. Structure—FCC	Stable for 3 months. Resist growth of E. coli, S. aureus and P. aeruginosa Act as promising anti-biofouling agent
20	Das et al., 2012	Mycelia of Rhizopus oryzae	Size—~15 nm Shape—sph. Structure—FCC	Stable for 3 months, Antimicrobial to E. coli and B. subtilis, Used for treating contaminated water and adsorption of pesticides
21	El-Rafie et al., 2013	Crude hot water soluble polysaccharide extracted from different marine algae	Size—7 - 20 nm Shape—sph	Stability: 6 months, Ag-NPs treated cotton fibers antibacterial to E. coli and S. aureus
22	Suresh et al., 2014	Filtered aqueous extract of Delphinium denudatum root powder	Size—85 nm Shape—sph. Structure—FCC Nature—PD	Anti-bacterial against S. aureus, B. cereus, E. coli and P. aeruginos Larvicidal to Aedes aegypti
23	Zuas et al., 2014	Filtered aqueous extract of Myrmecodia pendan plant.	Size—10 - 20 nm Shape—sph. Structure—FCC	Promising therapeutic value
24	Vijaykumar et al., 2014	Aqueous extract of Boerhaavia diffusa plant powder.	Size—~25 nm Shape—sph. Structure—FCC, Cub	Antibacterial to fish pathogens *A. hydrophilia, F. branchiophilum, P. fluorescens*

25	Elumalai et al., 2014	Filtered coconut water	Size—70 - 80 nm Structure—FCC Nature—PD	Metabolites and proteins served as capping agents.

Note: PD—Polydispersed, MD—Monodispersed, WD—Well Dispersed, Cryst—Crystalline. FCC- Face centered cubic; Tri- Triangular; Sph- Spherical; cryst- crystalline; Cub- cubic

The synthesized Ag-NPs vary in size, shape, surface electric charge, and in other physiological characteristics. Therefore, green synthesis procedure of Ag-NPs could be potential because of its cost effectiveness, environmental hostility, and overall easy synthesis process.

1.3 Effect of Ag-NPs' physicochemical properties on cytotoxicity

1.3.1 Effects of particle size variability

The cytoxicity of Ag-NPs is influenced by the variation in particle size (Gliga et al., 2014). Ag-NPs showed a vital effect on cell viability, lactate dehydrogenase (LDH) activity (Gliga et al., 2014), and ROS generation (Carlson et al., 2008) in a size-dependent manner in different cell lines. It is evident that surface area, volume ratio, and surface reactivity can be changed with particle size (Carlson et al., 2008, Britto et al., 2014). Moreover, sedimentation velocity, mass diffusivity, attachment efficiency, and deposition velocity of NPs over the biological or solid surfaces are considerably influenced by particle size (Liu et al., 2010). Particle size can also influence the mammalian cell interaction (Nel et al., 2006). Several studies have been carried out to determine the particle size effect of Ag-NPs on different cell lines. Table 1.2 shows some size-dependent studies of Ag-NPs on different cell lines. The studies reported in Table 1.2 reflect the hypothesis that smaller particles can induce greater toxicity.

Table 1.2 Size dependent effects of Ag-NPs on different cell lines

Particle sizes (nm)	Cell type	Findings	References
15, 30, 55	Rat Alveolar macrophages	Small particles induce more toxicity than larger particles	(Carlson et al., 2008)
10, 50, 100	HepG2	Ag-NPs induced size dependent toxicity through autophagy	(Mishra et al., 2016)
5, 20, 50	A549, SGC-7901, HepG2 and MCF-7	EC_{50} values were size dependent and smaller particles can enter easily than larger particles	(Liu et al., 2010)
13 ± 4.7	HeLa & U937	Ag-NPs induced cytotoxicity in both HeLa and U937 cell lines	(Kaba et al., 2015)
10	HepG2	Cytotoxicity induced through the oxidative stress	(Greulich et al., 2009)
20, 80, 113	RAW 264.7 & L929	Ag NPs induced cytotoxicity depends on cell type and Np size	(Park et al., 2010)
5–10	HepG2	Ag NPs induced Oxidative changes in HepG2 cell	(Lankoff et al., 2012)
30–50	A431A549	Ag NP's toxicity depends on particle size and surface potential	(Le et al., 2010)
1-10	HIV virus	Interaction of Ag NPs with HIV virus is size dependent	(Elechiguerra et al., 2005)
7–20	A431HT-1080	Apoptosis induced in both A431 and HT-1080 cell lines	(Arora et al., 2009)
15, 30, 55	alveolar macrophages cells	ROS and LDH generated in a size dependent manner	(Sriram et al., 2012)

Different synthesis processes result diverse types of Ag-NPs e.g., spherical, triangular, square, cubic, rectangular, rod, oval, and flower (Fig. 1.1). From the nano-toxicological point of view, it is unknown whether particle shape has any significant effect on the biological system. This might depend on multiple factors rather than a single one.

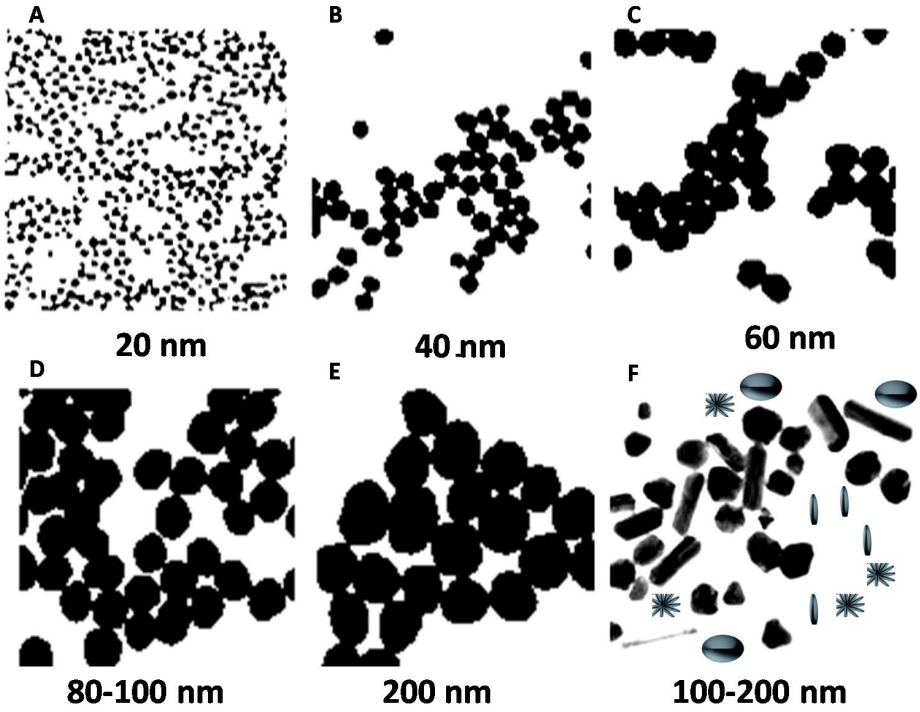

Fig. 1.1 TEM images of synthesized Ag-NPs with various sizes and shapes (A-F). Spherical, oval, rod, and flower shaped Ag-NPs can be obtained from green synthesis. Spherical shaped Ag-NPs mostly obtained by chemical synthesis. The size variability is independent to the synthesis process. Ag-NPs change color as they change their size (color not shown). Scale bars are 100 nm. Modified and redrawn from Stoehr et al. (2011)

1.3.2 Effects of concentration

The concentration of NPs is another important factor affecting toxicity. It is critical to determine the minimum concentration level of NPs that induces toxicity and its variation in different subjects. Mostly, Ag-NPs showed cytotoxicity in a concentration-dependent manner. In RAW 264.7 cells, 0.2 µg/mL of Ag-NPs reduced cell viability by 20%, whereas 1.6 µg/mL of Ag-NPs reduced viability by 40% (Park et al., 2010). The same trend was also observed in human Chang liver cells, where cell viability decreased in a concentration- and dose-dependent manner (Piao et al., 2011). In a rat liver cell line (BRL 3A), 25 µg/mL of Ag-NPs was reported to be the most toxic concentration, with toxicity observed at concentrations ranging from 1–25

µg/mL. Depending on the cell type, Ag-NPs cytotoxicity varies significantly, and this should be taken into consideration for their application in consumer products and in examining environmental effects. Table 1.3 shows the effects of Ag-NPs at different concentration ranges on different cell lines.

Table 1.3 Effects of Ag-NPs of different ranges of concentration on different cell lines

Concentration range	Effects of Ag-NPs in different ranges	References
25-75 µg/mL	In rat alveolar macrophage cell line, cytotoxicity increase in a concentration dependent manner	(Carlson et al., 2008)
5, 15, 40, 125 µg/mL	Cytotoxicity occurred through mitochondrial depolarization	(Aueviriyavit et al., 20014)
10–50 g/mL	Induce cytotoxicity in BRL 3A rat liver cell through ROS generation GSH depletion and reduction of mitochondrial membrane potentiality	(Piao et al., 2011)
20 µg/mL	Induce mitochondrial swelling in HSCs cell line after giving treatment for 2 days	(Stoehr et al., 2011)
20-250 µg/mL	Apoptosis and necrosis induced in HSCs cell line	(Singh et al., 2012)
40-80 µg/mL	40 µg/mL was considered as IC50 value for MCF-7 cell line and apoptosis occurred at the concentration of 80 µg/ml. more than 80 µg/mL induce necrosis when percentage of apoptosis being decreased.	(Jiao et al., 2014)
10-25 µg/mL	In MDA-MB- 231 cell line, DNA damage occur in presence or absence of concurrent radiation treatment	(Yilma et al., 2013)
50 µg/mL	Antioxidant capacity increased in Caco-2 cells	(Kalishwaralal et al., 2009)

1, 2, 4 µg/mL	Cell viability decreased in a concentration dependent manner	(Wang et al., 2009)
10-50 µg/mL	In THP-1-derived human macrophages cell line cell viability decreased in a concentration dependent manner	(Haase et al., 2011)
5 µg/mL	promote epigenetic dysregulation in HT22 cells through cell proliferation, DNA damage response and DNA methylation	(Mytych et al., 2016)
0.4 and 0.8 µg/mL	Arrest G1 phase in cell cycle in RAW 264.7 cell line	(Park et al., 2011)

Taken together, it can be concluded that cytotoxicity of Ag-NPs varies from cell to cell. Moreover, the cell type, particle size, and exposure time also play vital roles in cytotoxicity. However, the minimum or highest concentration of Ag-NPs needed to induce toxicity is not fixed and might vary based on the organism.

1.3.3 Effects of coatings

To prevent aggregation of Ag-NPs, coating is a way to produce electrostatic as well as electrosteric repulsions between particles, which further helps to stabilize the NPs. Uncoated Ag-NPs significantly decreased cell viability in a time-and dose-dependent manner, and coating is used to provide protection against cytotoxicity. The type of coating depends on the capping agent properties such as organic capping agents (polysaccharides, citrates, polymers, proteins, NOM, etc.) and inorganic capping agents (sulfide, chloride, borate, and carbonate). Since the capping material plays a role in maintaining the surface chemistry of Ag-NPs by stabilizing, giving a definite shape, and reducing Ag^{+}, the potentiality of modulating the bioactivity of coated Ag-NPs is significant. In this section, we will discuss the possible effects of Ag-NP coatings on their toxicological phenomena. Ag-NPs-induced cytotoxicity may vary depending on several factors including the type of coating materials. Usually the processes involved in toxicity induction involve ROS generation, depletion of antioxidant defense systems, and loss of mitochondrial membrane potential. Surface coating of Ag-NPs can affect shape, aggregation, and dissolution ratio. However, the method and extent of Ag-NPs toxicity varies based on the coating materials. For example, chitosan-derived polysaccharide-coated Ag-NPs showed antimicrobial activity with no toxicity to eukaryotic cells (Travan et al., 2009).

Polystyrene-coated Ag-NPs caused fewer changes in genetic induction and repression compared to Ag-NPs and $AgCO_3$ in HepG2 cells (Kawata et al., 2009). Furthermore, citrate- and polyvinylpyrrolidone (PVP)-coated Ag-NPs were tested to compare their toxicity with uncoated Ag-NPs using J774A.1 macrophages and HT29 epithelial cells (Nguyenet et al., 2013). Both citrate and PVP-coated Ag-NPs proved to be less cytotoxic than uncoated ones in tested cell lines. Cytokine expression as well as oxidative stress pathway analysis corroborates the possible mechanism of toxicity induction in epithelial cells and macrophages. Citrate coatings can improve the stability of colloidal Ag-NPs and decrease their toxicity. In contrast, PVP-modified Ag-NPs maintain good stability and cause negligible toxic effects in human skin HaCaT keratinocytes. However, no significant changes were observed between uncoated and PVP- and oleic acid-coated Ag-NPs in terms of bioaccumulation and toxicity in earthworms (*Eisenia fetida*) (Shoults et al., 2011). In contrast, polysaccharide-coated Ag-NPs resulted in greater DNA damage than uncoated Ag-NPs by increasing the likelihood of entering into the mitochondria and the nucleus (Zhang et al., 2014). The stability of thiol-coated Ag-NPs reported by Andrieux et al., 2013 was due to their corrosive properties and affinity for the cell membrane proteins (Andrieux-Ledier et al., 2013). It is evident from the above discussion that coating materials and their characteristics play a vital role in Ag-NPs induced cytotoxicity.

1.3.4 Effects of agglomeration

NPs have high potential tendency to aggregate or agglomerate in solution and in ambient air. The interaction potentiality of NPs with cells is dependent on diffusion, gravitation, and convection forces (Lison et al., 2008). The agglomeration process might be affected by the pH, electrolyte or salt content, and protein composition in the culture medium (Vippola et al., 2009). Several studies showed that the binding capacity of NPs with protein is different based on the composition of both the NPs and protein (Kittler et al., 2009).

Ag-NPs have a high agglomeration tendency in culture medium because of their high surface area (Bae et al., 2013). This agglomeration may induce toxicity rather than the ionic metal-induced toxicity. Sometimes, aggregation plays a role in the various types of intracellular responses. Hence, from the point of view of toxicological interest, it is very important to know how agglomeration or aggregation states of NPs affect different biological responses (Lankoff et al., 2012, Liu et al., 2011).

1.4 Cytotoxicity mechanism of Ag-NPs

1.4.1 Mechanism of toxicity induced by Ag-NPs

Despite the wide applications of Ag-NPs, little research has been conducted concerning their impact on human health and the environment. The toxicological mechanism is still unclear. Regardless, there are a number of publications available describing both *in vitro* and *in vivo* NPs toxicity experiments. Results showed that the cytotoxic and genotoxic effect of Ag-NPs is dependent on their concentration, size, exposure time, and environmental factors. In addition, nanosilver surface-coating agents, such as citric acid, amino acids, acetyl trimethylammonium bromide, and sodium dodecyl sulfate are noncovalently attached to nanosilver particles and can be released into the environmental and biological media with or without interaction with biological macromolecules, and inorganic and organic ions cause the NPs to be unstable in media (Mc Shan et al., 2014). Additionally, particle aggregation, surface oxidation to form silver oxide, and oxidation of silver oxide release both Ag^{+} and Ag^{0} into the media, which eventually results in accumulation of ionic silver in the environmental media, biological media, and inside the cell through diffusion or endocytosis, causing mitochondrial dysfunction (Reidy et al., 2013). Ag-NPs then interact with cell membrane proteins and activate signaling pathways to generate reactive oxygen species (ROS), leading to damage of proteins and nucleic acids caused by the strong affinity of silver for sulfur and finally causing apoptosis and inhibition of cell proliferation (Haase et al., 2012). Most of the research has pointed to the above-mentioned cytotoxicological pathways of Ag-NPs.

Generally, in *in vitro* tests, Ag-NPs are highly toxic at concentrations ranging from 5–10 μg mL^{-1} and sizes from 10–100 nm, and they disrupt mitochondrial function (Arora et al., 2009, Ahamed et al., 2008). It can be assumed from several studies that Ag-NPs are transported across cell membranes, especially into the mitochondria, but it is unknown whether nanomaterials target the mitochondria directly or enter the organelle secondary to oxidative damage (Foley et al., 2002). Cytotoxicity of Ag-NPs was mainly induced through the mitochondrial pathway by reducing glutathione (GSH), high lipid peroxidation, and ROS responsive genes causing DNA damage, apoptosis, and necrosis (Haase et al., 2012). On the other hand, a few *in vivo* studies showed that Ag-NPs cause adverse effects on reproduction, malformations, and morphological deformities in different non-mammalian animal models, in addition to the above-mentioned *in vitro* effects (Zhang et al., 2015).

There is another debate regarding whether Ag-NPs or Ag^{+} induce toxicity in biological systems. Ag^{+} is released through the surface oxidation and then reacts with biological molecules (Yu et al., 2013). Though it is controversial, there is strong evidence supporting the

idea that it is Ag^+ that is responsible for the Ag-NPs-mediated toxicity and not the NP itself (Xiu et al., 2012). A recent study revealed that cytotoxicity of Ag-NPs occurs due to the minimum release of Ag^+ (Beer et al., 2012). Therefore, distinguishing the part of the Ag-NPs that leads to toxicity is challenging.

1.4.2 Uptake mechanism of Ag-NPs

Uptake of Ag-NPs into cells may differ from cell to cell. Diffusion, phagocytosis, and endocytosis are some potential modes of entry into the cell (Murugan et al., 2015). In human macrophages, Ag-NPs can enter cells in phagocytic and non-phagocytic ways (Haase et al., 2011). In medium, some Ag-NPs aggregate and enter into the cells through phagocytosis, but other particles that are not in an aggregated form enter through alternate ways. Sometimes, Ag-NPs are engulfed by mammalian cells, and the uptake range of NPs depends on the particle size and type of cell (Sahu et al., 2014). The membrane flip flop mechanism or direct penetration via the ion channel is another possible route of Ag-NPs uptake. In this case, active transport also exists with passive transport (Haase et al., 2011). Intracellular uptake of Ag-NPs was confirmed in the HT22 cell line even 96 hours after removal of Ag-NPs from the medium (Mytych et al., 2016).

1.4.3 ROS generation in Ag-NPs-induced toxicity

Most of the cellular and biochemical alterations in the cells are caused by ROS-mediated toxicity, and this has been confirmed by several *in vitro* models (Aerle et al., 2013). Oxidative stress is considered as the probable mechanism of Ag-NPs-induced toxicity. Superoxide radical (O_2^-) and H_2O_2 can act as ROS, which are essential for maintaining normal physiological processes. However, excessive ROS can collapse the antioxidant defense system, leading to the damage of DNA, proteins, and lipids (Sriram et al., 2012). Mitochondria mainly release ROS, leading to oxidative stress, disruption of ATP synthesis, DNA damage, and eventually apoptosis (Gurunathan et al., 2015). Likewise, Ag-NPs usually generate ROS after entering into the cell (Aerle et al., 2013). As ROS levels increase, the GSH level decreases dramatically and at the same time LDH increases in the medium, which ultimately induces apoptosis (He et al., 2012). Increased levels of ROS ensure oxidative stress that might cause calcium dysregulation or neurodegeneration in neuronal cell (Wang et al., 2009). Oxidative stress resulting from Ag-NPs can damage the antioxidant defense capacity of the cell, damage DNA, and finally lead to apoptosis, especially in human cell lines (Aerle et al., 2013). Intracellular oxidative stress causes MMP3 to secrete a specific amount of MMP, an extracellular matrix (ECM) digester protease (Nagase et al., 2006). Moreover, ROS generation also affects redox homeostasis at the intracellular level, and as a result, lipid peroxidation and

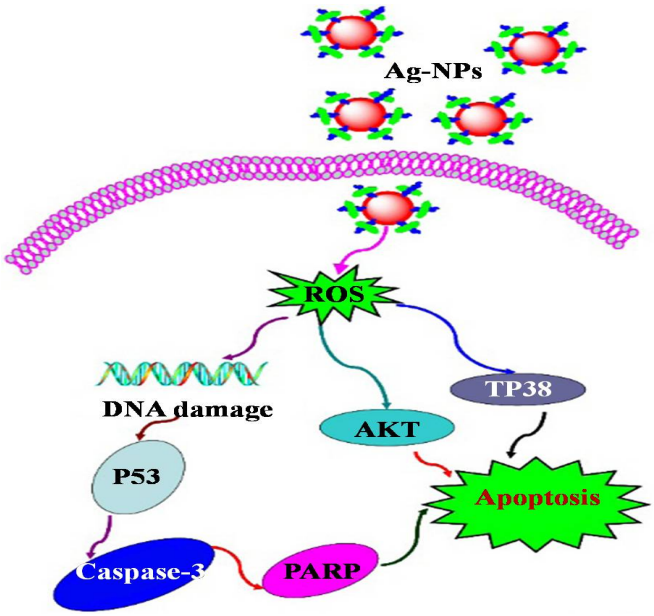

Fig. 1.2 Apoptosis inducing signaling pathway mediated by p53, AKT, MAPK activation to suppress ROS generated by Ag-NPs (Li et al., 2016).

protein carbonylation occurs. At the same time, the glutathione level and antioxidant enzyme activity are decreased. Thus, glutathione level, antioxidant enzyme activity, and protein bound sulfhydryl group depletion promote apoptosis (Miethling et al., 2014). Therefore, the main cytotoxic effect of Ag-NPs is apoptosis-mediated cell death (Gusseme et al., 2011).

1.4.4 Different signaling pathways of Ag-NPs induced toxicity

Ag-NPs induce cytotoxicity following different pathways. Several studies have shown that Ag-NPs induced toxicity is triggered by the increase of ROS generation (Foldbjerg et al., 2009). *In vitro* instillation of Ag-NPs into the cell could generate overproduction of intracellular ROS, which activates cell death-regulating pathways such as p53, AKT, and MAPK signaling apoptotic pathways (Li et al., 2016). Over production of ROS causes the down regulation of total AKT, which increases the expression of proapoptotic kinase p38. Meanwhile, decrease in PARP (poly ADP ribose polymerase) expression resulting significant increase of caspase-3, H2X, p-p53 (phosphorylated p53), and total p53 expressions (Li et al., 2016). Thus Ag-NPs can induce apoptosis following p53 signaling pathway (Fig. 1.2). Mitochondrion is an important centre of apoptosis signal. Effect of Ag-NPs on mitochondrial membrane permeability could cause loss of mitochondrial integrity, which may regulate JNK (Jun N-terminal Kinase) mediated caspase dependent apoptosis (Piao et al., 2011).

Loss of mitochondrial membrane potential ($\Delta\Psi$) regulate down-regulation of Bcl-2, up-regulation of BAX and release of cytochrome c into the cytosol. Down-regulation of Bcl-2 can be influenced by JNK (Jun amino –terminal kinases). JNK is a member of MAPK family which participates in apoptosis via phosphorylation of Bcl-2, consequences inactivation of Bcl-2. Release of cytochrome c into the cytosol initiates a cascade that leads to the initiation of caspase 3 through apaf-1 and caspase 9 (Li et al., 1997). Thus Ag-NPs can induce apoptosis via mitochondria and caspase dependent pathway mediated by JNK (Fig. 1.3). Epigenetic dysregulation can also be induced by Ag-NPs, which may have long term effects on gene expression reprogramming. (Mytych et al., 2016). Ag-NPs could have effect on the cell cycle and induction of DNA hypermethylation following the p53 or p21 pathway, which may have effect on epigenomic level (Mytych et al., 2016).

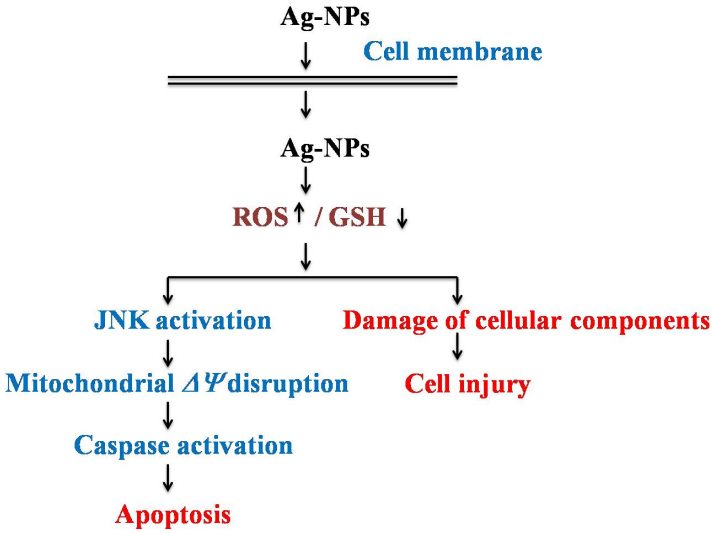

Fig. 1.3 A proposed pathway for Ag-NPs induced ROS generation and intracellular GSH depletion, damage to cellular components, and apoptosis (Piao et al., 2011).

Several studies have compared the toxicity mechanism of Ag-NPs with the Trojan-horse-type molecular pathway (Park et al., 2010) For instance; Ag-NPs can be phagocytosed by RAW 265 cells, making them available in the cytosol and culture medium of active cells, but not in damaged cells. It is possible that NPs released from the damaged cell into the culture medium promote a further biological response referred to as a "Trojan-horse-type" mechanism. Disappearance of Ag-NPs inside the damaged cells suggests that the NPs were ionized inside the cell resulted to cell damage. It is also worth noting, phagocytosis of Ag-NPs can generate ROS which stimulate inflammatory signaling TNF-α. The increase of TNF- α. causes the

damage of cell membrane and apoptosis. Thus, it is speculated to be caused by ionization of Ag-NPs in the cell which is expressed as Trojan-horse type mechanism (Park et al., 2010).

Like other nanoparticles, Ag-NPs also provoke oxidative stress in to the cell through ROS generation (Limbach et al., 2007). Moreover, in Ag-NPs treated cells, generation of ROS can be decreased by pretreatment of cells with NAC, suggesting involvement of intracellular antioxidant defense system (Piao et al., 2011). GSH is one of the major endogenous antioxidant scavengers that able to bind to and reduce ROS. Thus, GSH mediated antioxidant scavenge system is considered as a critical defense system for cell survival (Dewanjee et al., 2009). GSH is formed in two steps by γ-GCL and GSS. First, γ-GCL catalyses and produce glutamylcysteine in the process of cellular GSH biosynthesis. Then finally glutamylcysteine is catalyzed by GSS and adds a glycine residue to form glutamylcysteinglycine or glutathione (Piao et al., 2011). Ag-NPs raised intracellular ROS by the reduction of GSH level through the inhibition of GSH synthesizing enzyme (Piao et al., 2011). However superoxide dismutase and catalase is also intracellular antioxidant defensive enzyme.

Kelch-like ECH-associated protein 1 (Keap-1)-Nrf2 is another defensive signaling pathway which plays an important role in preventing cellular stress (Fig. 1.4). Nrf2 can play a central role in regulating the cellular protection from oxidative, electrophilic, and nitrosative stress, especially in the intestinal cell, through the induction of antioxidant-responsive (ARE) genes and genes of the phase II detoxifying enzyme (Uruno et al., 2011). Oxidation of Keap-1 dissociates Nrf2 and it is then translocated into the nucleus and ultimately activated (Uruno et al., 2005). Thus, activation of Nrf2 influences the generation of cytoprotectors such as hemeoxygenase (HO-1). HO-1 is an enzyme of heme catabolism, which counteracts cell death by producing equimolar quantities of Fe^{2+}, biliverdin, and carbon monoxide to neutralized ROS (Zhu et al., 2011).

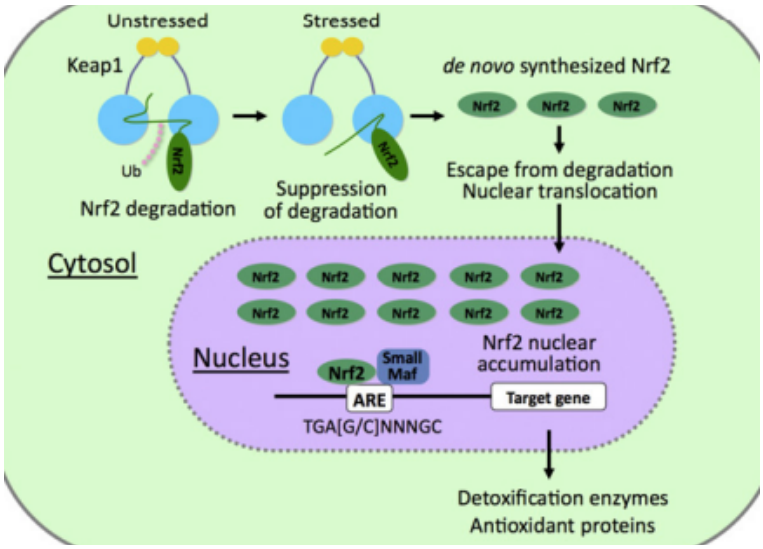

Fig. 1.4 Keap-1-Nrf2 pathway for both stressed and unstressed condition (Uruno et al., 2011).

In summary, Ag-NPs can enter into the cell through the process of diffusion, phagocytosis or endocytosis. Inside the cell, Ag-NPs itself or ionized Ag^{+} generate ROS cause oxidative stress. Over production of ROS can denature different antiapoptotic proteins and initiate proapoptotic proteins expression. Thus, expressions of apoptotic proteins initiate apoptosis signaling pathway (Fig. 1.5).

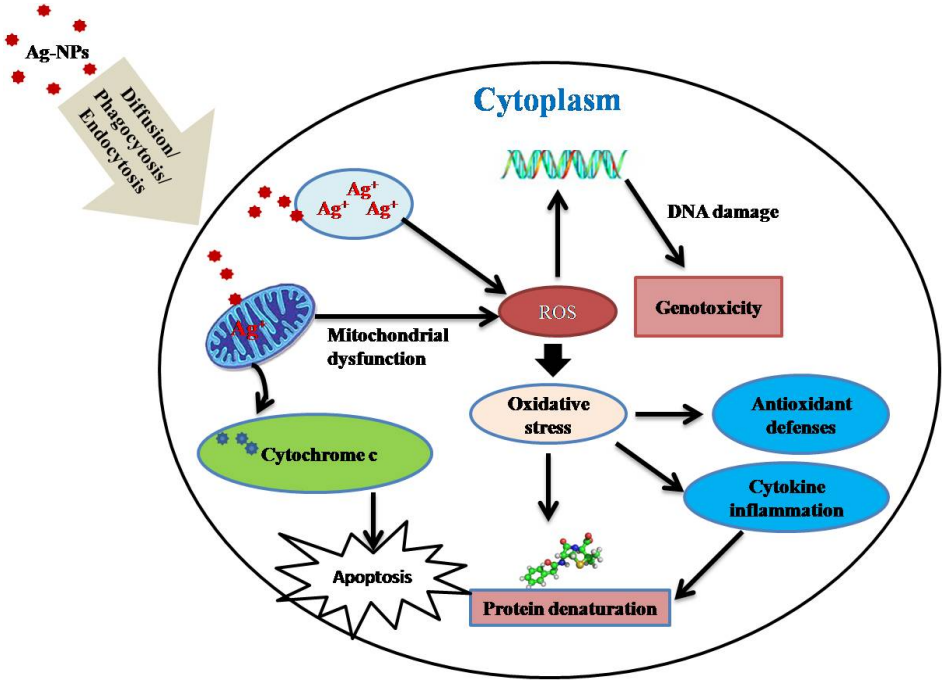

Fig. 1.5 Possible uptake process and mechanism of cytotoxicity induced by Ag-NPs in different cell lines based on the metadata from several studies.

1.5 Role of Ag-NPs against cancer cell

Anticancer activities of Ag-NPs are explored in different cell lines; biogenic Ag-NPs showed anticancer effect on MCF-7 cell line (Jeyaraj et al., 2013) and in A549 cell line (Gengana, et al., 2013) as well. Ag-NPs induce apoptotic cell death in MCF-7 cell line following mitochondrial intrinsic pathway; where DNA damage occurred through generation of ROS, indicating Ag-NPs could help to find an alternative therapeutic agent against MCF-7 cell line. (Jeyaraj et al., 2013). Biologically synthesized Ag-NPs showed antitumor effect on DLA (Dalton's lymphoma ascites) tumor system by activating caspase-3, a well-known enzyme having potential inhibitory effect on disease progression in a mouse model (Muthu et al., 2010). Another recent study has reported that *Albizia adianthifolia* mediated Ag-NPs showed potential cytotoxic effect against A549, human lung cancer cell line, and surprisingly no adverse effect on normal cell line (Gengan et al., 2013). Ag-NPs induced ROS dependent cytotoxic effect was found on HepG2 cell line where DNA damage occurred through oxidative damage dependent pathway and Ag-NPs itself is responsible for the behavior but not silver ion (Kim et al., 2009). However, Caco-2 cell line showed high sensitivity to Ag-NPs, slow gene expression kinetics, and at the same time no size dependent responses. Therefore, a complete mechanism of Ag-NPs induce anticancer effect on Caco-2 cell line is still unclear (Meike et al., 2016).

1.6 *Brassica rapa* var. *nipposinica / japonica* for green Ag-NPs synthesis

Brassica juncea or rapa var. *japonica* plant (locally known as Mizuna) belongs to the mustard family, and has long, broad, serrated, and deeply cut finished leaves with thin trailing stems. *Brassica rapa var. japonica* grows almost round the year in Japan, China and Korea and it is very popular in salad, soup and hot pot. It flavours as bright piquant with a slight earthiness, and contains vitamins A, C, K and E with high glucosinolate compounds (Sahin et al., 2016). It is also rich in antioxidants and has several unique benefits to health. Some of the beneficial aspects of *Brassica rapa* var. *japonica* are (Long et al., 2010):

- High in antioxidant
- Supports blood clotting
- Strengthens bones
- Improves immune health
- Promotes eye health

Previous studies reported that Mizuna plant contains kaempferol, a compound that act as an antioxidant. Kaempferol has been shown to block the spread of cancer cells, protect healthy

cells and reduce chronic inflammation (Allen et al., 2013). Vitamin K is believed to promote the healthy formation of blood clots and may help to prevent bone fracture (Guangliang et al., 2017). Mizuna improves the working efficiency of immune system as well as reduce risk of prostate cancer and helps to refrain from dry skin, eyes, night blindness, hazy vision, and blindness due to its high content of vitamin C and vitamin A (Gale et al., 2003). Therefore, *Brassica rapa* var. *japonica* leaf extract can be a potential candidate as a source of reducing and capping agent for the green synthesis of Ag-NPs.

1.7 Research motivation

"Green Ag-NPs could be a potential antibacterial agent as well as therapeutic agent against cancer cell" is simply be stated as motivation of current research. In this section, some important facts behind the research motivation is depicted. It is said that "Ag -NPs will be a material for future" and also predicted that in 2025, production of Ag -NPs will be reached at 800 ton (Jolanta et al., 2016). This information clearly demonstrates the enormous applications of Ag-NPs in every sector of recent civilization. But unfortunately, conventional commercial nanoparticle synthesis method is energy and time consuming; and most importantly not environment friendly. Therefore, to minimize those disadvantages it is now being high concern to invent alternative synthesis process of NPs synthesis and regarding this issue green synthesis got premium attraction. Green synthesis of nanomaterials mostly known as bio-synthesis has got increased attention to the researchers because of its simplicity, fastness, non-toxicity, and economical approach (Edberg et al., 2000). Moreover, plant mediated bio-synthesis of NPs known as green phyto-synthesis which has upsurge applications in various sectors is said to have advantages such as easily available, safe to handle, and broad range of biomolecules such as alkaloids, terpenoids, phenols, flavanoids, tannins, quinines etc. (Soo et al., 2011).

In contrast, antibiotic resistant bacterial strains with different mechanisms are found continually and thus new drugs are required (Streit et al., 2004). Therefore, the finding of new antimicrobial agents with novel mechanisms of action is essential and extensively pursued in antibacterial drug discovery (Coates et al., 2002). Microbial resistance to antibiotics is a world-wide problem in human and animals. It is generally accepted that the main risk factor for the increase in the antibiotic resistance is an extensive use of antibiotics. This has led to the emergence and dissemination of resistant bacteria and resistance genes in animals and human (Bogaard et al., 2000). The antibiotic resistance of pathogens can be a result of several different factors. Resistance among bacteria is continuously increasing. Nanotechnology is expected to open a new avenue to fight and prevent diseases using atomic scale tailoring of materials.

Recently, it has been demonstrated that metal and metal oxide NPs exhibit excellent biocidal and biostatic actions against Gram-positive and Gram-negative bacteria (Bogaard et al., 2000).

Colorectal cancer is one of the death leading cancers all over the world. Though conventional drug is available for treatment but still nothing is fully satisfactory because of the side effect. Therefore, researchers are now looking for the alternative therapeutic agent for colorectal cancer treatment and the most importantly nanoparticles are considered as potential one. Consequently, It was hypothesized that green Ag-NPs could be a potential antibacterial as well as therapeutic agent for colorectal cancer treatment which motivated us to find a noble environment friendly green method of Ag-NPs synthesis using *Brassica rapa* var. *nipposinica/ japonica* leaf extract to ensure its biomedical applications such as the high antibacterial activity and anticancer property as well.

1.8 Aims and objectives

The aim of this research is to elucidate the biomedical applications of green synthesized Ag-NPs and underlying possible mechanisms of Ag-NPs induce cytotoxicity. To achieve the goal a set of specific objectives is outlined as follows:

a) To synthesize Ag-NPs using *Brassica rapa* var. *nipposinica/ japonica* leaf extract and evaluate their antibacterial activity and cytotoxicity to compare with commercially synthesized Ag-NPs
b) To synthesize Ag-NPs using *Brassica rapa* var. *nipposinica / japonica* leaf extract under controlled temperature and characterized their properties
c) To investigate the anticancer potentiality of Brassica Ag-NPs against colorectal cancer cell line (Caco-2) and their underlying mechanisms

1.9 Outline of the thesis

This thesis comprises of five consecutive chapters including the first chapter on general introduction. In the Chapter 1, a comprehensive background matter is discussed on emerging concern of Ag-NPs in the light of its applications in different sectors, aspect of green synthesis of Ag-NPs, and interaction of Ag-NPs with different cell lines in the light of concentration and coating effect of Ag-NPs. In addition, effect of Ag-NPs on different cancer cell lines is also discussed. However, on the bases of the discussion of Chapter 1, a review article entitled "A systematic review on silver nanoparticles induced cytotoxicity: physicochemical properties and perspectives" has already been published in a reputed international peer reviewed journal "Journal of Advanced Research" 9 (2018) 1-16. Moreover, possible mechanism of Ag-NPs

induce cytotoxicity in different cell lines is also explained in a brief. After that green synthesized Ag-NPs (Brassica Ag-NPs) was compared with commercial Ag-NPs in terms of cytotoxicity on PC 12 cells and evaluate the antibacterial activity with other green synthesized Ag-NPs in Chapter 2. One research article has also been published with these findings in an international journal "Journal of Inorganic and Organometallic Polymers and Materials", 28 (2018) 1483-1493. Then the effect of temperature on biomolecules encapsulation of Ag-NPs synthesized using the green synthesis approach discussed in Chapter 3. Furthermore, effect of Brassica Ag-NPs as a therapeutic agent against colorectal cancer cells is discussed in Chapter 4. Then in Chapter 5 an overall conclusion is being taking place. This chapter is intended to summarize all the findings in a common platform with focusing the importance of green synthesis of Ag-NPs and their biomedical applications in respect of cytotoxicity, antibacterial activity, and potentiality as a therapeutic agent against colorectal cancer cell line *in vitro*.

References

Aerle, R.V., Lange, A., Moorhouse, A., Paszkiewicz, K., Ball, K., Johnston, B.D., Bastos, E.D., Booth, T., Tyler, C.R., Santos, E.M., 2013. Molecular mechanisms of toxicity of silver nanoparticles in zebrafish embryos. Environ Sci Technol. 47, 8005-8014

Ahamed, M., Karns, M., Goodson, M., Rowe, J., Hussain, S.M., Schlager, J.J., Hong, Y., 2008. DNA damage response to different surface chemistry of silver nanoparticles in mammalian cells. Toxicol. Appl. Pharm. 233, 404-410

Ajitha, A., Reddy, Y., A.K., Reddy, P.S., 2014. Biogenic Nano-Scale Silver Particles by Tephrosia purpurea Leaf Extract and Their Inborn Antimicrobial Activity. Spectrochim Acta A Mol Biomol Spectrosc . 121, 164-172

Allen, Y., Chen, Yi., Charlie, Chen., 2013. A review of the dietary flavonoid, kaempferol on human health and cancer chemoprevention. Food chem. 138, 2099-20107

Andrieux-Ledier, A., Tremblay, B., Courty, A., 2013. Stability of Self-Ordered Thiol-Coated Silver Nanoparticles: Oxidative Environment Effects. Langmuir. 29, 13140-13145

Arora, S., Jain, J., Rajwade, J.M., Paknikar, K.M., 2009. Interactions of silver nanoparticles with primary mouse fibroblasts and liver cells. Toxicol. Appl. Pharm. 236, 310-318

Ashokkumar, S., Ravi, S., Kathiravan, V., Velmurugan, S., 2015. Synthesis of Silver Nanoparticles Using A. indicum Leaf Extract and Their Antibacterial Activity. Spectrochim Acta A Mol Biomol Spectrosc. 134, 34-39

Aueviriyavit, S., Phummiratch, D., Maniratanachote, R., 2014. Mechanistic study on the biological effects of silver and gold nanoparticles in Caco-2 cells – Induction of the Nrf2/HO-1 pathway by high concentrations of silver nanoparticles. Toxicol Lett. 224, 73-83

Bae, E., Lee, B.C., Kim, Y., Choi, K., Yi., J., 2013. Effect of agglomeration of silver nanoparticle on nanotoxicity depression. Korean. J. Chem. Eng. 30, 364-368

Bagherzade, G., Tavakoli., M.M., Namae, M.H., 2017. Green synthesis of silver nanoparticles using aqueous extract of saffron (Crocus sativus L.) wastages and its antibacterial activity against six bacteria. Asian Pac J Trop Biomed. 7, 227-233

Beer, C., Foldbjerga, R., Hayashi, Y., Sutherlandb, D.S., Autrupa H. 2012. Toxicity of silver nanoparticles-nanoparticle or silver ion?. Toxicol Lett. 208, 286–292

Bhor, G., Maskare, S., Hinge, S., Singh, L., Nalwade, A., 2014. Synthesis of Silver Nanoparticles Using Leaflet Extract of Nephrolepi sexaltata L. and Evaluation Antibacterial Activity against Human and Plant Pathogenic Bacteria. Asian Journal of Pharmaceutical Technology and Innovation. 6, 23-31

Bogaard, A.E., Stobberingh, E.E., 2000. Epidemiology of resistance to antibiotics. Links between animals and humans. Int. J. Antimicrob. Agents. 14, 327-335

Britto, J.D., Gracelin, D.H.S, Kumar, P.B.J.R., 2014. Antibacterial Activity of Silver Nanoparticles Synthesized from a Few Medicinal Ferns. Int J Pharm Res Dev. 6, 25-29

Bruchez, M., Moronne, M., Gin, P., Weiss, S., Alivisatos, A.P., 1988. Semiconductor nanocrystals as fluorescent biological labels. Science. 281, 2013-2016

Camargo, P.H.C., Satyanarayana, K.G., Wyypych, F., 2009. Nanocomposites: synthesis, structure, properties and new application opportunities. Mat. Res. 12, 1-39

Carlson, C., Hussain, S.M., Schrand, A.M., Braydich-Stolle, L.K., Hess, K.L., Jones, R., L., Schlager, J.J., 2008. Unique cellular interaction of silver nanoparticles: Size-dependent generation of reactive oxygen species. J Phy Chem B. 112, 13608–13619

Cheng, K.M., Hung, Y.W., Chen, C.C., Lin, C.C., Yong, J.J., 2014. Green Synthesis of Chondroitin Sulfate Capped Silver Nanoparticles: Characterization and Surface Modification. Carbohydr Polym. 110, 195-202

Chen, M., Feng, Y.G., Wang, X., Li, T.C., Zhang, J.Y., 2007. Qian DJ. Silver Nanoparticles Capped by Oleylamine: Formation, Growth, and Self-Organization. Langmuir. 23, 5296-5304

Chen, S.F., Zhang, H., 2012. Aggregation kinetics of nanosilver in different water conditions. Adv. Nat. Sci.: Nanosci. Nanotechnol. 035006 (4pp)

Chen, Q., Jiang, H., Ye, H., Li, J., Huang, J., 2014. Preparation, Antibacterial, and Antioxidant Activities of Silver/Chitosan Composities. J Carbohydr Chem. 33, 298-312

Chernousova, S., Epple, M., 2013. Silver as antibacterial agent: ion, nanoparticle, and metal. Angew Chem Int Ed Engl. 52, 1636–1653

Cho, J-G., Kim, K-T., Ryu, T-K., Lee, J-W., Kim, J-E., Kim, J., Lee, B-C., Jo, E-H., Yoon, J., Eom, I-c., Choi, K., Kim, P., 2013. Stepwise Embryonic Toxicity of Silver Nanoparticles on Oryzias latipes. Bio Med Research International. 1-7

Coates, A., Hu, Y., Bax, R., Page, C., 2002. The future challenges facing the development of new antimicrobial drugs. Nat. Rev. Drug Discov. 1, 895-910

Daima, H.K., Bansal, V., Chapter-10: Influence of physico-chemical properties of nanomaterials on their antibacterial applications, Nanotechnology in Diagnosis, Treatment and Prophylaxis of Infectious Diseases, 2015, pp. 151-166. Book published at Boston by Academic Press/ Elsevier, edited by Mahendra Rai and Kateryna Kon, DOI: 10.1016/B978-0-12-801317-5.00010-4.

Das, S.K., Khan, M.M.R., Guha, A.K., Das, A.K., Mandal, A.B., 2012. Silver-NanoBiohybrid Material: Synthesis, Characterization and Application in Water Purification. Bioresour Technol. 124, 495-499

Dewanjee, S., Maiti, A., Sahu, R., Dua, T.K., Mandal, V., 2009. Effective control of type 2 diabetes through antioxidant defense by edible fruits of Diospyros peregrina. Evid Based Complement Alternat. Med. doi:10.1093/ecam/nep080

Edberg, S.C., Rice, E.W., Karlin, R.J., Allen, MJ., 2000. Escherichia coli: the best biological drinking water indicator for public health protection. Appl Microbiol. 88,1068-1168

Edwards-Jones V., 2009. The benefits of silver in hygiene, personal care and healthcare. Lett Appl Microbiol. 49,147–152

Elechiguerra, J.L., Burt, J.L, Morones, J.R., Camacho, B.A., Gao, X., Lara, H.H., Yacaman, M.J., 2005, Interaction of silver nanoparticles with HIV-1. J. Nanobiotechnol. 3: doi:10.1186/1477-3155-3-6

El-Rafie, H.M., El-Rafie, M.H., Zahran, M.K., 2013. Green Synthesis of Silver Nanoparticles Using Polysaccharides Extracted from Marine Macro Algae. Carbohydr Polym. 96, 403-410

Elumalai, E.K., Kayalvizhi, K., Silvan, S., 2014. Coconut Water Assisted Green Synthesis of Silver Nanoparticles. J Pharm Bioallied Sci. 6, 241-245

Foldbjerg, R., Olesen, P., Hougaard, M., Dang, D.A., Hoffmann, H.J., Autrup, H., 2009. PVP-coated silver nanoparticles and silver ions induce reactive oxygen species apoptosis and necrosis in THP-1 monocytes. Toxicol. Lett. 190, 156–162

Foley, S., Crowley, C., Smaihi, M., Bonfils, C., Erlanger, B., Seta, P., Larroque, C., 2002. Cellular localisation of a water-soluble fullerene derivative. Biochem. Biophys. Res. 294, 116–119

Gale, C., Hall, N.F., Phillips, D.I., Martyn, C.N., 2003. Lutein and zeaxanthin status and risk of age-related macular degeneration. Invest Opthalmol. Vis Sci. 44, 2461-2465

Gengan, R.M., Anand, K., Phulukdaree, A., Chuturgoon, A., 2013. A549 lung cell line activity of biosynthesized silver nanoparticles using Albiziaadianthifolia leaf, Colloids Surf B Biointerfaces. 105, 87-91

Gliga, A.R., Skoglund, S., Wallinder, I.O., Fadeel, B., Karlsson, H.L., 2014. Size-dependent cytotoxicity of silver nanoparticles in human lung cells: the role of cellular uptake, agglomeration and Ag release. Part Fibre Toxicol. https://doi.org/10.1186/1743-8977-11-11

Greulich, C., Kittler, S., Epple, M., Muhr, G., Koller, M., 2009. Studies on the biocompatibility and the interaction of silver nanoparticles with human mesenchymal stem cells (hMSCs). Langenbeck Arch. Surg. 394, 495–502

Guangliang, H., Md., Mingyoung, Gu., Chen, Chen., Qiang, Zhang., Guichun, Zhang., Xuecheng, Cao., 2007. Vitamin K intake and the risk of fractures. Medicine. 96,1-12

Gurunathan, S., Park, J.H., Han, J.W., Kim, J.H., 2015. Comparative assessment of the apoptotic potential of silver nanoparticles synthesized by Bacillus tequilensis and Calocybe indica in MDA-MB-231 human breast cancer cells: Targeting p53 for anticancer therapy. Int. J. Nanomed. 10, 4203–4222

Gusseme, D.B., Hennebel, T., Christiaens, E., Saveyn, H., Verbeken, K., Fitts, J.P., Boon, N., Verstraete, W., 2011. Virus disinfection in water by biogenic silver immobilized in polyvinylidene fluoride membranes. Water Res. 45, 1856-1864

Haase, A., Rott, S., Mantion, A., Graf, P., Plendi, J., Thunemann, A.F., Meier, W.P., Taubert, A., Luch, A., Reiser, G., 2012. Effects of silver nanoparticles on primary mixed neural cell cultures: uptake, oxidative stress and acute calcium responses. Toxicol Sci. 126, 457-468

Haase, A., Tentschert, J., Jungnickel, H., Graf, P., Mantion, A., Draude, F., Plendl, J., Goetz, M.E., Galla, S., Masic, A., Thuenemann, A.F., Taubert, A., Arlinghaus, H.F., 2011. Luch A. Toxicity of silver nanoparticles in human macrophages: uptake, intracellular distribution and cellular responses. J Phys. 304, 012030 (14pp)

Hamzeh, M., Sunahara, G.I., 2013. In vitro cytotoxicity and genotoxicity studies of a titanium dioxide (TiO_2) nanoparticles in Chinese hamster lung fibroblast cells. Toxicol In vitro. 27: 864-873

He, D., Dorantes-Aranda., J.J, Waite, T.D. 2012. Silver nanoparticleealgae interactions: oxidative dissolution, reactive oxygen species generation and synergistic toxic effects. Environ Sci Technol. 46, 8731–8738

Jolanta, P.k., Marcin, B., 2016. silver nanoparticles- a material of the future? Open chem. 14, 76–91

Jeyaraj, M., Sathishkumar, G., Sivanandhana, G., Mubarak, Ali., D., Rajesha, M., Arunc, R., Kapildev, G., Manickavasagam, M., Thajuddin, N., Premkumar, K., Ganapathi., 2013. A. Biogenic silver nanoparticles for cancer treatment: An experimental report. Colloids Surf . B. 106, 86– 92

Jiao, Z.H., Li, M., Feng, Y.X., Shi, J.C., Zhang, J., Shao, B., 2014. Hormesis effects of silver nanoparticles at Non-Cytotoxic doses to human hepatoma cells. PLoS ONE. 9: doi: 10.1371/journl .pone.0102564

Kaba, S.I., Egorova, E.M., 2015. In vitro studies of the toxic effects of silver nanoparticles on HeLa and U937 cells. Nanotechnol Sci Appl. 8, 19–29

Kalishwaralal, K., Banumathi, E., Pandian, S.R.K., Deepak, V., Muniyandi, J., Eom, S.H., Gurunathan, 2009. S. Silver nanoparticles inhibit VEGF induced cell proliferation and migration in bovine retinal endothelial cells. Colloid Surf. B. 73, 51–57

Kathiraven, T., Sundaramanickam, A., Shanmugam, N., Balasubramanian, T., 2014. Green Synthesis of Silver Nanoparticles Using Marine Algae Caulerpa resmosa and Their Anti-Bacterial Activity against Some Human Pathogens. Applied Nanoscience. 5, 499-504

Kawata, K., Osawa, M., Okabe, S., 2009. In vitro toxicity of silver nanoparticles at noncytotoxic doses to HepG2 human hepatoma cells. Environ Sci Technol. 43, 6046–51

Kim, S., Choi, J.E., Choi, J., Chung, K.H., Park, K., Yi., J, Ryu., 2009. Oxidative stress-dependent toxicity of silver nanoparticles in human hepatoma cells. Toxicol In Vitro. 23, 1076–1084

Kittler, S., Greulich, C., Gebauer, J.S., Diendorf, J., Treue, I.L., Ruiz, L., 2009. The influence of proteins on the dispersability and cell-biological activity of silver nanoparticles. J Mater Chem. 20, 512–518

Lankoff, A., Sandberq, W.J., Weqierek-Ciuk, A., Lisowska, H., Refsnes, M., Sartwarze, B., Schwarze, P.E., 2012. The effect of agglomeration state of silver and titanium dioxide nanoparticles on cellular response of HepG2, A549 and THP-1 cells. Toxicol Lett. 208,197-213

Le, A.T., Huy, P.T., Tam, P.D., Huy, T.Q., Cam, P.D., Kudrinskiy, A.A., Krutyakov Y.A., 2010. Green synthesis of finely-dispersed highly bactericidal silver nanoparticles via modified Tollens technique. Curr. Appl. Phys.10, 910-916

Limbach, L.K., Wick, P., Manser, P., Grass, R.N., Bruinink, A., Stark, W.J,. 2007. Exposure of engineered nanoparticles to human lung epithelial cells: Influence of chemical composition and catalytic activity on oxidative stress. Environ Sci Technol. 41, 4158–4163

Lison, D., Thomassen, L.C., Rabolli, V., Gonzalez, L., Napierska, D., Seo, J.W., Kirsch-Volders., M., Hoet., P., Kirschhock., CE., Martens., J.A., 2008. Nominal and effective dosimetry of silica nanoparticles in cytotoxicity assays. Toxicol Sci. 104, 155–162

Li, P., Nijhawan, D., Budihardjo, I., Srinivasula, S.M., Ahmad, M., Alnemri, E.S., Wang, X., 1997. Cytochrome c and d ATP-dependent formation of Apaf- 1/caspase-9 complex initiates an apoptotic protease cascade. Cell. 91, 479– 489

Liu, H.H., Surawanvijit, S., Rallo, R., Orkoulas, G., Cohen, Y., 2011. Analysis of Nanoparticle Agglomeration in Aqueous Suspensions via Constant-Number Monte Carlo Simulation. Environ Sci Technol. 45, 9284–9292

Liu, W., Wu, Y., Wang, C., Li, H.C., Wang, T., Liao, C.Y., Cui, L., Zhou, Q.F., Yan, B., Jiang, G.B., 2010. Impact of silver nanoparticles on human cells: effect of particle size. Nanotoxicology. 4, 319-30

Li, Y., Guo, M., Lin, Z., Zhao, M., Xiao, M., Wang, C., Xu, T., et al., 2016. Polyethylenimine-functionalized silver nanoparticle-based co-delivery of paclitaxel to induce HepG2 cell apoptosis. Int J Nanomedicine. 11, 6693–6702

Long-Z, L., James, M.H., 2010. Phenolic component profiles of Mustard Greens. Yu Choy and 15 other Brassica vegetables. J Agric food chem. 58, 6850–6857

McShan, D., Ray, P.C., Yu, H., 2014. Molecular toxicity mechanism of nanosilver. J Food Drug Anal. 22,16-127

Meike, V., Anna, K.U, Evelien, K., Marco, M., 2016. Different responses of Caco-2 and MCF-7 cells to silver nanoparticles are based on highly similar mechanisms of action. Nanotoxicology. 10,1431-1441

Mishra, A.R., Zheng, J., Tang, X., Goering, P.L., 2016. Silver Nanoparticle-Induced Autophagic-Lysosomal Disruption and NLRP3-Inflammasome Activation in HepG2 Cells is Size-Dependent. Tox Sci. 150, 473-87

Miethling-Graff, R., Rumpker, R., Richter, M., Verano-Braga, T., Kjeldsen, F., Brewer, J., Hoyland, J., Rubahn, H.G., 2014. Exposure to silver nanoparticles induces size- and dose-dependent oxidative stress and cytotoxicity in human colon carcinoma cells. Toxicol In Vitro. 28, 1280–1289

Mondal, N.K., Chaudhury, A., Mukhopadhya, P., Chatterjee, S., Das, K., Datta, J.K., 2014. Green Synthesis of Silver Nanoparticles and its Application for Mosquito Control. Asian Pac J Trop. 4, 204-210

Muthu, I.S., Selvaraj, B.M.K., Kalimuthu, K., Sangiliyandi, G., 2010. Antitumor activity of silver nanoparticles in Dalton's lymphoma ascites tumor model. Int j nanomedicine. 5, 753-762

Murugan, K., Choonara, Y.E., Kumar, P., Bijukumar, D., Toit, D.L.C., Pillay, V., Parameters and characteristics governing cellular internalization and trans-barrier trafficking of Nanostructures. Int J Nanomedicine. 10, 2191-2206

Mytych, J., Zebrowski, J., Lewinska, A., Wnuk, M., 2016. Prolonged effects of silver nanoparticles on p53/p21pathway-mediated proliferation, DNA damage response, and methylation parameters in HT22 Hippocampal neuronal cells. Mol Neurobiol. 54, 1-16

Naidu, K.B., Govender, P., Adam, J.K., 2015. Biomedical applications and toxicity of Nanosilver: A review. Medical technology. 29, 13-19

Nagase, H., Visse, R., Murphy, G., 2006. Structure and function of matrix metalloproteinases and TIMPs. Cardiovasc Res. 69, 562–573

Nalwade, A.R., Badhe, M.N., Pawale, C.B., Hinge, S.B., 2013. Rapid Biosynthesis of Silver Nanoparticles Using Fern Leaflet Extract and Evaluation of Their Antibacterial Activity. Int J Biol Technol. 4, 12-18

Nel, A., Xia, T., Madler, L., Li, N., 2006. Toxic Potential of Materials at the Nanolevel. Science. 311, 622-627

Nguyen, K.C., Seligy, V.L., Massarsky, A., Moon, W., Rippstein, P., Tan, J., Tayabali, A.F., 2013. Comparison of toxicity of uncoated and coated silver nanoparticles. J. Phys: Conf. Ser. 429, Doi:10.1088/1742-6596/429/1/012025

Park, E.J., Yi, J., Kim, Y., Choi, K., Park, K., 2010. Silver nanoparticles induced toxicityby a Trojan-horse type mechanism. Toxicol In Vitro. 24, 872–878

Park, M.V.D.Z., Neigh, A.M., Vermeulen, J.P., de, la, Fonteyne, L.J.J., Verharen, H.W., Briedé, J.J., et al., 2011. The effect of particle size on the cytotoxicity, inflammation, developmental toxicity and genotoxicity of silver nanoparticles. Biomaterials. 32, 9810-9817

Piao, M.J., Kang, K.A., Lee, I.K., Kim, H.S., Kim, S., Choi, J.Y., Choi, J., Hyun, J.W., 2011. Silver nanoparticles induce oxidative cell damage in human liver cells through inhibition of reduced glutathione and induction of mitochondria-involved apoptosis. Toxicol Lett. 201, 92-100

Rahimi-Nasrabadi, M., Pourmortazavi, S.M., Shandiz, S.A.S., Ahmadi, F., Batooli, H., 2014. Green Synthesis of Silver Nanoparticles Using Eucalyptus leucoxylon Leaves Extract

and Evaluating the Antioxidant Activities of the Extract. Natural Product Research. 28, 1964-1969

Reidy, B., Haase, A., Luch, A., Dawson, K.A., Lynch, I., 2013. Mechanisms of silver nanoparticle release, transformation and toxicity: a critical review of current knowledge and recommendations for future studies and applications. Materials. 6, 2295-2350

Roe, D., Karandikar, B., Bonn, S.N., Gibbins, B., Roullet, J.B., 2008. Antimicrobial surface functionalization of plastic catheters by silver nanoparticles. J. Antimicrob. Chemoth. 61, 869-876

Sahin, F.H., Aktas, T., Acikgoz, F.E., Akcay, T., 2016. Some Technical and Mechanical Properties of 3 Mibuna (Brassica rapa var. Nipposinica) and Mizuna (Brassica rapa var. japonica), Peer J PrePrints. https://doi.org/10.7287/peerj.preprints.1698v1

Sahu, S.C., Zheng, J., Graham, L., Chen, L., Ihrie, J., Yourick, J.J., Sprando, R.L., 2014. Comparative cytotoxicity of nanosilver in human liver HepG2 and colon Caco2 cells in culture. J Appl Toxicol. 34, 1155–1166

Sadeghi, B., and Gholamhoseinpoor, F., 2015. A Study on Stability and Green Synthesis of Silver Nanoparticles Using Ziziphora tenuior (Zt) Extract at Room Temperature. Spectrochim Acta A Mol Biomol Spectroc. 134, 310-315

Sadeghi, B., Rostami, A., Momeni, S.S., 2014. Facile Green Synthesis of Silver Nanoparticles Using Seed Aqueous Extract of Pistacia Atlantica and Its Antibacterial Activity. Spectrochim A Mol Biomol Spectrosc. 134, 326-332

Sant, D.G., Gujarathi, T.R., Harne, S.R., Ghosh, S., Kitture, R., Kale, S., Chopade, B.A., Pardesi, K.R., 2013. Adiantum phillipenseL. Frond Assisted Rapid Green Synthesis of Gold and Silver Nanoparticles. J. Nanopart. 2013: 9pp: http://dx.doi.org/10.1155/2013/182320

Sato, B.R., Redón, R., Vázquez, O.A., Saniger J.M., 2009. Silver nanoparticles synthesized by direct photoreduction of metal salts. Application in surface-enhanced Raman spectroscopy. J. Raman Spectrosc. 40, 376-380

Shoults-Wilson, W.A., Reinsch, B.C., Tsyusko, O.V., Bertsch, P.M., Lowry, G.V., Unrine, J.M., 2011. Effect of silver nanoparticle surface coating on bioaccumulation and reproductive toxicity in earthworms (Eisenia fetida). Nanotoxicology. 5, 432-444

Siegel, J., Kvítek, O., Ulbrich, P., Kolská, Z., Slepička, P., Švorčík, V., 2012. Progressive approach for metal nanoparticle synthesis. Mater. Lett. 89, 47-50

Singh, P.K., Bhardwaj, K., Dubey, P., Prabhune, A., 2015. UV-Assisted Size Sampling and Antibacterial Screening of Lantana camara Leaf Extract Synthesized Silver Nanoparticles. RSC Advances. 5, 24513-24520

Singh, R.P., Ramarao, P., 2012. Cellular uptake, intracellular trafficking and cytotoxicity of silver nanoparticles. Toxicol. Lett. 213, 249–259

Soo-HK, Lee, H.S., Ryu, D.S., Choi, S.J., Lee, D.S., 2011. Antibacterial Activity of Silver-nanoparticles Against Staphylococcus aureus and Escherichia coli. Korean J. Microbiol. Biotechnol. 39, 77–85

Sriram, M.I., Kalishwaralal, K., Barathmanikanth, S., Gurunathani, S., 2012. Size-based cytotoxicity of silver nanoparticles in bovine retinal endothelial cells. Nanosci. Methods. 1, 56–77.

Stoehr, L.C., Gonzalez, E., Stampf, A., Casals, E., Duschl, A., Puntes, V., Oostingh, G.J., 2011. Shape matters: Effects of silver nanospheres and wires on human alveolar epithelial cells. Part. Fibre Toxicol. 8, 425–430

Streit, J.M., Fritsche, T.R., Sader, H.S., Jones, R.N., 2004. Worldwide assessment of dalbavancin activity and spectrum against over 6,000 clinical isolates. Diagn. Microbiol. Infect. Dis. 48,137-143

Suresh, G., Gunasekar, P.H., Kokila, D., Prabhu, D., Dinesh, D., Ravichandran, N., Ramesh, B., Koodalingam, A., Siva, G.V., 2014. Green Synthesis of Silver Nanoparticles Using Delphinium denundatum Root Extract Exhibits Antibacterial and Mosquito Larvicidal Activities. Spectrochim Acta A Mol Biomol Spectrosc. 127, 61-66

Tang, J., Xiong, L., Zjou, G., Xi, T., 2010. Silver nanoparticles crossing through and distribution in the blood-brain brrier in vitro. J. Nanosci. Nanotechnol. 10, DOI: 10.1166/jnn.2010.2625

Tagad, C.K., Dugasani, S.R., Aiyer, R., Park, S., Kulkarni, A., Sabharwal, S., 2013. Green Synthesis of Silver Nanoparticles and Their Application for the Development of Optical Fiber Based Hydrogen Peroxide Sensor. Sens Actuators. B: 183, 144-149

Travan, A., Pelillo, C., Donati, I., Marsich, E., Benincasa, M., Scarpa, T., Semeraro, S., et al. 2009. Non-cytotoxic silver nanoparticle-polysaccharide nanocomposites with antimicrobial activity. Biomacromolecules. 10,1429–35

Uruno, A., Motohashi, H., 2011. The Keap1-Nrf2 system as an in vivo sensor for electrophiles Nitric Oxide. 25,153–160

Velichkova, M., Hasson, T., 2005. Keap1 Regulates the oxidation-sensitive shuttlingof Nrf2 into and out of the nucleus via a Crm1-dependent nuclear export mech-anism. Mol Cell Biol. 25, 4501–4513

Vijaykumar, P.P.N., Pammi, S.V.N., Kollu, P., Satyanarayana, K.V.V., Shameem, U., 2014. Green Synthesis and Characterization of Silver Nanoparticles Using Boerhaavia diffusa Plant Extract and Their Antibacterial Activity. Ind Crops Prod. 52, 562-566

Vimala, R.T.V., Satishkumar, G., Sivramakrishnan, S., 2015. Optimization of Reaction Conditions to Fabricate Nano Silover Using Couroupita guianensis Aubel(Leaf & Fruit) and Its Enhanced Larvicidal Effects. Spectrochim Acta A Mol Biomol Spectrosc. 135, 110-115

Vippola, M., Falck, G.C., Lindberg, H.K., Suhonen, S., Vanhala, E., Norppa., H., et al., 2009. Preparation of nanoparticle dispersions for in-vitro toxicity testing. Hum Exp Toxicol. 28, 377-385

Wang, J.Y., Rahman, M.F., Duhart, H.M., Newport, G.D., Patterson, T.A., Murdock, R.C., Hussain, S.M., Schlager, J.J., Ali, S.F., 2009. Expression changes of dopaminergic system-related genes in PC12 cells induced by manganese, silver, or copper nanoparticles. Neurotoxicology. 30, 926–933

Xiu, Z.M., Zhang, Q.B., Puppapa, H.L., Colvin, V.L., Colvin, P.J., 2012. Negligible particle-specific antibacterial activity of silver nanoparticles. Nano Lett. 12, 4271-5

Yasin, S., Liu, L.,Yao, J., 2013. Biosynthesis of Silver Nanoparticles by Bamboo Leaves Extract and Their Antimicrobial Activity. Journal of Fiber Bioengineering and Informatics. 6, 77-84

Yilma, A.N., Singh, S.R., Dixit, S., Dennis, V.A., 2013. Anti-inflammatory effects of silver-polyvinyl pyrrolidone (Ag-PVP) nanoparticles in mouse macrophages infected with live Chlamydia trachomatis. Int. J. Nanomed. 8, 2421–2432

Yu, S-J., Yin., Y-G., Liu, J-F., 2013. Silver nanoparticles in the environment. Environ Sci Proc Impacts. 15, 78-92

Yugang, S., Younan, X., 2002. Shape-Controlled Synthesis of Gold and Silver Nanoparticles. Science. 298, 2176-2179

Zhang, M., Zhang, K., Gusseme, B.D., Verstraete, W., Field, R., 2014. The Antibacterial and Anti-Biofouling Performance of Biogenic Silver Nanoparticles by Lactobacillus fermentum. Biofouling: The Journal of Bioadhesion and Biofilm Research. 30, 347-357

Zhang, T., Wang, L., Chen, Q., Chen, C., 2014. Cytotoxic Potential of Silver Nanoparticles. Yonsei Med. J. 55, 283-291

Zhang, X.F., Gurunathan, S., Kim, J.H., 2015. Effects of silver nanoparticles on neonatal testis development in mice. Int J Nanomedicine. 10, 6243–6256

Zuas, O., Hamim, N., Sampora, Y., 2014. Bio-Synthesis of Silver Nanoparticles Using Water Extract of Myrmecodia pendan (Sarang Semut Plant). Materials Letters. 123, 156-159

Zhu, X., Fan, W.G., Li, D.P., Kung, H., Lin, M.C., 2011. Heme oxygenase-1 systemand gastrointestinal inflammation: a short review. World J Gastroenterol. 17, 4283-4288

Chapter 2

Brassica rapa var. *nipposinica/ japonica* leaf extract mediated green synthesis of crystalline silver nanoparticles and evaluation of their stability, cytotoxicity and antibacterial activity

Abstract

Silver nanoparticles (Ag-NPs) were successfully synthesized from the reduction of Ag^+ using $AgNO_3$ solution as a precursor and *Brassica rapa* var. *nipposinica/ japonica* leaf extract as a reducing and capping agent. This study was aimed at synthesis of Ag-NPs, exhibiting less toxicity with high antibacterial activity. The characterization of Ag-NPs was carried out using UV-Vis spectrometry, energy dispersive X-ray spectrometry, fourier transform infrared spectrometry, field emission scanning electron microscopy, X-ray diffraction, atomic absorption spectrometry, and transmission electron microscopy analyses. The analyses data revealed the successful synthesis of nano-crystalline Ag possessing more stability than commercial Ag-NPs. The cytotoxicity of Brassica Ag-NPs was compared with commercial Ag-NPs using *in vitro* PC12 cell model. Commercial Ag-NPs reduced cell viability to 23% (control 97%) and increased lactate dehydrogenase activity at a concentration of 3 ppm, whereas, Brassica Ag-NPs did not show any effects on both of the cytotoxicity parameters in PC12 cells. Moreover, Brassica Ag-NPs exhibited antibacterial activity in terms of zone of inhibition against *E. coli* (11.1$\pm$0.5 mm) and *Enterobacter* sp. (15$\pm$0.5 mm) which was higher than some previously reported green-synthesised Ag-NPs. Thus, this finding can be a matter of interest for the production and safe use of green- Ag-NPs in consumer products.

2.1 Introduction

Enormous uses of silver nanoparticles (Ag-NPs) in cosmetics have been increased in recent decades due to their unique physicochemical properties and antibacterial activities (Gajbhiye et al., 2016). Recent researches have revealed that 12% of the total NPs used in cosmetics is Ag-NPs (Akter et al., 2018). In particular, Ag-NPs have widely used in soaps, face creams, toothpastes, wet tissues, deodorants, lip products, face and body foams (Gajbhiye et al., 2016). These huge applications of Ag-NPs could be threatening for human health, because the particles having size up to 1000 nm can across through skin and reach to inside of the cells (Rouse et al., 2007). Moreover, the absorption of NPs is enhanced in acne, eczema or wounds; subsequently the particles enter into the blood stream and induce complications (Prow et al.,

2011). It is also reported that, NPs (5-20 nm) can penetrate into the skin and interact with the immune system (Kreilgaard et al., 2002). Besides, Ag-NPs could be penetrated through the human skin at a range of 0.2% - 2%, if barrier capacity in the skin was disrupted (Kokura et al., 2010). Several *in vitro* and *in vivo* studies revealed that Ag-NPs can induce toxicity to organisms (Akter et al., 2018). The cytotoxic effects of Ag-NPs in A-549, NIH- 3T3, PC12 and HepG2 cell lines were reported in literature (Sambale et al., 2015). Prolonged effects of Ag-NPs were also warning for the possible adverse impacts on epigenetic dysregulation and gene expression reprogramming (Mytych et al., 2016). Hence, it is worthwhile to develop suitable method/s for the synthesis of Ag-NPs, which would be less toxic. Moreover, Ag-NPs having antibacterial activity could promote the safe use in dietary supplements, food packaging, cosmetics and anti-acne preparation. Consequently, it is important to establish a synthesis route of Ag-NPs having less toxicity with high antibacterial activity for the safe use of them in terms of human health concerns.

In recent years, numerous conventional methods are reported for Ag-NPs synthesis such as chemical reduction (Guzmán MG et al., 2009), electrochemical (Starowicz et al., 2006), and sonochemical (Xu et al., 2013) processes. However, green synthesis method is being prominent as it is eco-friendly, cost effective and rapid with high substrate availability (Velmurugan et al., 2016). Green synthesis of Ag-NPs was firstly reported by Gardea-Torresdey et al., 2003. Chandran et al. 2006. synthesized Ag-NPs using *Aloe vera* plant extract and described that the presence of ammonia in the *Aloe vera* facilitated the bioreduction of Ag^{+} ion for the formation of metallic Ag-NPs. The studies evaluated the use of plants and their tissues for Ag-NPs synthesis. *Aloe vera* leaf (Ashraf et al., 2016), *Musa paradisiaca* peels (Narayanamma et al., 2016), *Cocos nucifera* coir (Roopan et al., 2013), *Annona squamosa* peel (Jagtap UB et al., 2013), *Citrus aurantium* peel (Kahrilas et al., 2014), and *Citrullus lanatus* rind (Velmurugan et al., 2016) extracts mediated synthesis of Ag-NPs have been reported. The successful green synthesis can be a potential candidate to replace conventional chemical synthesis of NPs. Thus, scientists all over the world have been searching for the new substrates from the nature.

Green synthesis of NPs by bacteria, fungi, yeast and plant extract are the best alternatives to develop the cost effective, less labour, non-toxic environmentally friendly NPs for avoiding the adverse effects in many nanomaterials' applications. The synthesis of NPs using plants extracts is more effective than microbes, because the presence of bio-molecules in plants can act as reducing agents as well as stabilizer and thus enhance the rate of reduction and stabilization of NPs. *Brassica rapa* var. *nipposinica/ japonica*plant (locally known as

Mizuna) contains a good number of phenolic acids and flavonoids (Khanam et al.,2012). It was speculated that the bio-molecules present in the *Brassica rapa* var. *nipposinica /japonica* plant would act both reducing and capping agents (Huang et al., 2007). Mizuna belongs to the mustard family, and has long, broad, serrated and deeply cut finished leaves with thin trailing stems. It flavours as bright piquant with a slight earthiness and contains vitamins A, C, and E with high glucosinolate compounds (Sahin et al., 2016). Moreover, *Brassica rapa* var. *nipposinica/ japonica* grows almost round the year in Japan, China and Korea, and it is very popular in salad, soup and hot pot. Therefore, Brassica rapa var. nipposinica /japonica leaf extract can be a potential candidate as a source of naturally available reducing and capping agent for the green synthesis of Ag-NPs.

The aim of this study was to establish a method of synthesis of crystalline Ag-NPs, as crystalline materials are generally known as more stable than the amorphous phase, to ensure their stability in biological medium in order to show less toxicity along with enhanced antibacterial activity. The toxicity of Ag-NPs on cells was evaluated from the cell viability and LDH assay experiments from their exposure to PC12 cells, a well-known model cell line in molecular biology to assess cytotoxicity (Jiang et al., 2014). The antibacterial activity of Ag-NPs was assessed using *E. coli* and *Enterobacter* sp. *E. coli* is a coliform Gram-negative bacteria which is considered as the best biological indicator of drinking water and widely used in bacterial study (Edberg et al., 2000). It is abundant on the body surface of mammals and sometimes results acute infection (Kim et al., 2011). *Enterobacter* sp. is a pathogenic bacteria cause nosocomial infection and can be replicated easily in contaminated fluid (Joseph et al., 1994). Finally, the cytotoxic effect of *Brassica rapa* var. *japonica* leaf extract mediated green synthesized Ag-NPs was compared with commercially available Ag-NPs (Com Ag-NPs) and the antibacterial activity was compared with some of other reported green synthesized Ag-NPs.

2.2 Materials and methods

2.2.1 Materials

Commercially available 10 nm sized, sodium citrate coated Ag-NPs was purchased from Sigma Aldrich (St. Louis Missouri, USA). 0.1 M $AgNO_3$ was purchased from Wako Pure Chemical Industries (Osaka, Japan). *Brassica rapa* var. *japonica* plants were collected locally from Sapporo, Japan. PC12 cell line was obtained from the American type culture collection (USA and Canada). Dulbacos modified eagles medium (DMEM) was purchased from Sigma (St. Louis, MO, USA). Fetal bovine serum was purchased from Biosera (Kansas City, MO,

USA). Trypan blue stain solution (4%) was purchased from Bio Rad (Hercules, CA, USA). Bacto trypton, bacto agar and yeast extract were purchased from Difco Laboratories (Detroit, MI, USA) and sodium chloride from Wako Pure Chemical Company (Osaka, Japan). All other reagents and chemicals used in this study were of analytical grade.

2.2.2 Preparation of Brassica rapa var. japonica *leaf extract*

Fresh and healthy leaves of *Brassica rapa var. japonica* were collected locally and then thoroughly washed with tap water followed by distilled water for several times to remove the visible dust. Then, the leaves were dried naturally for 10 days, and blended with a blender to make leaf powder. After that 1 g of leaf powder was mixed with 50 mL of distilled water and boiled at 100 °C for 10 min. After cooling at room temperature (25 °C), the leaf broth was filtered through Whatman filter paper (Cat No 1001 090, diameter: 9 cm, pore size: 11µm). The filtrate was then stored at 4 °C for further experiments (Fig. 2.1).

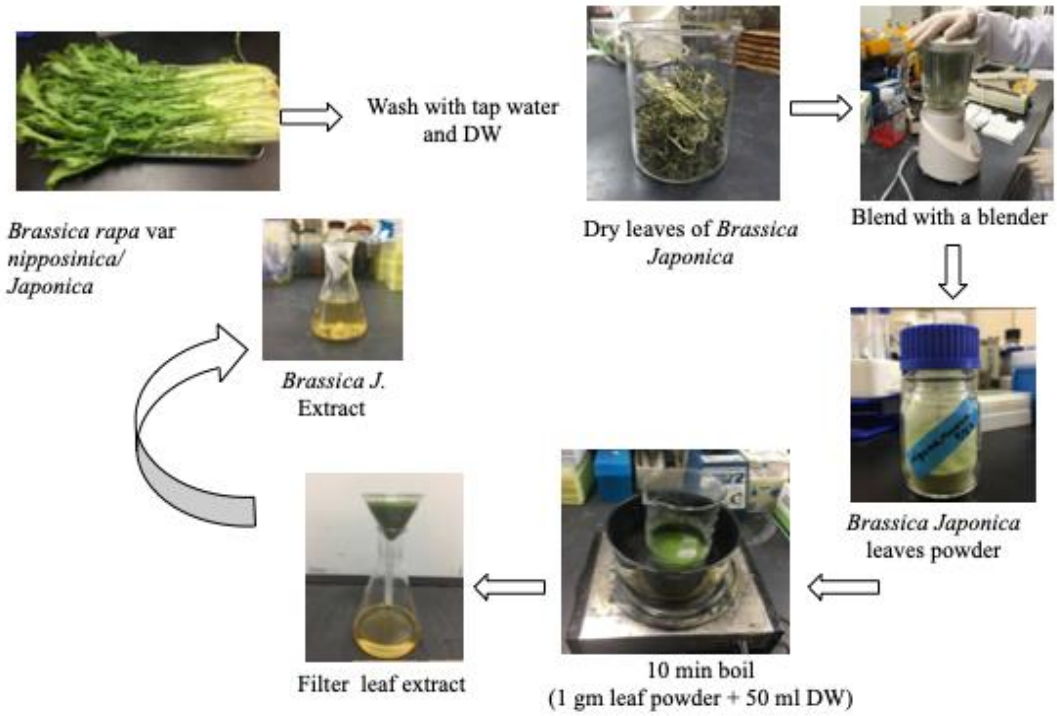

Fig. 2.1 Schematic diagram of preparation of *Brassica rapa* var. *nipposinica/ japonica* leaf extract

2.2.3 Synthesis of Ag-NPs using Brassica rapa *var. nipposinica/ japonica leaf extract*

In this study, 10 mL of *Brassica rapa* var. *japonica* leaf extract was added with 100 mL of 1 mM $AgNO_3$ solution drop wise at a rate of around one drop per second under constant stirring on a magnetic stirrer. The stirring was continued for one hour and then kept undisturbed at room temperature (25° C) for 24 h. The reduction of Ag^+ ions to Ag^0 was monitored by the

change of colour from gray to reddish yellow. The broth was then centrifuged at 10,000 rpm for 10 min and the precipitates were washed with deionized water and centrifuged repeatedly to remove the impurities. The precipitates were dried at 60 °C for overnight and stored in a desiccator for further analysis (Fig 2.2).

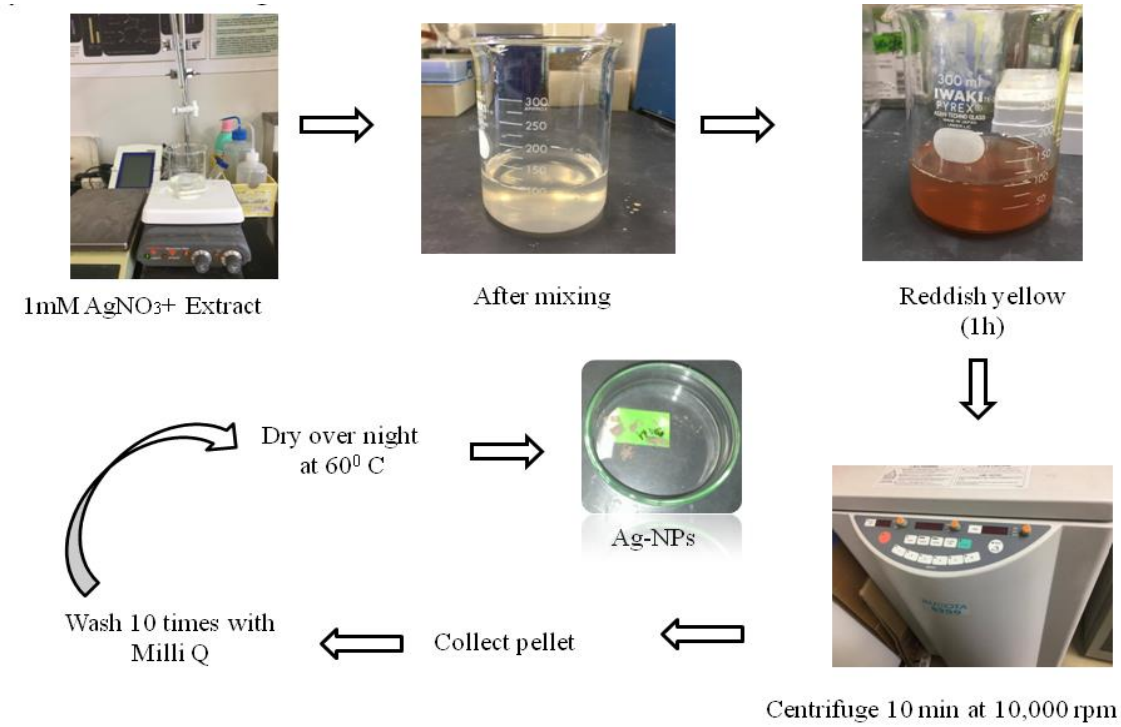

Fig. 2.2 Schematic diagram of synthesis of *Brassica rapa* var. *nipposinica/ japonica* leaf extract mediated Ag-NPs

2.2.4 UV-Vis. spectra analysis

The formation of Ag-NPs from the reduction of Ag^+ ion was analyzed by monitoring the UV–Vis. spectra. Sample was diluted for 20 times with deionized water and spectra of Brassica Ag-NPs and commercial Ag-NPs suspension were recorded at wavelength of 200-700 nm using a UV-Vis. spectrophotometer (JASCO V-650, Japan). During the experiment, deionized water was used as blank to adjust the baseline of the UV-Vis. spectra. This experiment was repeated three times for the reproducibility.

2.2.5 Field emission scanning electron microscopy (FESEM) and Energy dispersive X-ray (EDX) spectrometry analyses of Ag-NPs

The surface morphology of Ag-NPs was monitored using FESEM (JEOL, model JSM 6500 F, Japan). The elemental composition was obtained from EDX spectrometer (JEOL,

model JSM 6500 F, Japan). The operating condition of the instrument was 15 kV acceleration voltage and 12 μA emission current.

2.2.6 X-ray diffraction (XRD) Analysis of Ag-NPs

Crystalline phase was measured by XRD technique (Rigaku, MiniFlex, Japan). During XRD, sample was placed on XRD grid and spectra were recorded at 40 KeV and 30 mA of voltage and current respectively with CuKα radiation.

2.2.7 Transmission electron microscopy (TEM) analysis of Ag-NPs

The sizes of Ag-NPs were measured by TEM (JEOL, JEM 2010, Japan). A suspension of Ag-NPs with ethanol was prepared, and 1 μL of the suspension was placed on formver coated grid, allowed to dry at room temperature (25ºC) and then kept on a specimen holder in order to perform TEM analysis. The images were viewed at an accelerating voltage of 120 kV.

2.2.8 Fourier transform infrared (FT-IR) analysis

FT-IR spectra of Ag-NPs and *Brassica rapa* var. *japonica* leaf powder was recorded to find the presence of functional groups that bound distinctively with the Ag-NPs surfaces. 1 % (w/w) samples were mixed with KBr powder and pressed into a sheer slice. FT-IR spectra of the samples were measured from 500 to 5000 cm^{-1} with a JASCO FT/IR-4100, Japan.

2.2.9 Assessment of stability of Ag-NPs

The stability of Ag-NPs was assessed from the silver ion release test measured by atomic absorption spectrophotometer (AAS) (HITACHI, model U-135, Kyoto, Japan). Hollow cathode lamp with 7.5 mA lamp current, 328.1 nm wavelength and 0.3 nm slit was used in the AAS. The purity of C_2H_2 gas was 99.99%. 1 μg/mL suspensions of both commercial and Brassica Ag-NPs were prepared using deionised water and kept at room temperature (25 °C) for 1 h and 24 h respectively. Suspensions were centrifuged at 3000 rpm for 5 min before taking the absorbance. To ensure the reproducibility of the results, silver ion release test was performed for three times.

2.2.10 Assessment of cytotoxicity of Ag-NPs

2.2.10.1 Cell viability assay

PC12 cells were cultured in DMEM medium supplemented with 10% FBS in a humidified incubator at 37 °C with 5% CO_2 in 25 cm^2 culture flasks. Then, the Ag-NPs were added into the flasks, and incubated for 48 h. In every treatment, fresh medium was added prior to

treatment. The cell viability of PC12 cells after the exposure of Ag-NPs was measured by trypan blue exclusion assay method (Rahman et al., 2017). After 48h incubation with Ag-NPs exposure, cell viability was measured using Bio-Rad automated cell counter (Herculis CA, USA). Cell viability was expressed as percentage of the total cell counts against the stained cell counts. Each experiment was performed at least three times to make sure the reproducibility and statistical validity.

2.2.10.2 Lactate dehydrogenase (LDH) activity assay

The LDH activity in the treatment medium after the exposure of Ag-NPs to PC 12 cells was measured using a nonradioactive cytotoxicity assay kit (Promega, state of Wisconsin, WI, USA) (Rahman et al., 2018). The cells were cultured in a medium and treated with 0, 1 and 3 ppm of Ag-NPs. After 48 h cultivation, 50 µL medium was taken into a 1.5 mL eppendorf tube, and then substrate mixture containing tetrazolium salts was added. After 30 min incubation at room temperature, stop solution was added, and the total amount of formazan dye formed was determined by measuring absorbance at 490 nm using DU65 spectrophotometer (Beckman, CA, USA). LDH assay was also performed at least three times to ensure reproducibility and statistical validity.

2.2.11 Antibacterial activity of Brassica Ag-NPs

The antibacterial activity of Ag-NPs was measured by disc diffusion method (Saravanan et al., 2011). *E. coli* (JM-109 strain) and *Enterobacter* sp. were used as Gram-negative bacteria. Bacteria were cultured in Luria Broth (LB) medium (tryptone 1.5%, yeast extract 0.75%, sodium chloride 1.2%) at 37 °C with 60 rpm shaking in water bath. Fresh culture containing 6.6×10^6 bacteria measured by the optical density at 600 nm was used for the experiments (Saravanan et al., 2011). To measure the inhibition zone, 50 µL of medium containing bacteria were poured into LB plate with 1% agar. For disc preparation, filter paper was punched, autoclaved and dried at 60 °C for overnight. Subsequently, the discs (5 mm sized) were soaked with 15 µL of Ag-NPs suspensions and placed on culture plate at 37 °C for 24 h.

2.2.12 Statistical analyses

To ensure the reproducibility of the results, each of the experiments was repeated at least three times. Statistical analyses were conducted following unpaired student's *t*- test. All data were presented as the mean ± standard error of mean (SEM). Significance level was calculated at $p<0.05$, where difference between means were considered as statistically significant.

2.3 Results

2.3.1 Characterization of Ag-NPs

The formation of Ag-NPs through the reduction of Ag^{+} was primarily monitored using UV-Vis. spectra analysis. It is reported that Ag-NPs exhibit UV-Vis. absorption maxima at wavelength range of 400-500 nm because of the surface plasmon resonance (Ashraf et al., 2016). In the present study, an absorption maxima was observed at 420 nm after 1 h reaction as shown in Fig. 2.3 indicating the formation of Ag-NPs (Ashraf et al., 2016). In addition, in commercial Ag-NPs, a broad peak at 509 nm was also observed (Fig. 2.3).

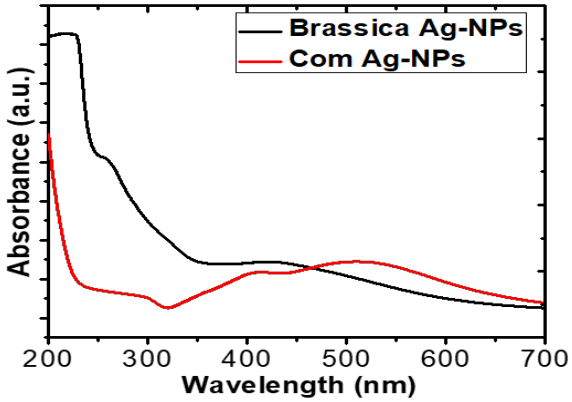

Fig. 2.3 UV- Vis. absorption spectra of Brassica Ag-NPs and Com Ag-NPs showing absorption maxima at 420 nm and 509 nm, respectively.

Dispersion and aggregation of both *Brassica rapa* var. *japonica* mediated Ag-NPs (Brassica Ag-NPs) and commercial Ag-NPs (Com Ag-NPs) were examined using FESEM as shown in Fig. 2.4a and 2.4b, respectively. From the images, it was evidenced that both the Brassica and Com Ag-NPs were uniformly dispersed, referred a very few aggregations of particles

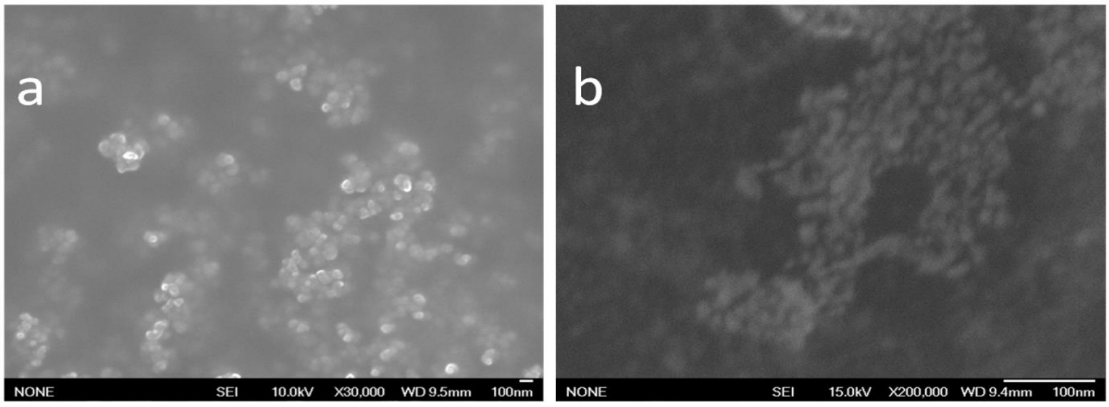

Fig. 2.4 FESEM images of (a) Brassica Ag-NPs and (b) Com Ag-NPs showing the evenly dispersion of Ag-NPs

EDX analysis confirmed the presence of high percentage of silver signalling strong peak for both of the Brassica Ag-NPs (Fig. 2.5a) and commercial Ag-NPs (Fig 2.5b). However, some weaker peaks were also found for oxygen and carbon in Brassica Ag-NPs.

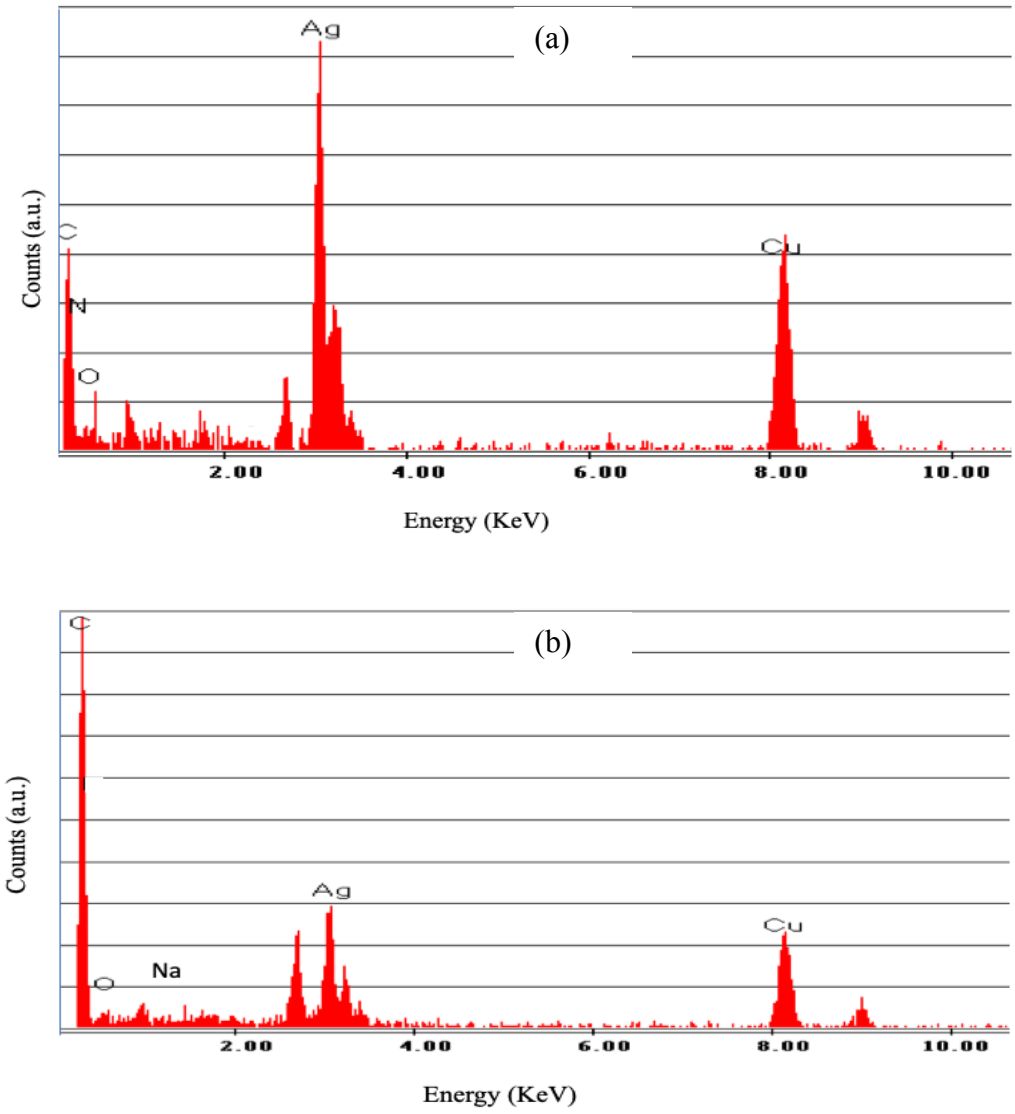

Fig. 2.5 EDX of (a) Brassica Ag-NPs and (b) Com Ag-NPs

Crystallinity and solid phase microstructure of Brassica Ag-NPs was characterized by XRD (Fig. 2.6) at a scanning range of 35-85º (2θ). Five distinct diffraction peaks were found at 38.04º, 44.24º, 64.4º, 77.24º and 81.48º, which were indexed as the planes 111, 200, 220, 311 and 222 respectively. The crystalline phase was found to be cubic and the value of lattice constant was measured using Nelson-Riley function (Ullah et al., 2017). The average lattice constant was found to be 4.0904 Å which agreed with reported value (4.077 Å) (Sagar et al.,

2012)). The crystallite size was calculated using Debye-Scherrer approximation (Alam et al., 2017) and the value was found to be 15 nm.

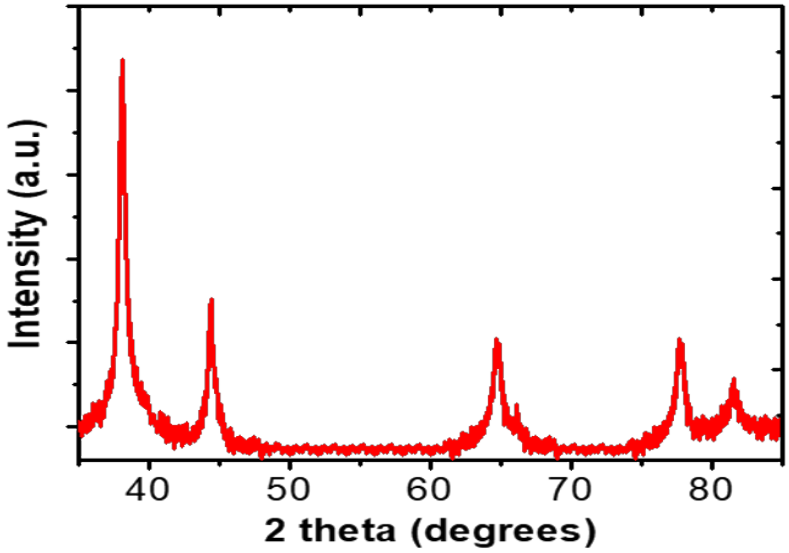

Fig. 2.6 XRD pattern of Brassica Ag-NPs demonstrating crystalline phase of nanosilver.

Moreover, from TEM analysis, size and surface morphologies was observed and it was revealed that both types of Ag-NPs were of spherical in shape (Figs. 2.7a and 2.7b). The sizes were ranged from 15-30 nm and 10-15 nm for Brassica and Com Ag-NPs, respectively. The size of Brassica Ag-NPs measured from the TEM analysis agreed with the crystallite size calculated from the XRD patterns.

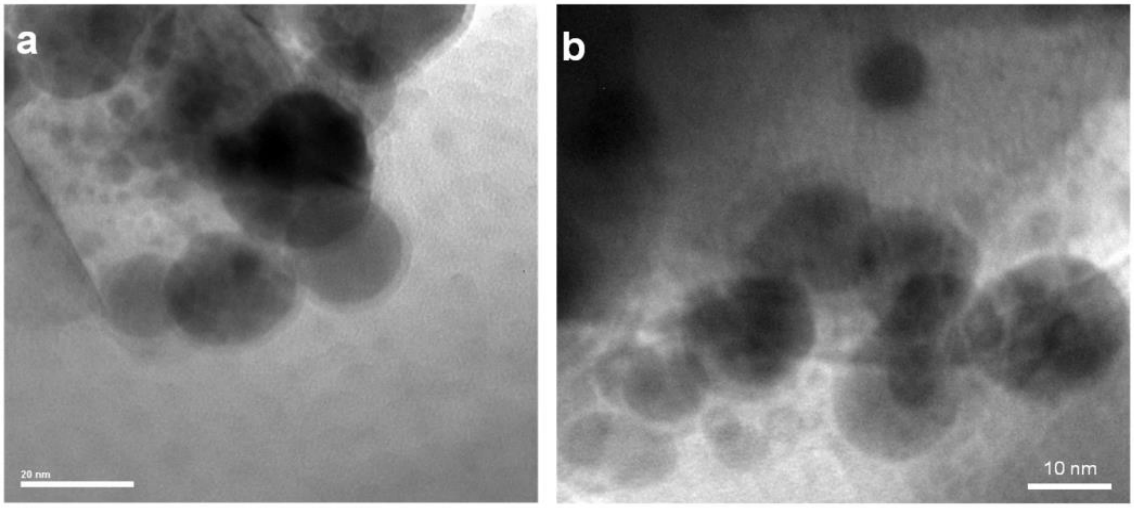

Fig. 2.7 TEM images of a Brassica Ag-NPs showing the spherical shaped NPs with the size of 15 to 30 nm and b Com Ag-NPs indicating the particle size of 10 to15 nm

The FT-IR spectra obtained for the *Brassica rapa* var. *Japonica* leaf aqueous extract and synthesized Ag-NPs between the wavenumber of 500-4000 cm^{-1} are shown in Fig. 2.8. From the FT-IR spectra obtained for the aqueous leaf extract, it can be seen that three strong peaks are appeared in the spectra at the wave number values of 1095, 1631 and 3452 cm^{-1}, respectively. These peaks are representing the stretching vibration bands of C–O–C, –C=O and –OH, respectively (Huang et al., 2007). Some weak peaks are also appeared at the values of 1375, 2852 and 2926 cm^{-1}, respectively. These peaks are indicating the stretching vibration bands of C-N of amine, N-H and C-H, respectively. From FT-IR spectrum obtained for synthesized Ag-NPs, it may be seen that four strong peaks are appeared in the spectra at the wavenumber values of 1099, 1382, 1631 and 3464 cm^{-1}, respectively, which are representing the stretching vibration bands of C–O–C, C-N of amine, –C=O and –OH, respectively. The weak peaks appeared at 2870 and 2954 cm^{-1} are indicating the stretching vibration bands of N-H and C-H, respectively (Yamamoto et al., 2004).

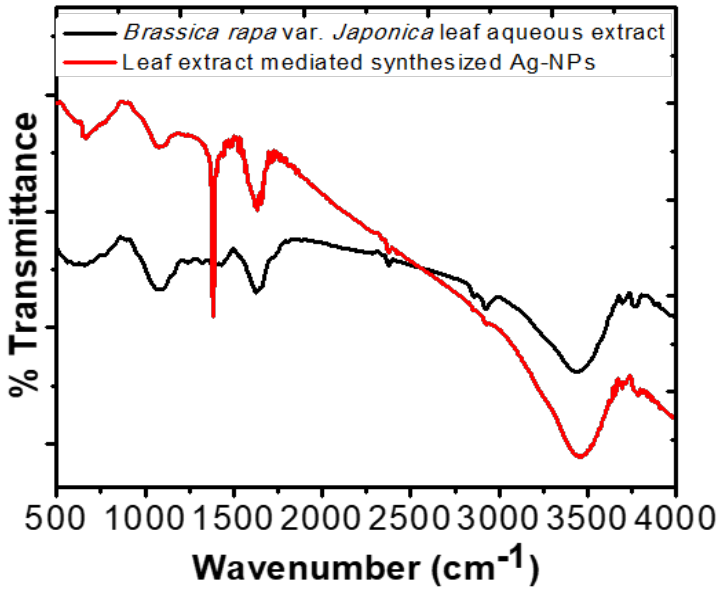

Fig. 2.8 FT-IR spectra of *Brassica rapa.* var *japonica* leaf aqueous extract and Brassica Ag-NPs

2.3.2 Stability assessment of Ag-NPs

1 µg/mL of both Brassica Ag-NPs and Com Ag-NPs suspension in deionized water were taken and release of ion was measured after 1 h and 24 h incubation under room temperature. Released silver ion from Brassica Ag-NPs was measured as 0.014 and 0.120 1µg/mL of

solution after 1 h and 24 h incubation, respectively whereas, with the same incubation, released silver ion was measured as 0.628 and 0.937 1 µg/mL respectively for Com Ag-NPs (Fig. 2.9).

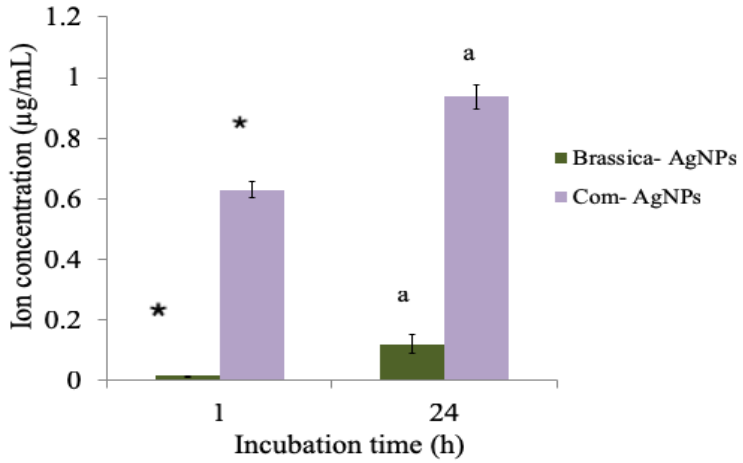

Fig. 2.9 Silver ion release from Brassica Ag-NPs and Com Ag-NPs after 1h and 24 h incubation. Error bars indicate mean ± SEM (n=3). Asterisk and a denote significant change from Com Ag-NPs to Brassica Ag-NPs at $p<0.05$

2.3.3 Cytotoxicity analysis of Ag-NPs

2.3.3.1 Cell viability assay

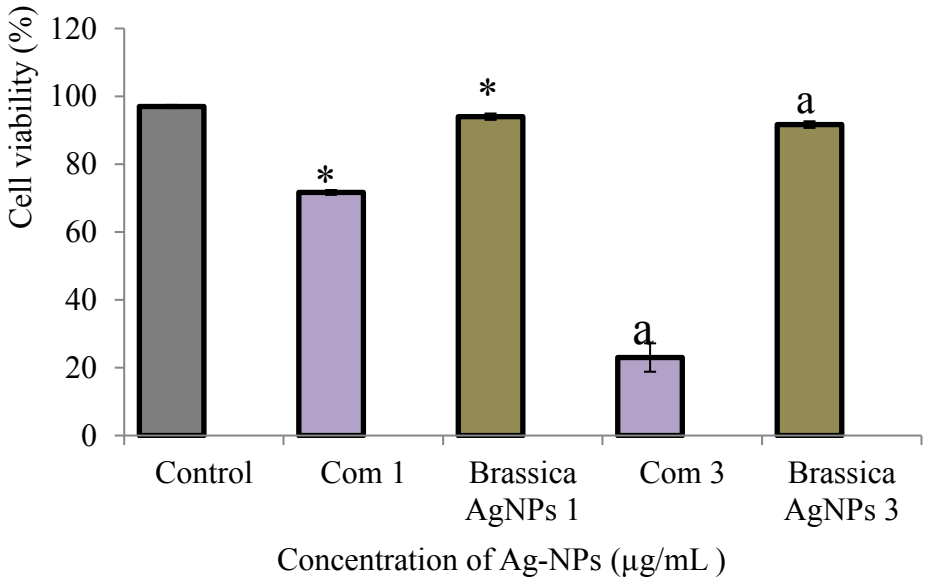

Fig.2.10 Cell viability of PC12 cells measured by trypan blue staining method with/without treated by Com Ag-NPs and Brassica Ag-NPs in two different concentrations (1 and 3 µg/mL) for 24 h of incubation. Control group contains cells with medium. Error bars indicate mean± S.E.M (n=3). Asterisk* and a denote significant change from com Ag-NPs to Brassica Ag-NPs at $p<0.05$

To assess the relative cytotoxicity of. Brassica and Commercial Ag-NPs (Com Ag-NPs), both types of NPs at two different concentrations of 1 and 3 µg/mL were exposed to PC12 cells. Then cell viability was measured by trypan blue exclusion method at 48 h after incubation with/without NPs exposures. In case of Com Ag-NPs, the viability was decreased to 70% and 20% for the treatment with 1 and 3 µg/mL of Brassica Ag-NPs (Fig. 2.10) whereas, no significant cell death was observed for Brassica Ag-NPs in the studied concentrations.

2.3.3.2 LDH assay

To confirm whether Brassica Ag-NPs have no cytotoxicity, LDH activity in the culture medium of PC12 cells treated with Brassica and Com Ag-NPs were measured. A significant difference of LDH activity between the Com Ag-NPs-treated group (1 and 3 µg/mL) and control group was observed but no significant change was observed between control group and Brassica Ag-NPs-treated groups. However, a significant difference was found between Com Ag-NPs and Brassica Ag-NPs in both applied concentrations (Fig. 2.11). The LDH activity results corroborated with the cell viability assay results. Therefore, both assays confirmed the Brassica Ag-NPs showed less cytotoxicity than the Com Ag-NPs in PC12 cells.

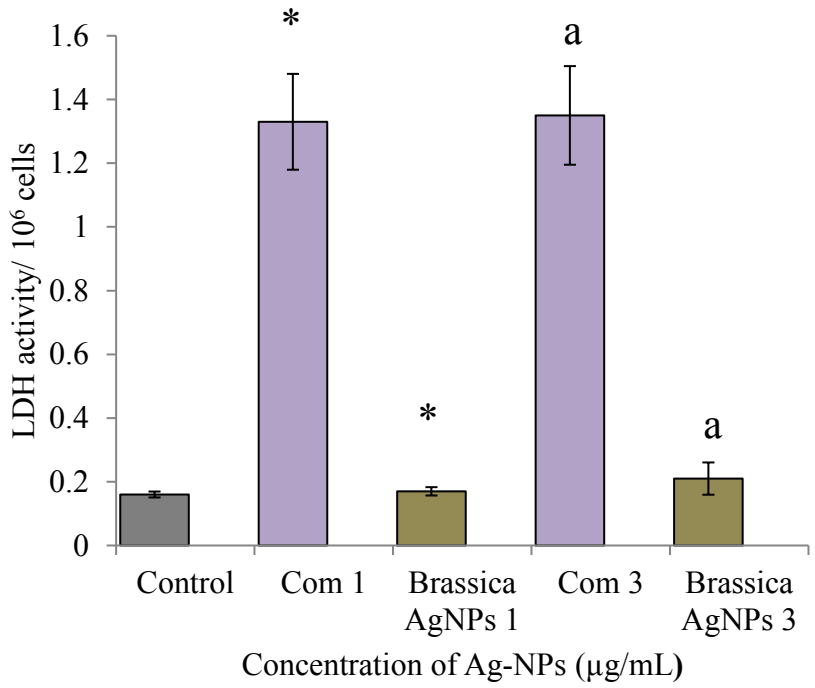

Fig. 2.11 LDH activity in the culture medium of PC12 cells after treatment with/without Com Ag-NPs and Brassica Ag-NPs after 48 h of incubation. Error bars indicate mean± S.E.M (n=3). Asterisk*and a denote significant change of LDH activity from Com Ag-NPs to Brassica Ag-NPs at $p<0.05$

2.3.4 Antibacterial activity analysis

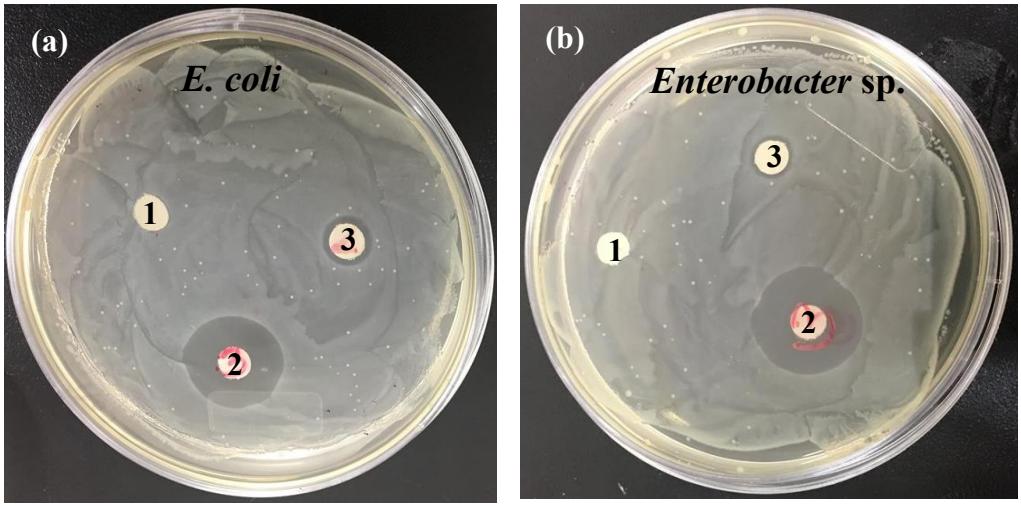

Fig. 2.12 Antibacterial activity of Brassica Ag-NPs against *E. coli* (a) and Enterobacter sp. (b) in terms of zone of inhibition at a concentration of 10 µg/mL. 1, 2 and 3 denote blank, Brassica Ag-NPs and amphicillin respectively. Amphicillin represents positive control and blank represents negative control as well.

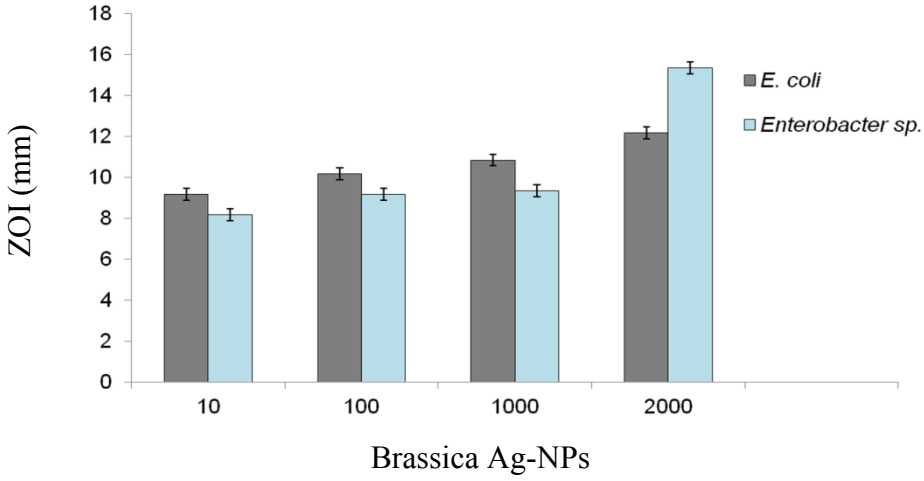

Fig. 2.13 Antibacterial activity of Brassica Ag-NPs against *E. coli* and *Enterobacter* sp. in terms of zone of inhibition (ZOI) at different concentrations. Error bars indicate mean± SD (n=3).

The antibacterial activity of Brassica Ag-NPs was assessed in terms of the zone of inhibition (ZOI) measurement against two-Gram negative bacteria, *E. coli* and *Enterobacter* sp. Amphicillin disc and blank disc were used as positive and negative controls, respectively. No effect on bacterial growth was found for the negative control whereas, the positive control

showed a clear ZOI. Using different concentrations (10 µg/mL) of Brassica Ag-NPs disc, a clear ZOI was detected for both of the *E. coli* (Fig. 2.12a) and *Enterobacter* sp. (Fig. 2.12b).

2.4. Discussion

The huge uses of Ag-NPs particularly, in cosmetics raise a grave concern for their toxicity (Hoet PHM et al., 2004). We have shown in our previous review study that Ag-NPs can induce toxicity in different cell lines (Akter et al., 2018). Consequently, to ensure the safe applications of Ag-NPs in consumer products it was aimed to establish a suitable synthesis method for Ag-NPs having less toxicity and high antibacterial activity; moreover, it was desirable that this development would be environmentally friendly and cost effective. In this study, for the synthesis of novel green Ag-NPs, $AgNO_3$ solution was taken as a precursor, and *Brassica rapa* var. *japonica* leaf extract was chosen as a source of reducing and capping agent.

A successful reduction of Ag^+ to Ag^o was visualized through the distinct change of colour from gray to reddish yellow due to Ag-NPs formation (Krishnaraj et al., 2010). It is well established that this reddish yellow colour arises, due to the excitation of Surface Plasmon Resonance (SPR) vibration occur in the Ag-NPs (Huang et al., 2007). Furthermore, from the UV–Vis. spectrometry, the formation of Ag-NPs in the Ag suspension was also evident. A strong peak was appeared at the wavelength of 420 nm indicating the presence of nano silver, resulted from the reduction of Ag^+ (Huang et al., 2007; Vadiraj KT, 2016). Moreover, in case of Com Ag-NPs, a broad peak was obtained at 509 nm.

The FESEM images depicted the presence of Ag-NPs with minimal agglomeration for both the Brassica Ag-NPs and Com Ag-NPs (Figs. 2.4a and 2.4b) which might be due to the presence of phytochemicals and sodium citrate that stabilized the particles, respectively (Sathishkumar et al., 2012). EDX spectra of Brassica Ag-NPs revealed the presence of Ag-NPs. Silver showed a signature peak at 3 keV (Fig. 2.5). Several weaker peaks were also found corresponding to materials containing carbon, oxygen and nitrogen, might be originated from *Brassica rapa* var. *japonica* leaf extract. Crystalline formation of newly synthesized Brassica Ag-NPs was further confirmed by XRD analysis. Five distinct characteristic peaks were observed at $2\theta = 38.04^{\circ}$, 44.24°, 64.4°, 77.24° and 81.48° corresponded to the planes 111, 200, 220, 311 and 222 respectively (Fig. 2.6), which were identified as face cantered cubic Ag in accordance with JCPDS card of Ag (JCPDS Card number 87-0597) (Hsueh et al., 2015). The value of lattice constant was calculated as 4.0904 Å which was in good agreement with the earlier work (4.077 Å) (Sagar et al., 2012).

The size and surface morphologies of both Brassica and Com Ag-NPs was assessed by TEM analysis. The TEM images showed that Ag-NPs were spherical in shape with smooth edges in both Brassica and Com Ag-NPs. The sizes of both Brassica and Com Ag-NPs were also measured as about 15-30 and 10-15 nm, respectively (Figs. 2.7a and 2.7b) which supported with the crystallite size calculated from the XRD patterns of Brassica Ag-NPs.

On comparing the FT-IR spectra obtained for the *Brassica rapa* var. *Japonica* leaf aqueous extract and synthesized Ag-NPs as shown in Fig. 2.8, it can be said that alike functional groups are existed both in the leaf extract and synthesized Ag NPs. But, the extents of the band intensities of the relevant peaks are different. It may be seen that the intensity of the stretching vibration modes of C=O and C-N are prominent than those of other groups in the synthesized Ag-NPs. Authors (Ashraf et al., 2016) have reported that –OH and –NH existing in the leaf powder act as a reducing agent and are capable of to reduce Ag^{+} ion to metallic nanosilver, i.e., nano Ag^{0}, in the ambient condition. On the other hand, heterocyclic compounds like alkaloids and flavones which show strong stretching bands of C–O–C and –C=O in FT-IR act as capping agent of NPs (Huang et al., 2007). In the present study, the functional groups relevant to reduction of Ag^{+} to Ag^{o} and capping of Ag-NPs are found to be in place both in the leaf extract and Ag-NPs. It may be speculated that amides present in the *Brassica rapa* var. *Japonica* leaf aqueous extract and its intense presence in the NPs kept additional contribution in the present Ag-NPs synthesis.

From the stability assay performed by AAS analysis it was found that Brassica Ag-NPs showed more stability than Com Ag-NPs which agreed with the results of XRD, EDX and FT-IR analyses. This might be due to the crystalline nature of Brassica Ag-NPs, confirmed from the XRD patterns and due to the presence of capping agent on Brassica Ag-NPs confirmed from the EDX and FT-IR analyses.

To evaluate the comparative cytotoxicity of Brassica and Com Ag-NPs, both types of NPs were exposed to PC12 cells, a widely used model cell line for toxicity assessment. It is reported that commercially synthesized Ag-NPs induce toxicity in different cell lines, e.g., HeLa, U937 (Kaba and Egorova, 2015), and human hepatoma cell line (Kim et al., 2009). In our study, Com Ag-NPs showed a significant decrease of cell viability of PC12 whereas, no significant change was observed for Brassica Ag-NPs in 1 and 3 µg/mL (Fig. 2.10). It was reported that 7-20 nm sized Com Ag-NPs showed toxicity on A431 cell line where toxicity threshold was measured at 1.56 µg/mL (Arora et al., 2008). However, 15-25 nm size of Brassica Ag-NPs did not show any toxic effect on PC12 cells for the exposure dose of 1 and 3 µg/mL.

LDH activity measurements (Fig. 2.10) supported the same manner for Com Ag-NPs (showing toxicity) and Brassica Ag-NPs (showing no toxicity) compared as cell viability experiments. LDH activity determines cell membrane integrity (Hussain et al., 2005), therefore, increased trend of LDH activity was a sign of more cell damage in response to toxic effects. Recently different biogenic materials have been used for Ag-NPs synthesis. In Table-2.1, we compared cytotoxic effect of Brassica Ag-NPs with various source mediated green synthesised Ag-NPs. Ag-NPs synthesized from *Albizia adianthifolia* (Gengan et al., 2013), *S. grandiflora* leaf extract (Jeyaraj et al., 2013) and watermelon rind extract (Velmurugan et al., 2016) induce toxicity in different cell line at a concentration of 10, 5 and 4 µg/mL respectively.

Table 2.1 Effect of Ag-NPs on cell viability obtained from different sources

Source	Cell line	Conc. (µg/mL)	Viability (%)	References
Albizia adianthifolia	A549	10	79	(Gengan et al., 2013)
S. grandiflora leaf extract	MCF-7	5	50	(Jeyaraj et al., 2013)
Humicola sp.	NIH3T3	250	79.17	(Syed et al., 2013)
Humicola sp	MDA-MB-231	250	57.82	(Syed et al., 2013)
Watermelon rind extract	Rat splenocytes	4	67	(Velmurugan et al., 2014)
Chitosan	HEHEK293	15.07	50	(Noghabi et al., 2017)
Commercial Ag-NPs (<150nm)	RAW 264.7	1.6	70	(Park et al., 2010)
Commercial Ag-NPs (13.5nm)	HeLA	2	20	(Kaba and Egorova, 2015)
Commercial Ag-NPs (13.5nm)	U937	2	10	(Kaba and Egorova, 2015)

Comparing to those green synthesized Ag-NPs, Brassica Ag-NPs showed less toxicity than other phytosynthesized Ag-NPs, but chitosan (Noghabi et al ., 2017) and fungi (Syed et al., 2013) synthesized Ag-NPs appeared less toxic than any other phytosynthesized Ag-NPs. In addition, commercial Ag-NPs showed severe toxicity comparing green synthesised Ag-NPs (Renugadevi et al., 2012). The mechanism behind the cytoxicity of Ag-NPs is remained contradictory, however, it is speculated that, Ag-NPs induce cytotoxicity through troazan horse type mechanism, favouring the ionization of NPs inside the cell is the initiator of different toxicity inducing pathway (Akter et al., 2018). Thus, stability of NPs might be a fact of toxicity issue. In this study, we found that Com Ag-NPs are less stable than Brassica Ag-NPs, suggesting more ionization tendency of Com Ag-NPs resulting to more toxicity.

Therefore, ionized silver easily induce toxicity by initiating toxicity inducing pathway. However, the actual mechanism of toxicity of Ag-NPs is needed to be further study.

Potentiality of green synthesized Ag-NPs as antibacterial and antifungal agents is highlighted in the previous reports (Velmurugan et al., 2014). Consequently, prior to use Ag-NPs as an antibacterial agent, it is highly required to evaluate their antibacterial activity. In our study, antibacterial activity of Brassica Ag-NPs was evaluated by determining their activity against *E. coli* and *Enterobacter* sp. Brassica Ag-NPs showed potential antibacterial activity against both *E. coli* (Fig. 2.11) and *Enterobacter* sp. (Fig. 2.12) at the lowest concentration of 10 ppm. It was also reported earlier that Ag-NPs synthesized from green synthesis routes showed antibacterial activities against *E. coli and Enterobacter* sp. as listed in Table 2.2. Ag-NPs synthesized using the extracts of *Azadirachta indica,* Capsicum and tea leaf showed zones of inhibition against *E. coli* which were recorded as 9 mm (Renugadevi et al., 2012), 10 mm (Abdullah and Hamid, 2013) and 0.5 mm (Sun et al., 2014), respectively, while Ag-NPs synthesized using *Brassica rapa* var. *japonica* leaf extract showed higher antibacterial ability as compared with them. However, green synthesized Ag-NPs using phlomis leaf extract and penicillin showed almost equivalent antibacterial activity against *E. coli* (Allafchian et al., 2016*;* Maliszewska et al., 2009). Moreover, *Azadirachta indica* mediated Ag-NPs induce 6 mm zone of inhibition against *Enterobacter* sp. (Renugadevi et al., 2012) whereas, *Brassica rapa* var. *japonica* leaf extract mediated Ag-NPs induced 9-15 mm zone of inhibition at different concentrations (Fig.11). Eventually, in comparison with some other reported green synthesized Ag-NPs, it is clear that *Brassica rapa* var. *japonica* mediated Ag-NPs was confirmed to be excellent antibacterial ability.

Table 2.2: Various green synthesized Ag-NPs induced zone of inhibition against *E. coli* and *Enterobacter* sp.

Microorganism	Extracted substances	Zone of inhibition (mm)	References
E. coli	*Azadirachta indica*	9	(Renugadevi et al., 2012)
Enterobacter sp.	*Azadirachta indica*	6	(Renugadevi et al., 2012)
E. coli	Phlomis leaf	15.1	(Allafchian et al., 2016)
E. coli	Tea leaf extract	0.5	(Sun et al., 2014)
E. coli	Capsicum	10	(Abdullah and Hamid, 2013)
E. coli	Penicillin	14	(Maliszewska et al., 2009)

Exact mechanism behind antibacterial activity of Brassica Ag-NPs is still unclear. Therefore, we assume a three steps antibacterial mechanism for our synthesized Ag-NPs which is also supported by Morones et al (Morones et al., 2005). At first, sufficiently small diameter Ag-NPs were attached to the cell wall of the bacteria, where Ag-NPs were interacted with bacterial cell wall and subsequently disrupted their proper function like permeability and respiration. Then Ag-NPs were entered inside the bacteria caused further damage by the interaction with sulfur and phosphorus containing compounds and destroyed their activity. Thus, Ag-NPs could interact with DNA which eventually hampered their replication ability resulting of initiation of cell death (Fig. 2.14). Further investigation would be needed to clarify the precise mechanism of antibacterial activity caused by Brassica Ag-NPs.

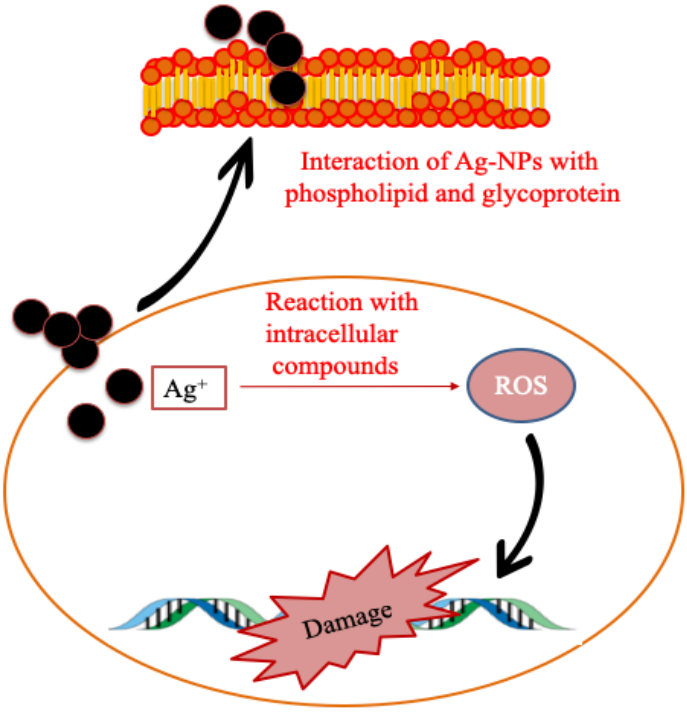

Fig. 2.14 Schematic diagram of Probable mechanism of interaction between bacteria and Ag-NPs

2.5. Conclusion

It is the first report of Ag-NPs showing less toxicity and high antibacterial activity, where *Brassica rapa* var. *nipposinica/ Japonica* was used as a reducing and capping agent for the synthesis of Ag-NPs. Crystalline phased Brassica Ag-NPs showed less toxicity than Com Ag-NPs on PC12 cells. Moreover, at the same concentration, Brassica Ag-NPs showed excellent potentiality of antibacterial activity against gram negative bacteria, *E. cloi* and

Enterobacter sp. in comparison with some other reported green synthesised Ag-NPs. The less cytotoxic activity of Brassica Ag-NPs might be due to their stability, which was for the presence of capping agent on Ag-NPs provided by *Brassica rap* var. *japonica*. Therefore, easy and cost-effective Brassica Ag-NPs could be a potential candidate for their safe use in consumer products.

References

Abdullah, A., Hamid, Z., 2013. Antimicrobial activity of Silver nanoparticles from Capsicum sp. against Staphylococcus sp., Bacillus sp., Pseudomonas sp. and Escherichia coli. J. Biol. Agric. Healthc. 3, 67–72.

Akter, M., Sikder, M.T., Rahman, M.M., Ullah, A.K.M.A., Hossain, K.F.B., Banik, S., Hosokawa, T., Saito, T., Kurasaki, M., 2018. A systematic review on silver nanoparticles-induced cytotoxicity: Physicochemical properties and perspectives. J. Adv. Res. 9, 1–16. https://doi.org/10.1016/j.jare.2017.10.008

Alam, H.M.B., Das, R., Shajahan, M., Atique Ullah, A.K.M., Kibria, A.K.M.F., 2017. Surface characteristics and electrolysis efficiency of a Palladium-Nickel electrode. Int. J. Hydrogen Energy 43, 1998–2008. https://doi.org/10.1016/j.ijhydene.2017.12.027

Allafchian AR, Mirahmadi-Zare SZ, Jalali SAH, Hashemi SS, V.M., 2016. Green synthesis of silver nanoparticles using phlomis leaf extract and investigation of their antibacterial activity. J. Nanostructure Chem. 6, 129–135.

Arora, S., Jain, J., Rajwade, J.M., Paknikar, K.M., 2008. Cellular responses induced by silver nanoparticles: In vitro studies. Toxicol. Lett. 179, 93–100. https://doi.org/10.1016/j.toxlet.2008.04.009

Ashraf, J.M., Ansari, M.A., Khan, H.M., Alzohairy, M.A., Choi, I., 2016. Green synthesis of silver nanoparticles and characterization of their inhibitory effects on AGEs formation using biophysical techniques. Sci. Rep. 6, 1–10. https://doi.org/10.1038/srep20414

Atique Ullah, A.K.M., Fazle Kibria, A.K.M., Akter, M., Khan, M.N.I., Tareq, A.R.M., Firoz, S.H., 2017. Oxidative Degradation of Methylene Blue Using Mn3O4 Nanoparticles. Water Conserv. Sci. Eng. 1, 249–256. https://doi.org/10.1007/s41101-017-0017-3

Chandran, S.P., Chaudhary, M., Pasricha, R., Ahmad, A., Sastry, M., 2006. Synthesis of gold nanotriangles and silver nanoparticles using Aloe vera plant extract. Biotechnol. Prog. 22, 577–583. https://doi.org/10.1021/bp0501423

Edberg SC, Rice EW, Karlin RJ, A.M., 2000. Escherichia coli: the best biological drinking water indicator for public health protection. Appl Microbiol 88, 1068–1168.

Gajbhiye Swati, S.S., 2016. Silver Nanoparticles in Cosmetics. J. Cosmet. Dermatological Sci. Appl. 6, 48–53. https://doi.org/10.4236/jcdsa.2016.61007

Gardea-Torresdey, J.L., Gomez, E., Peralta-Videa, J.R., Parsons, J.G., Troiani, H., Jose-Yacaman, M., 2003. Alfalfa sprouts: A natural source for the synthesis of silver nanoparticles. Langmuir 19, 1357–1361. https://doi.org/10.1021/la020835i

Gengan, R.M., Anand, K., Phulukdaree, A., Chuturgoon, A., 2013. A549 lung cell line activity of biosynthesized silver nanoparticles using Albizia adianthifolia leaf. Colloids Surfaces B Biointerfaces 105, 87–91. https://doi.org/10.1016/j.colsurfb.2012.12.044

Guzmán MG, Dille J, G.S., 2009. Synthesis of silver nanoparticles by chemical reduction method and their antibacterial activity. Int. J. Chem. Biomol. Eng. 2, 114–111.

Hoet PHM, Bruske-Hohlfeld I, S.O., 2004. Nanoparticles- known and unknown health risks. J. Nanobitechnology 2, 1–15.

Hsueh, Y.H., Lin, K.S., Ke, W.J., Hsieh, C. Te, Chiang, C.L., Tzou, D.Y., Liu, S.T., 2015. The antimicrobial properties of silver nanoparticles in bacillus subtilis are mediated by released Ag+ ions. PLoS One 10, 1–17. https://doi.org/10.1371/journal.pone.0144306

Huang, J., Li, Q., Sun, D., Lu, Y., Su, Y., Yang, X., Wang, H., Wang, Y., Shao, W., He, N., Hong, J., Chen, C., 2007. Biosynthesis of silver and gold nanoparticles by novel sundried Cinnamomum camphora leaf. Nanotechnology 18, 1–11. https://doi.org/10.1088/0957-4484/18/10/105104

Hussain, S.M., Hess, K.L., Gearhart, J.M., Geiss, K.T., Schlager, J.J., 2005. In vitro toxicity of nanoparticles in BRL 3A rat liver cells. Toxicol. Vitr. 19, 975–983. https://doi.org/10.1016/j.tiv.2005.06.034

Jagtap UB, B.V., 2013. Biosynthesis, characterization and antibacterial activity of silvernanoparticles by aqueous Annona squamosa L. Leaf extract at room temperature. J. Plant Biochem. Biotechnol. 22, 434–440.

Jeyaraj, M., Sathishkumar, G., Sivanandhan, G., MubarakAli, D., Rajesh, M., Arun, R., Kapildev, G., Manickavasagam, M., Thajuddin, N., Premkumar, K., Ganapathi, A., 2013. Biogenic silver nanoparticles for cancer treatment: An experimental report. Colloids Surfaces B Biointerfaces 106, 86–92. https://doi.org/10.1016/j.colsurfb.2013.01.027

Jiang C,Yuan Y, Hu F, Wang Q, Z.K.W.Y. et al, 2014. Cadmium induces PC12 cells apoptosis via an extracellular signal-related kinase and c-jun N-terminal kinase-mediated mitochondrial apoptotic pathway. Biol. Trace Elem. Res 158, 249–258.

Joseph W. Chow, Victor L. Yu, D.M.S., 1994. Epidemiologic perspectives on Enterobacter for the infection control professional. Am J Infect Control 22, 195–201.

Kaba, S.I., Egorova, E.M., 2015. In vitro studies of the toxic effects of silver nanoparticles on HeLa and U937 cells. Nanotechnol. Sci. Appl. 8, 19–29. https://doi.org/10.2147/NSA.S78134

Kahrilas GA, Wally LM, Fedrick SJ, Hiskey M, Prieto AL, J.E., 2014. Microwave–Assisted Green Synthesis of Silver Nanoparticles Using Orange Peel Extract. ACS Sustain. Chem 2, 367–376.

Khanam, U.K.S., Oba, S., Yanase, E., Murakami, Y., 2012. Phenolic acids, flavonoids and total antioxidant capacity of selected leafy vegetables. Journa of functional foods. 4.979-987

Kim, S., Choi, J.E., Choi, J., Chung, K.H., Park, K., Yi, J., Ryu, D.Y., 2009. Oxidative stress-dependent toxicity of silver nanoparticles in human hepatoma cells. Toxicol. Vitr. 23, 1076–1084. https://doi.org/10.1016/j.tiv.2009.06.001

Kim, S.H., Lee, H.S., Ryu, D.S., Choi, S.J., Lee, D.S., 2011. Antibacterial activity of silver-nanoparticles against Staphylococcus aureus and Escherichia coli. Korean J. Microbiol. Biotechnol. 39, 77–85. https://doi.org/10.5897/AJMR2016.7908

Kokura, S., Handa, O., Takagi, T., Ishikawa, T., Naito, Y., Yoshikawa, T., 2010. Silver nanoparticles as a safe preservative for use in cosmetics. Nanomedicine Nanotechnology, Biol. Med. 6, 570–574. https://doi.org/10.1016/j.nano.2009.12.002

Kreilgaard, M., 2002. Influence of microemulsions on cutaneous drug delivery. Adv. Drug Deliv. Rev. 54. https://doi.org/10.1016/S0169-409X(02)00116-3

Krishnaraj, C., Jagan, E.G., Rajasekar, S., Selvakumar, P., Kalaichelvan, P.T., Mohan, N., 2010. Synthesis of silver nanoparticles using Acalypha indica leaf extracts and its antibacterial activity against water borne pathogens. Colloids Surfaces B Biointerfaces 76, 50–56. https://doi.org/10.1016/j.colsurfb.2009.10.008

Maliszewska I, S.Z., 2009. Synthesis and antibacterial activity of silver nanoparticels. J. Phys. 146. https://doi.org/10.1088/1742-6596/146/1/012024

Morones JR, Elechifuerra AC, Holt K, Kouri JB, Ramirez JT, Y.M., 2005. The bacterial effect of silver nanoparticles. Nanotechnology 16, 2346–53.

Mytych, J., Zebrowski, J., Lewinska, A., Wnuk, M., 2016. Prolonged Effects of Silver Nanoparticles on p53/p21 Pathway-Mediated Proliferation, DNA Damage Response, and Methylation Parameters in HT22 Hippocampal Neuronal Cells. Mol. Neurobiol. 54, 1285–1300. https://doi.org/10.1007/s12035-016-9688-6

Narayanamma, A., 2016. Natural Synthesis of Silver Nanoparticles by Banana Peel Extract and as an Antibacterial Agent. IOSR J. Polym. Text. Eng. 3, 17–25. https://doi.org/10.9790/019X-03011725

Noghabi MP, Parizadeh MR, Mobarhan MG ,Taherzadeh D, D.H., 2017. Green synthesis of silver nanoparticles and investigation of their colorimetric sensing and cytotoxicity effects. J Mol Struct 1146, 499–503.

Park, E.J., Yi, J., Kim, Y., Choi, K., Park, K., 2010. Silver nanoparticles induce cytotoxicity by a Trojan-horse type mechanism. Toxicol. Vitr. 24, 872–878. https://doi.org/10.1016/j.tiv.2009.12.001

Prow, T.W., Grice, J.E., Lin, L.L., Faye, R., Butler, M., Becker, W., Wurm, E.M.T., Yoong, C., Robertson, T.A., Soyer, H.P., Roberts, M.S., 2011. Nanoparticles and microparticles for skin drug delivery. Adv. Drug Deliv. Rev. 63, 470–491. https://doi.org/10.1016/j.addr.2011.01.012

Rahman, M.M., Ukiana, J., Uson-Lopez, R., Sikder, M.T., Saito, T., Kurasaki, M., 2017. Cytotoxic effects of cadmium and zinc co-exposure in PC12 cells and the underlying mechanism. Chem. Biol. Interact. 269, 41–49. https://doi.org/10.1016/j.cbi.2017.04.003

Rahman, M.M., Uson-Lopez, R.A., Sikder, M.T., Tan, G., Hosokawa, T., Saito, T., Kurasaki, M., 2018. Ameliorative effects of selenium on arsenic-induced cytotoxicity in PC12 cells via modulating autophagy/apoptosis. Chemosphere 196, 453–466. https://doi.org/10.1016/j.chemosphere.2017.12.149

Renugadevi K, A.R., 2012. Microwave irradiation assisted synthesis of silver nanoparticle using Azadirachta indica leaf extract as a reducing agent and invitro evaluation of its antibacterial and anticancer activity. Int. J. Nanomater. Biostructures 2, 5–10.

Roopan, S.M., Rohit, Madhumitha, G., Rahuman, A.A., Kamaraj, C., Bharathi, A., Surendra, T. V., 2013. Low-cost and eco-friendly phyto-synthesis of silver nanoparticles using

Cocos nucifera coir extract and its larvicidal activity. Ind. Crops Prod. 43, 631–635. https://doi.org/10.1016/j.indcrop.2012.08.013

Rouse, J.G., Yang, J., Ryman-Rasmussen, J.P., Barron, A.R., Monteiro-Riviere, N.A., 2007. Effects of mechanical flexion on the penetration of fullerene amino acid-derivatized peptide nanoparticles through skin. Nano Lett. 7, 155–160. https://doi.org/10.1021/nl062464m

Sagar, G., Bhosale, A,. 2012. Green synthesis of silver nanoparticles using Aspergillus niger and itsefficacy against human pathogenes. Eur. J.Exp. Bio. 2, 1654-1658

Sahin Fusun Hasturk , Aktas Turkan , Acikgoz Funda Eryilmaz, A.T., 2016. Some Technical and Mechanical Properties of 3 Mibuna (Brassica rapavar. Nipposinica) and Mizuna (Brassica rapa var. japonica). Peer J Prepr. 80–83.

Sambale, F., Wagner, S., Stahl, F., Khaydarov, R.R., Scheper, T., Bahnemann, D., 2015. Investigations of the toxic effect of silver nanoparticles on mammalian cell lines. J. Nanomater. 2015. https://doi.org/10.1155/2015/136765

Saravanan, M., Vemu, A.K., Barik, S.K., 2011. Rapid biosynthesis of silver nanoparticles from bacillus megaterium (ncim 2326) and their antibacterial activity on multi drug resistant clinical pathogens. Colloids Surfaces B Biointerfaces 88, 325–331. https://doi.org/10.1016/j.colsurfb.2011.07.009

Sathishkumar, G., Gobinath, C., Karpagam, K., Hemamalini, V., Premkumar, K., Sivaramakrishnan, S., 2012. Phyto-synthesis of silver nanoscale particles using Morinda citrifolia L. and its inhibitory activity against human pathogens. Colloids Surfaces B Biointerfaces 95, 235–240. https://doi.org/10.1016/j.colsurfb.2012.03.001

Starowicz M, Stypula B, B.J., 2006. Electrochemical synthesis of silver nanoparticles. Electrochem. commun. 8, 227–230.

Sun, Q., Cai, X., Li, J., Zheng, M., Chen, Z., Yu, C.P., 2014. Green synthesis of silver nanoparticles using tea leaf extract and evaluation of their stability and antibacterial activity. Colloids Surfaces A Physicochem. Eng. Asp. 444, 226–231. https://doi.org/10.1016/j.colsurfa.2013.12.065

Syed, A., Saraswati, S., Kundu, G.C., Ahmad, A., 2013. Biological synthesis of silver nanoparticles using the fungus Humicola sp. And evaluation of their cytoxicity using normal and cancer cell lines. Spectrochim. Acta - Part A Mol. Biomol. Spectrosc. 114, 144–147. https://doi.org/10.1016/j.saa.2013.05.030

Ullah, A.K.M.A., Kibria, A.K.M.F., Akter, M., Khan, M.N.I., Maksud, M.A., Jahan, R.A., Firoz, S.H., 2017. Synthesis of Mn3O4nanoparticles via a facile gel formation route and study of their phase and structural transformation with distinct surface morphology upon heat treatment. J. Saudi Chem. Soc. 21, 830–836. https://doi.org/10.1016/j.jscs.2017.03.008

Ullah, A.K.M.A., Kabir, M.F., Akter, M., Tamanna, A.N., Hossain, A., Tareq, A.R.M., Khan, M.N.I., Kibria, A.K.M.F., Kurasaki, M., Rahman, M.M., 2018. Green synthesis of bio-molecule encapsulated magnetic silver nanoparticles and their antibacterial activity. RSC Advances. 8: 37176-37183

Vadiraj KT, belagali S., 2016. Synthesis and optical characterization of nickel doped zinc sulphide without capping agent. j Mater Sci Mater Electron 27, 2885–2889.

Velmurugan P, Hong SC, Aravinthan A, Jang SH, Yi PI, Song YC et al., 2016. comparison of the physical characteristics of green synthesized and commercial silver nanoparticales: Evaluaiton of antimicrobial and cytotoxic effects. Arab. J. Sci. Eng. 42, 201–208.

Velmurugan, P., Iydroose, M., Mohideen, M.H.A.K., Mohan, T.S., Cho, M., Oh, B.T., 2014. Biosynthesis of silver nanoparticles using Bacillus subtilis EWP-46 cell-free extract and evaluation of its antibacterial activity. Bioprocess Biosyst. Eng. 37, 1527–1534. https://doi.org/10.1007/s00449-014-1124-6

Xu, H., Zeiger, B.W., Suslick, K.S., 2013. Sonochemical synthesis of nanomaterials. Chem. Soc. Rev. 42, 2555–2567. https://doi.org/10.1039/c2cs35282f

Yamamoto, Y., Miura, T., Suzuki, M., Kawamura, N., Miyagawa, H.,zNakamura, T., Kobayashi, K., Teranishi, T., Hori, H., 2004. Direct observation of ferromagnetic spin polarization in gold nanoparticles. Physical Review Letters. 93, 116801 (1-4)

Yang, F., Zhao, M., Zheng, B., Xiao, D., Wu, L., Guo, Y., 2012. Influence of pH on the fluorescence properties of graphene quantum dots using ozonation pre-oxide hydrothermal synthesis. J. Mater. Chem. 22, 25471–25479. https://doi.org/10.1039/c2jm35471cc

Chapter 3

Bio-molecule encapsulation of silver nanoparticles via a facile green synthesis approach: an effect of temperature

Abstract

The synthesis of Ag-NPs was performed at four different reaction temperatures 25 °C (room temperature), 60, 80, and 100 °C in order to find the effect of reaction temperature on the particles' size and encapsulation. The synthesized Ag-NPs were characterized using UV-vis. spectrophotometer, X-ray diffractometer (XRD), transmission electron microscope (TEM), and dynamic light scattering (DLS) techniques. The characterization of the synthesized materials indicates that Ag-NPs synthesized at 60 °C resulted in the particles of the highest size. The increase of the particle size was due to the aggregation of Ag-NPs resulting from the increase in the rate of nucleation. In contrast, particles synthesized at 100 °C yielded to the formation of Ag-NPs with the lowest size which was due to the encapsulation of the particles. The encapsulation of Ag-NPs obstructs the aggregation of Ag-NPs. Thus, the reaction temperature was found to play an important role for the encapsulation of Ag-NPs where bio-molecules present in the *Brassica rapa* var. *japonica* leaf participated in the encapsulation

3.1. Introduction

Silver nanoparticles (Ag-NPs) have drawn a remarkable interest to the researchers due to their wide range of potential technological applications in medicine, medicinal devices, pharmacology, biotechnology, electronics, engineering, magnetic fields, and environmental remediation (Yu et al., 2013). In our previous review, we briefly summarized the enormous applications of Ag-NPs which elevate them one of the most important and demandable materials (Akter et al., 2018, Edward et al., 2009). It is noteworthy to mention that, the surface enhanced Raman scattering (SERS) made Ag-NPs superior over other metal NPs (Kneipp et al., 2006). Consequently, in recent past significant research efforts have been grown up on Ag-NPs synthesis (Bruchez et al., 2013).

Ag-NPs are generally synthesized employing physical, chemical, and sonochemical processes (Hangxum et al., 2013). In most of the cases, these synthesis processes require toxic chemicals which are detrimental to human health as well as environment. Eventually, there is a growing need of developing eco-friendly synthesis process of Ag-NPs, and green synthesis might be a solution of environmentally benign Ag-NPs synthesis. Green synthesis of Ag-NPs

possesses the highest advantages over the other types of syntheses because it is eco-friendly, cheaper, convenient, single step method, and does not require high pressure, energy, and toxic chemical (Prathna et al., 2011, Sintubin et al., 2011).

The surface morphology of NPs plays a vital role to their multi-purpose applications. Numerous researches have been reported with a wide range of variation of surface morphology such as tetrahedral (Zhou et al., 2008), bipyramids (Wiley et al., 2006), cubes (Sun et al., 2002), disks (Mailard et al., 2003) decahedra (Gao et al., 2006), hexagons (An et al., 2007), triangular (Jin et al., 2001), octahedrons (Tao et al., 2006), rods (Pietrobon et al., 2008), and wires (Caswell et al., 2003). To synthesize colloidal Ag-NPs, mainly two major approaches such as direct chemical reduction and photochemical approaches are established. In the photochemical process, the reaction can easily be terminated by the removal of light irradiation which made it superior over the other process. Light absorbed by the system can create a hot electron which reduces the Ag^{+} for the formation of Ag^{0} and a hot hole in order to oxidize the citrate ion on the surface resulting to shape transformation (Caswell et al., 2003). It is reported that the rate of reaction or even the ratios of branching can be controlled by changing the reaction temperature in the thermal reduction process (Shan et al., 2014). However, a very little study has been reported on temperature-dependent green synthesis of Ag-NPs. To the best of our knowledge first time, we are reporting temperature dependent Mizuna (*Brassica rapa* var. *nipposinica / japonica)* leaf extract mediated green synthesis of Ag-NPs and its effect on the surface morphology of the NPs.

In our previous study, we have synthesized Ag-NPs using Mizuna leaf extract as a reducing agent and $AgNO_3$ solution as a precursor at room temperature. In the present study, we hypothesized that the variation of synthesis temperature may result in a morphological change of the particles. Thus, with the continuation of our previous study it was aimed to synthesis of Ag-NPs with the variation of synthesis temperature in the present study and assesses the morphological change with the encapsulation of Ag-NPs.

3.2. Materials and methods

3.2.1 Materials

Silver nitrate ($AgNO_3$) and Ethanol (C_2H_5OH) were purchased from Wako pure chemical industries (Osaka, Japan). Mizuna plants were collected locally from Sappporo, Japan. All the reagents and chemicals used in the synthesis and characterization of the synthesized Ag-NPs were of analytical grade.

3.2.2 Synthesis of Ag-NPs

Ag-NPs were synthesized at four different reaction temperatures 25 (room temperature), 60, 80, and 100 °C. The room temperature synthesis of Ag-NPs was carried out following our previously reported procedure (Akter et al., 2018) which is described in Chapter 2. In addition, the three other temperature dependent synthesis of Ag-NPs was performed just by varying the reaction temperature.

3.2.3 Characterization of Ag-NPs

The synthesized Ag-NPs were characterized by UV-vis. spectroscopy, energy dispersive X-ray (EDX) spectroscopy, X-ray diffraction (XRD), and transmission electron microscopy (TEM) analyses. All these techniques were described in Chapter 2. The distribution of particle size synthesized by varying the reaction temperature was performed by using a dynamic light scattering (DLS) instrument (Microtract Version 11.1.1-246W). Approximately 50 mg of Ag-NPs were added into 1L of ethanol to measure the particle size distribution.

3.3. Results

Ag-NPs were synthesized using $AgNO_3$ solution as a precursor and Mizuna leaf aqueous extract as a reducing and capping agent. To analyze the effect of reaction temperature on the surface encapsulation, Ag-NPs were synthesized at four different reaction temperatures 25 (room temperature), 60, 80, and 100 °C. After adding 10mL of leaf extract into 100mL of 1mM $AgNO_3$ solution with controlled temperature, the solution of $AgNO_3$ was turned from gray to reddish yellow confirming the formation of nano silver (Krishnaraj et al., 2010). The change of colour was visualized at different temperatures for the the variation of reaction temperature which was observed within 50, 20, 10, and 5 min for the reaction temperatures of 25, 60, 80, and 100 °C respectively. When the color of the reaction mixture was turned from gray to reddish yellow, UV-vis spectroscopy measurement was performed to confirm the formation of Ag^0 from Ag^+. It is reported that due to the surface plasmon resonance, Ag-NPs give UV-vis. absorption maxima at a wavelength of 400-500 nm (Ashraf et al., 2016). In the present study, four different absorption maxima of wavelengths 425, 427, 420, and 418 nm were obtained for the Ag-NPs synthesized at four different reaction temperatures of 25, 60, 80, and 100 °C respectively as shown in Fig. 3.1

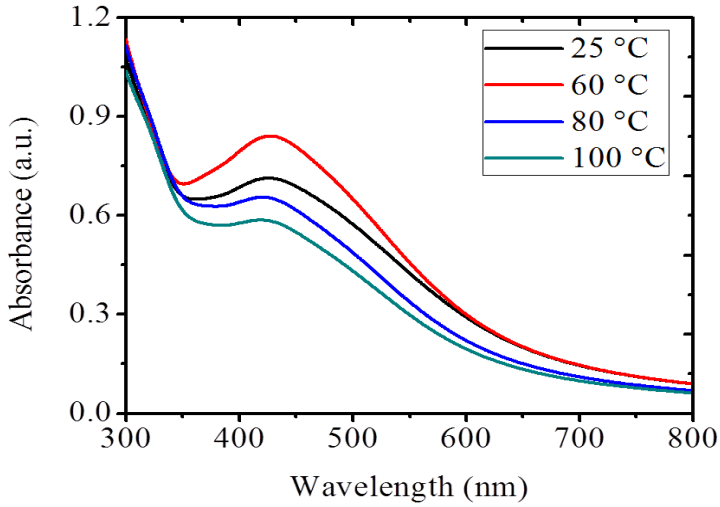

Fig. 3.1 UV- Vis. absorption spectra of Ag-NPs. Ag-NPs show absorption maxima at 425, 427, 420 and 418 nm in the UV- Vis. spectra for the synthesis temperatures of 25, 60, 80, and 100 °C, respectively

The solid phase crystal structural characterization was carried out using an XRD analysis at a scanning range of 35-85° (2θ). The XRD patterns of Ag-NPs obtained for four different reaction temperatures are shown in Fig. 3.2. Five distinct diffraction peaks were found at 38.20, 44.40, 64.60, 77.60, and 81.76 ° that were indexed as the planes of (111), (200), (220), (311), and (222) respectively. XRD patterns of Ag-NPs clearly demonstrate that the peak broadenings were happened for the change of reaction temperatures.

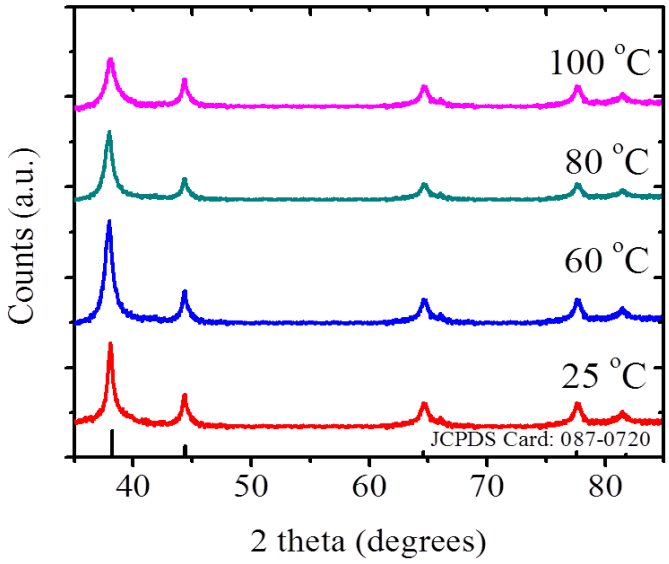

Fig. 3.2 XRD patterns of Ag-NPs synthesized at 25, 60, 80, and 100 °C reaction temperatures

The size and encapsulation of Ag-NPs obtained from the reaction of $AgNO_3$ solution and Mizuna leaf extract at four different reaction temperatures 25, 60, 80, and 100 °C were viewed by TEM analysis as shown in Fig. 3.3. The figure indicates that for the increase of temperature from 25 °C to 60 °C there is an aggregation of Ag-NPs resulting into the increase of particle size. Then the particle size decreased with the increase in temperatures for 80 °C, and 100 °C. It is interesting to quote here that an intense look on the Ag-NPs clearly indicates a surface coating starting to form for the synthesis temperature of 80 °C and finally almost all particles were visualized to be encapsulated for the Ag-NPs synthesized at 100 °C which was the primary objective of the present study.

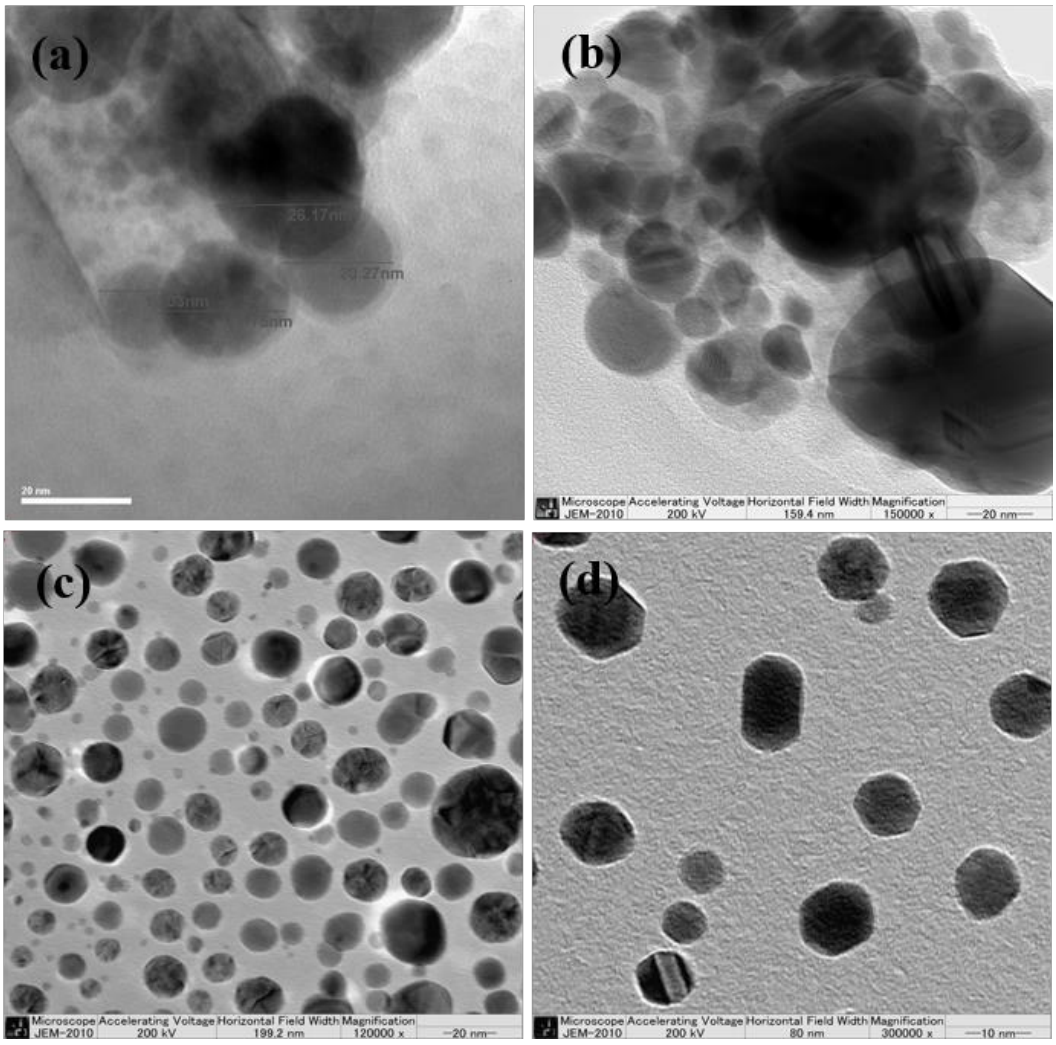

Fig. 3.3 TEM images of Ag-NPs synthesized at (a) 25 °C- indicating spherical and uncoated (b) 60° C- showing uncoated spherical and aggregated (c) 80° C- indicating almost round shaped and partially coated (d) 100° C- showing completely encapsulated Ag-NPs

The hydrodynamic size distribution of Ag NPs was measured by DLS as shown in Fig. 3.4. DLS analysis showed that the size distribution of Ag NPs was varied due to the difference of materials synthesis temperature. The size distribution of Ag NPs was found for four different synthesis temperatures of 25, 60, 80, and 100 °C as an average hydrodynamic size of 18, 40, 31, and 21 nm respectively.

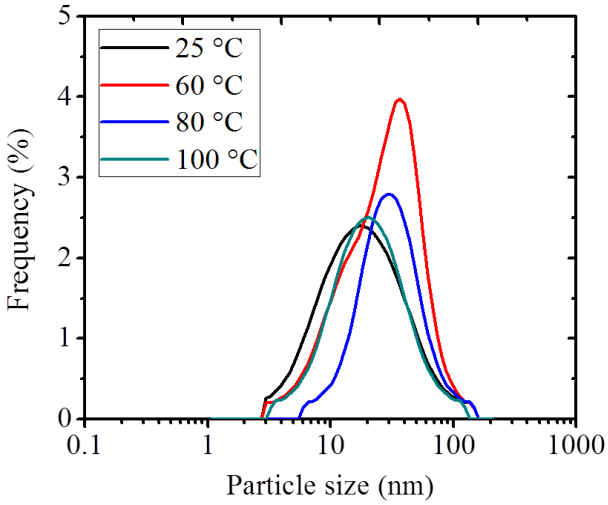

Fig. 3.4 Hydrodynamic particle size distribution of Ag-NPs showing 18, 40, 31, and 21 nm of average size of particles obtained at the reaction temperatures of 25, 60, 80, and 100 °C respectively

3.4. Discussion

Temperature controlled synthesis of Ag-NPs were carried out with you view to find out the effect of reaction temperature on the encapsulation of the synthesized NPs by using Mizuna (*Brassica rapa* var. *nipposinica*) leaf extract as a simultaneous reducing and capping agent and $AgNO_3$ solution as a precursor. During the synthesis, all the conditions were kept constant except reaction temperature. Four different synthesis temperatures, 25 °C (room temperature), 60, 80, and 100 °C were selected to assess whether the difference of temperature retains any size and morphological changes on Ag-NPs. In this study, Ag-NPs were synthesized by adding 10 mL of Mizuna leaf extract into 100 mL of 1mM $AgNO_3$ solution dropwise on a magnetic stirrer maintaining the studied temperatures. The reaction mixture was stirred for about 1 hour and a product was found to be settled down. The broth was then centrifuged at 10,000 rpm for 10 min and washed several times to remove the impurities.

After complete mixing of leaf extract with the $AgNO_3$ solution, the colour of the $AgNO_3$ solution was changed from gray to reddish yellow which was a sign of formation of Ag^0 from Ag^+ (Krishnaraj et al., 2010). It is well established that this yellow colour appears due to the

excitation of surface plasmon resonance (SPR) vibration of the Ag-NPs (Parameshwar et al., 2013). For further confirmation of the formation of Ag^0, UV-vis spectroscopy measurement of the broths was performed, and the absorption maxima were obtained at a wavelength of 400-500 nm, indicating the formation of Ag^0 (Ashraf et al., 2016). The absorption maxima for the synthesized Ag-NPs were found in the wavelength of 425, 427, 420 and 418 nm for the Ag-NPs synthesized at four different reaction temperatures of 25 °C, 60 °C, 80 °C, and 100 °C respectively. The change of absorption maxima indicates that the variation of particle size was occurred depending upon the reaction temperatures (Saha et al., 20179). It is reported that with the increasing absorption maxima the particle size is decreased (Haytham et al., 2015). The UV-vis. data clearly depict that the synthesis temperature 60 °C resulted in the formation of particles with the highest size, whereas, 100 °C leaded to the formation of particles with the lowest size. This may be due to the fact that when the reaction temperature was increased there was an increase in reaction rate which turned the faster nucleation resulting in the increase in particle size (Park et al., 2007). In the case of reaction temperature 80 °C the size of the particles decreased and finally for 100 °C reaction temperature the size of the particles reached their lowest value. This may be due to the fact that at 80 °C, encapsulation process accelerates which hindered the aggregation and for 100 °C, a more encapsulation occurred which also reduced the aggregation and ultimately lowered the particles size.

In XRD (Fig. 3.5), at a scanning range of 35° - 85°, same distinct diffraction peaks at 38.20, 44.40, 64.60, 77.60, and 71.76 ° indexed as the planes of (111), (200), (220), (311), and 222 respectively, were obtained for four types of Ag-NPs synthesized at four different reaction temperatures. The diffraction peaks were matched with the JCPDS card of 097-0720 indicating the formation of face centre cubic structured Ag-NPs. The diffraction patterns also showed a good agreement with the earlier reported values (Sagar et al., 2012, Ullah et al., 2018). No other foreign peaks were found in the XRD patterns indicating the absence of any impure peak in the synthesized Ag-NPs. But, interestingly the peak broadenings were found to be changed with the change in reaction temperature. It is well established that with the increase in peak broadening, the particle size is decreased (Ullah et al., 2017). If we move from 25 to 60 °C, an intense look on the XRD patterns indicates that the peak broadening decreased which is an indication of the increase in particle size. Then when the reaction temperatures were changing from 60 to 100 °C the peak broadening was found to be increased which is an indication of the decrease of particle size. The results obtained from XRD are in good agreement with the UV-vis measurements. The aggregation and encapsulation of the presently synthesized Ag-NPs

were visualized from the TEM images (Fig. 3.3). The particles synthesized at room temperature (25 °C) showed a value of about 10-20 nm. However, at 60 °C temperature synthesized Ag NPs showed a higher value than the 25 °C synthesized Ag-NPs. An intense look on the figure indicates that an aggregation of Ag-NPs was found in this case. This may arise from the faster nucleation as with the increase in temperature the rate of reaction is also increased. When the temperature was increased to 80 °C, particles were found to be formed with a lower size than 60 °C. An intense look again demonstrates that particles were starting to be encapsulated and at 100 °C almost all of the particles were encapsulated which hampered the aggregation and ultimately reduced the size of the particles.

The hydrodynamic size distribution for Ag-NPs obtained atfour different synthesis temperatures of 25, 60, 80, and 100 °C was found with an average size of 18, 40, 31, and 21 nm respectively. The order of the particle size is in good agreement with the TEM analysis value. The particle size obtained from TEM and DLS are different which may be due to the varying principles used for measurements (Gengan et al., 2013).

3.5. Conclusion

We reported here a temperature dependent synthesis of Ag-NPs considering the synthesis temperature of 25 °C (room temperature), 60 °C, 80 °C, and 100 °C. The effect of reaction temperature on the size and surface morphology was examined from the UV-Vis, EDX, XRD, TEM, and DLS analyses. The adopted techniques clearly demonstrate that synthesis temperature affects the size and encapsulation of Ag-NPs. Thus, this might be a potential report to the scientists dealing with the encapsulation of nanoparticles.

References

Akter, M., Rahman, M.M., Ullah, A.K.M.A., Sikder, M.T., Hosokawa, T., Saito, T., Kurasaki, M., 2018. Brassica rapa var. japonica leaf extract mediated green synthesis of silver nanoparticles and evaluation of their stability, cytotoxicity and antibacterial activity. J. Inorganic Organometallic Polymers Mater. 28, 1483-1493

Akter, M, Sikder, M.T., Rahman, M.M., Ullah, A.K.M.A., Hossain, K.F.B., Banik, Hosokawa, S.T., Saito, T., Kurasaki, M., 2018. A systematic review on silver nanoparticles-induced cytotoxicity: Physicochemical properties and perspectives. J. Adv. Res. 9, 1-16

Ashraf, J.M., Ansari, M.A., Khan, H.M., Alzohairy, A.M.A., Choi, I., 2016. Green synthesis of silver nanoparticles and characterization of their inhibitory effects on AGEs formation using biophysical techniques. Scientific Reports. 6,1-10

An, J., Tang, B., Ning, X., Zhou, J., Xu, S., Zhao, B., Xu, W., Corredor, C., Lombardi, J.R., 2007. Photoinduced shape evolution: From triangular to hexagonal silver nanoplates, J. Phys. Chem. 111, 18055–18059

Bruchez, M., Moronne, M., Gin, P., Weiss, S., Alivisatos, A.P., 2013. Semiconductor nanocrystals as fluorescent biological labels. Science. 281, 2013–16

Caswell, K., Bender, C.M., Murphy, C.J., 2003. Seedless Surfactantless wet chemical synthesis of silver nanowires. Nano Letters. 3, 667–669

Edwards-Jones, V., 2009. The benefits of silver in hygiene, personal care and healthcare. Letters Appl. Microbio. 49, 147–52

Gao, Y., Jiang, P., Song, L., Wang, J., Liu, L., Liu, D., Xiang, Y., Zhang, Z., Zhao, X., Dou, X., 2006. Studies on silver nanodecahedrons synthesized by PVP-assisted N, N-dimethylformamide (DMF) reduction. J. Crystal Growth. 289, 376–380

Gengan, R.M., Anand, K., Phulukdaree, A., Chuturgoon, A., 2013. A549 lung cell line activity of biosynthesized silver nanoparticles using Albizia adianthifolia leaf. Colloids Surf B Biointerfaces. 105, 87–91

Haytham, M.M.I., 2015. Green synthesis and characterization of silver nano particles using banana peel extract and their antimicrobial activity against representative microorganisms. J. Radiation Res. Appl. Sci. 8, 265-275

Hangxun, X., Brad, W.Z., Suslick, K.S. 2013. Sonochemical synthesis of nanomaterials. Chem. synthesis reviews. 42, 2555-67

Jin, R., Cao, Y., Mirkin, C.A., Kelly, K., Schatz, G.C., Zheng, J., 2001. Photoinduced conversion of silver nanospheres to nanoprisms. Science. 294, 1901–1903

Kneipp, K., Kneipp, H., Kneipp, J., 2006. Surface-Enhanced Raman Scattering in Local Optical Fields of Silver and Gold Nano aggregates -From Single-Molecule Raman Spectroscopy to Ultrasensitive Probing in Live Cells. Accounts Chem. Res. 39, 443–450

Krishnaraj, C., Jagan, E.G., Rajasekar, S., Selvakumar, P., Kalaichelvan, P.T., Mohan N., 2010. Synthesis of silver nanoparticles using Acalypha indica leaf extracts and its antibacterial activity against water borne pathogens. Colloids Surf.B: Biointerfaces 76, 50–56

Lee, S.W., Chang, S.H., Lai, Y.S., Lin, C.C., Tsai, C.M., Lee, Y.C., Chen, J.C., Huang, C.L., 2014. Effect of Temperature on the Growth of Silver Nanoparticles Using Plasmon-Mediated Method under the Irradiation of Green LEDs. Materials. 7, 7781-7798

Maillard, M., Huang, P., Brus, L., 2003. Silver Nanodisk Growth by Surface Plasmon Enhanced Photoreduction of Adsorbed [Ag+]. Nano Letters. 3, 1611–1615

Pietrobon, B., McEachran, M., Kitaev, V., 2008. Synthesis of size-controlled faceted pentagonal silver nanorods with tunable plasmonic properties and self-assembly of these nanorods. ACS Nano. 39 21–26

Parameshwaran, R., Kalaiselvam, S., Jayavel, R., 2013. Green synthesis of silver nanoparticles using Beta vulgaris: role of process conditions on size distribution and surface structure. Mater. Chem. Phys. 140,135-147

Park, J., Joo, J., Kwon, S.G., Jang, Y., 2007. Synthesis of monodisperse spherical nanocrystals. Angewandte. Chemie- Int. Ed. T. 46, 4630-4660

Prathna, T.C., Chandrasekaran, N., Raichur, A.M., Mukherjee, A., 2011. Kinetic evolution studies of silver nanoparticles in a bio-based green synthesis process. Colloids Surf. A: Physicochem. Eng. Aspects. 377, 212-6

Sagar, G., Bhosale, A,. 2012. Green synthesis of silver nanoparticles using Aspergillus niger and itsefficacy against human pathogenes. Eur. J.Exp. Bio. 2, 1654-1658

Sarvamangala, D., Kondala, K., Sivakumar, N., Babu, M.S., Manga, S., 2013. Synthesis characterization and antimicrobial studies of Ag NPs using probiotics. Int. Res. J. Pharmacy. 4, 240-243

Saha, J., Begum, A., Mukherjee, A., Kumar, S., 2017. A novel green synthesis of silver nanoparticles and their catalytic action in reduction of Methylene Blue dye. Sustainable Env. Res. 27, 245-250

Sun, Y., Xia, Y., 2002. Shape-controlled synthesis of gold and silver nanoparticles. Science. 298, 2176–2179

Sintubin, L., Gusseme, B.D., Meeren, V. de., Pycke, B.F.G., 2011. Verstraete W, Boon N. The antibacterial activity of biogenic silver and its mode of action. Appl. Microbio. Biotech. 91:153-62

Tao, A., Sinsermsuksakul, P., Yang, P., 2006. Polyhedral silver nanocrystals with distinct scattering signatures. Angewandate Chemie. 45, 4597–4601

Ullah, A.K.M.A., Kibria, A.K.M.F., Akter, M., Khan, M.N.I., Maksud, M.A., Jahan, R.A., Firoz, S.H., 2017. Synthesis of Mn_3O_4 nanoparticles via a facile gel formation route and study of their phase and structural transformation with distinct surface morphology upon heat treatment. J. Saudi Chem. Soc. 21, 830-836

Ullah, A.K.M.A., Kibria, A.K.M.F., Akter, M., Khan, M.N.I., Tareq, A.R.M., Firoz, S.H., 2017. Oxidative Degradation of Methylene blue using Mn_3O_4 Nanoparticles. Water Conservation Sci. Eng. 1, 249–256

Ullah, A.K.M.A., Kabir, M.F., Akter, M., Tamanna, A.N., Hossain, A., Tareq, A.R.M., Khan, M.N.I., Kibria, A.K.M.F., Kurasaki, M., Rahman, M.M., 2018. Green synthesis of bio-molecule encapsulated magnetic silver nanoparticles and their antibacterial activity. RSC Advances. 8, 37176-37183

Wiley, B.J., Xiong, Y., Yuan, Z.L., Yin, Y., Xia, Y., 2006. Right bipyramids of silver: A new shape derived from single twinned seeds. Nano Letters. 6, 765–768

Xue, C., Métraux, G.S., Millstone, J.E., Mirkin, C.A., 2008. Mechanistic study of photomediated triangular silver nanoprism growth. J. American Chem. Soc. 130 8337–8344

Yu, S.J., Yin, Y.G., Liu, J.F., 2013. Silver nanoparticles in the environment. Environmental Science: Process and Impacts. 15, 78–92

Zhou, J., An, J., Tang, B., Xu, S., Cao, Y., Zhao, B., Xu, W., Chang, J., Lombardi, J.R., 2008. Growth of tetrahedral silver nanocrystals in aqueous solution and their SERS enhancement. Langmuir. 24, 10407–10413

Chapter 4

Beclin 1 mediated autophagy in colorectal cancer cells: implication in anticancer efficacy of Brassica Ag-NPs via inhibition of mTOR signaling

Abstract

Autophagy is a strictly regulated catabolic process and involves the degradation of intracellular components via lysosome. Although essential role of autophagy in homeostasis, cell growth and development are well understood. But its function and mechanism in cancer prevention is still unknown. On the other hand, green synthesized silver nanoparticles (Ag-NPs) showed promising effect on different cell line. Therefore, the aim of this study was to investigate the autophagy regulated anticancer effect of Brassica Ag-NPs against colorectal cancer cells (Caco-2 cells). We found that our synthesized Brassica rapa var. nipposinica/ japonica leaf extract mediated Ag-NPs induce Beclin 1 mediated autophagy in Caco-2 cells which further accelerate inducing autophagy via p53. Therefore, upregulation IkB inhibit activity of NFkB which stop DNA transcription. Finally, inhibition of Akt and mTOR further promote autophagy. Surprisingly no apoptotic protein expression found in this study. Taken together, we conclude that Brassica Ag-NPs induce Beclin 1 mediated autophagy via inhibition of mTOR in (Caco-2) cell; human colorectal cancer cells.

4.1. Introduction

Cancer is a multifactorial disease with a complex combination of genetics and environmental factors therefore, clear knowledge of the molecular, genetics and cellular basis of cancer is recommended for its new strategies of therapy (Mirim Buttacavoli et al., 2018). Though many anticancer drugs are available but most of the cases they showed inability to reach their target site in expected concentrations and efficiently cause irreversible unwanted injury to healthy tissues and cells (Pérez-Herrero E et al., 2015). Among all of the cancers, colorectal cancer is the second leading cause of cancer death for women and third for men worldwide (Silvia Fernandez de Mattos et al., 2008) and one of the main therapeutic option of colorectal cancer is platinum-based compounds. Another potential compound used as therapeutic agent in the treatment of colorectal cancer is cisplatin (Arimoto-Ishida et al.,2003). However, drug resistance is remaining one of the most crucial obstacles in cancer therapy.

Induction of autophagy mediated cell death is considered as an efficiency of anticancer activity (Meijuan Zou et al., 2012). Autophagy literally means as self-eating, is a strictly regulated self-digestive process, where cytoplasmic organelles are sequestered inside the double membrane vesicles known as autophagosomes and transported to the lysosome

for degradation and recycling as well (Meijuan Zou et al., 2012). More than 30 well conserved proteins (Atgs), from yeast to mammals are considered as autophagy regulator (Mizushima et al., 2011). Atg1is a serine/threonine kinase is an essential initiator of autophagy (Kabeya et al., 2005). Autophagy can also be regulated by phosphatidylinositol-3-kinase (PI3k) type III, a component of Atg 6 (Beclin-1) included multi-protein complex. PI3K promotes invagination of the membrane in the region of phosphatidylinositol-3-phosphate (PI3P) abundant region, called as omegasomes which initiate membrane isolation [Axe et al., 2008]. Subsequent expansion and inhibition of membrane isolation are regulated by two ubiquitin like conjugation pathways; Atg5-Atg-12 pathway and microtubule-associated protein 1light chain 3(LC-3) pathway (Mizushima et al., 2011). Therefore, four different stages; initiation, autophagosome formation, maturation and degradation are the process of progression of autophagy which subsequently results in lysosomal breakdown of cytoplasmic materials (E. A. Corcelle et al., 2009). Thus, excessive amount of autophagy can promote cell death due to the overconsumption of critical cellular organelles. This process is known as Atg dependent or type II programmed cell death (S.Roy et al., 2010, Rahman et al., 2018). It is generally agreed that, many diseases including liver diseases, neurodegenerative diseases and cancer are related to deregulation of autophagy (Y. S. Rajawat et al., 2008).

Over a decade ago the involvement of Beclin -1 in cancer was first indicated in MCF-7 cell line, demonstrated that its over expression could inhibit MCF-7 breast carcinoma xenograft tumor growth (Liang XH et al., 1999). In mouse model, heterozygous disruption of Beclin-1 expression promotes spontaneous tumorgenesis in mice, indicate Beclin-1 as a haploinsufficient tumor suppressor (Rasika A et al., 2016). In human tumors, frequent decrease of Beclin-1 mRNA and protein level often associated with poor prognosis which decrease overall survival potency of patient (Dong M et al., 2013). Taken together the mouse model and human tumor data support the hypothesis that reduced expression of Beclin-1 in human cancer may have contribution in disease progression (Rasika Aet al., 2016). Beclin-1 is a mammalian homolog of vacuolar protein of yeast associated with autophagy related protein Atg6 and functions in the core complex includes class III phosphatidinosytol (PI)-3 kinase and p150 subunit (Wirawan E et al., 2012). The activity of PI3KC3 is stimulated by Beclin-1 to generate phosphatidylinositol-3 phosphate (PI3P), which is necessary for the activity of effector protein containing a FYVE (Fab1p, YOTB, Vaclp, EEA1) or PX (Phox homology) domain that facilitate membrane fusion and trafficking events. Involvement of Beclin-1 has been found in multiple membrane trafficking pathways that require PI3P including autophagy, vacuolar protein shorting, phagocytosis, cytokinesis and endocytosis

(Wirawan E et al., 2012). This promising activity raises an important question regarding which of the Beclin-1 mediated pathway is important for the tumor suppressor function. Recently it is established that Beclin-1 can contribute to the regulation of the degradative process of autophagy. In contrast alternative function of Beclin-1 have also been reported in context of cancer. Thus, this is important that disruption of other autophagy pathway genes has not recapiluted the results from the $Becn1^{+/-}$ mice with regard to tumor development. Thus, this is a discrepancy that supports a potential role for autophagy –independent Beclin-1 function in cancer. However, nanotechnology offers an outstanding tools of cancer treatment where nanoparticles can pass away biological barriers and deliver therapeutic agent directly (Conde J et al., 2012). Metallic nanoparticles show some unique physicochemical properties such as high surface area to volume ratio, broad optical properties, surface functionalization and ease of synthesis offer new opportunities of cancer therapy (Poulose S, 2014).

Thus, green synthesis of Ag-NPs have attributed immense attention in order to the increasing demand of development of eco-friendly technologies in nano silver synthesis (Hulkoti NI et al., 2014) and already several methods have been established to synthesis noble Ag-NPs in both physical and chemical ones (Russo M et al., 2016). Therefore, different organisms and plants have been used as potential factories for the production of green Ag-NPs. The mechanism of the green synthesis of Ag-NPs is mainly depend on the capability of biopolymer to act as metal reducer and/or stabilizer (Kanmani P et al., 2013). However, in our previous study we synthesized Ag-NPs using *Brassica rapa* var. *japonica* leaf extract where $AgNO_3$ act as a precursor and Brassica leaf extract act as a reducing and capping agent (Akter et al., 2018). After characterization we found that Brassica Ag-NPs are face centered cubic in structured with a diameter of 15-30 nm. In continuation of our previous study our recent study has focused on the anticancer efficiency of green synthesized Ag-NPs (Brassica Ag-NPs) against colorectal cancer cell known as Caco-2 cell line *in vitro*.

Though the effect of Ag-NPs on colorectal cell is already studied, but mechanism of Ag-NPs induce autophagy type cell death is still unclear. Particularly to date there is no study on the effect of Ag-NPs inducing autophagy type cell death in Caco-2 cell line to use Ag-NPs as drugs in the treatment of colorectal cancer cells. Therefore, in this study we hypothesized that Brassica Ag-NPs might induce cytotoxic effect on colorectal cell line possibly by regulating beclin1 mediated autophagy (type II cell death). The effect of Brassica Ag-NPs might be type I (survival) autophagy or type II autophagy (cell death). Hence, our present study has been carried out to explore the effect of Brassica Ag-NPs on Caco-2 cells for the first time by unveil possible mechanism behind Beclin-1 induce autophagy type cell death.

4.2 Materials and methods

4.2.1 Materials

Brassica rapa var. *japonica* leaves were collected locally (Sapporo, Japan). $AgNO_3$ was purchased from Wako pure chemical industries (Osaka, Japan). Caco-2 cell lines were purchased from American type culture collection (USA and Canada). Eagle's minimum essential medium (EMEM), nonessential amino acid ethidium bromide, were bought from sigma (St. Louis, MO, USA). Fetal bovine serum (FBS) was purchased from Biosera (Kansas City, MO, USA). Proteinase K were purchased from Roche Diagnostics (Mannheim, Germany). Biotinylated goat anti-mouse IgG whole antibody and ECL western blotting detection reagent were purchased from Amersham Pharmacia Biotech (Buckinghamshire, England). Polyclonal antibodies beta-actin (GTX 109639, GeneTEX), Akt (Ser 473), NFkB (D14E12 CST) mTOR, p53, LC3-II, Bclin-1 (Cell signaling technology) was purchased. Trypan blue solution (0.4%) was obtained from Bio-Rad (Hercules, CA, USA). The DNA 7500 assay and LDH nonradioactive assay kits were purchased from Agilent Technologies (Waldbronn, Germany). All other chemicals and reagents used in this study were of analytical grade.

4.2.2 Brassica Ag-NPs synthesis, characterization and stability

Ag-NPs was synthesized using Brassica rapa var. nipposinica/ japonica leaf extract which is briefly explained in Chapter 2. For the characterization of Brassica Ag-NPs, FESEM, EDS, FTIR, XRD and TEM analyses was performed. Characterization techniques also explained in Chapter 2. After characterization we found that our synthesized Brassica Ag-NPs is 15-30 nm in size and evenly dispersed with a negligible agglomeration and face centered cubic structured (Akter et al., 2018)

4.2.3 Cell culture

Caco-2 cells were cultured in EMEM medium with supplemented 10% FBS and non-essential amino acid in a humidified incubator at 37ºC with 5% CO_2. Cells were pre incubated in a 25-cm^2 flasks for 24 h, then medium was replaced with serum EMEM medium with or without various concentrations of Ag-NPs. Cells were then incubated for 48 h and desired concentration of Ag-NPs was selected with a preliminary concentration of 1, 5, 10 and 20 µg/mL separately.

4.2.4 Cell viability

Cell viability was measured using Trypan blue exclusion assay. Caco-2 cells were cultured in EMEM culture medium at an approximate density of about 1×10^5 cells/flask and pre-incubated for 24 h. Cells were then treated without and with Brassica Ag-Nps separately.

Then the cells were incubated for another 12 h and 48 h. After that cells were harvested, subsequently number of total cells and trypan blue stained cells were counted using a Bio-Rad automated cell counter (Hercules, CA.USA). Cell viability was expressed as percentage of the counted trypan blue-stained cells. Each experiment was carried out at least three times to ensure biological reproducibility and statistical validity.

4.2.5 Lactate dehydrogenase (LDH) activity assay and visualization of cell wall integrity

Cytotoxicity was determined by measuring the LDH activity in the treatment medium using a nonradioactive assay kit (Promega) as described by Rahman et al. (2017). Caco-2 cells were (1×10^5 cells/flask) cultured in the medium without or with Brassica Ag-Nps (0, 1µg/mL, 51µg/mL, 25 1µg/mL) for 48 h. After 48 h incubation cells were collected in a 15 mL tube, centrifuge 1500 rpm for 3 min and collected medium. Then 50 µL medium transferred into the 96 well plates, added 50 µL substrate mixture and incubate 30 min in room temperature (25 ºC). After 30 min incubation stop solution was added and the amount of formazan dye formed were determined by measuring the absorbance at 490 nm using aiMark^{TM} immunoplate reader (biorad; Hercules, CA, USA). LDH activity was expressed as LDH activity/1×10^6 cells. This experiment was carried out three times to ensure biological reproducibility.

4.2.6 Measurement of oxidative stress marker (GSH level)

Intracellular level of free-SH was investigated following the protocol described by Rahman et al. (2018). Caco-2 cells (1×10^5) were pre- incubated for 24 h and then exposed Brassica AgNPs at a concentration of 0, 1 µg/mL, 5 µg/mL and 25 µg/mL for 48 h. After 48h incubation cells were harvested using 1× HEPES and Trypsin EDTA, washed with 1× phosphate buffer saline (PBS), added 150 µL of lysis buffer and incubated at room temperature (25ºC) for 10 min. Freeze- thaw sonication cycle was carried out for two times in order to rupture the cell membranes, then resultant solution was centrifuge 1500 rpm and supernatant was collected. Total protein of the collected supernatant was measured spectrophotometrically by using protein assay dye reagent (BIO-Rad, Hercules, CA, USA). Levels of GSH was determined by using 2.5mM 5,5′-dithiobis -2-nitrobenzoic acid (DTNB. pH7) assay kit. DTNB added to the lyset cell maintaining final concentration 200 µM and then absorbance was determined at 412 nm using DU-65 spectrophotometer (Beckman, CA, USA). Finally, the concentration of free SH present in Caco-2 cells was measured by using a molecular coefficient factor of 13,600 per cell number (1×10^5). The experiments were carried out three times to ensure biological reproducibility.

4.2.7 Isolation of genomic DNA from Caco-2 cell

After treatment of Caco-2 cells with Brassica Ag-NPs in various concentrations, the genomic DNA of Caco-2 cells were isolated using a high pure PCR template preparation kit according to the manufacture instruction. After 12h incubation, cells were harvested and obtained cells were centrifuge at 1500 rpm for 3 min to remove supernatant. To wash the cells 400 µL of 1× phosphate buffer saline (PBS) was added in to the cells and centrifuge at 1500 rpm for 5 min. The obtained solution containing DNA was incubated at 37 ºC for 15 min after adding 5 µg/mL RNase. After 15 min incubation ethanol and 3 MNaOAc buffer (pH 4.5) was added for ethanol precipitation and the total solution was kept in to a -20 ºC refrigerator overnight to allow DNA precipitation. On the very next day DNA was yielded using micro-centrifuge at 15,000 rpm for 8 min and the washed the precipitate with 70% ethanol at the same speed of centrifugation for 3 min. Then DNA sample was dried using a vacuum condenser approximately 15 min and concentration of DNA was measured adding 1× Tris/Borate/ EDTA (TBE) using a Gene Quant (GE Health Care; South East England, UK).

4.2.8 Agarose gel electrophoresis of genomic DNA

The fragmentation of DNA was analyzed via agarose gel electrophoresis. 4.0 µg of DNA was mixed with the loading dye and subjected to electrophoresis on a 1.5% agarose gel. Electrophoresis was carried out using a submarine-type electrophoresis system (Mupid-ex, Advance, Tokyo, Japan) at 100 V for 30 min. After electrophoresis agarose gel was soaked in to ethidium bromide solution for 10 – 15 min to visualize DNA fragmentation. Imaes of DNA was taken by using ChemiDoc XRS (Bio-Rad; Hercules, CA, USA). To visualize the fragmentation, the fluorescence intensity of the DNA in the gel was analysed by the software Quantity one. The amount of intact DNA was expressed as the ratio of DNA density to the fragmented DNA density. This experiment was conducted three times to confirm biological reproducibility.

4.2.9 Western blot analysis for determination of protein expression

After cultured Caco-2 cells with EMEM in supplement 10%FBS, different concentration of Brassica Ag-NPs was exposed to the cell for 12 h. Then procedure of western blot analysis was carried out following to the procedure described by Rahman et al. (2017). The total protein of Caco-2 cells was extracted by ice cold lysis buffer (2 mM HEPES, 100 mM Nacl, 10 mM EGTA, 0.1 µM MPMSF, 1 mM Na2MgO4, 5 mM 2-glycerophosphoric acid, 10 µM MgCl2, 2 mM DTT, 50 µM NaF and 1% triton X-100). The extracted protein concentration was measured spectrophotometrically using protein assay dye reagent (Bio-rad). The total protein (30 µg) from each sample was separated by 12.5/15%

sodium dodesyle sulphate polyacrylamide (SDS-PAGE) electrophoresis and then transferred on to nitrocellulose membrane using semi dry transfer method. Then membrane was blocked in to the 5% blocking buffer (Skim milk) at 4ºC overnight. Membrane was then sequentially incubated with desired primary and secondary antibodies. Finally, the protein present on the nitrocellulose membrane was visualized using enhanced chemiluminescence and the image of the detected band was analyzed using a Chemi Doc XRS (Bio-Rad, USA). The intensities of the bands were as the ratio to that of βactin. All experiments were conducted three times to ensure biological reproducibility.

4.2.10 Flow cytometry

Flow cytometry was carried out using BD FACSVerse ™ Flowcytometer, Ver 1.2. Caco-2 cells were treated with Brassica Ag-NPs at the concentration of 1, 5 and 10 µg/mL. After 12 h incubation cells were washed with PBS and added 400 µL ice cold 1×binding buffer. Then 5 µL of Annexin A5-FITC solution and 2.5 µL PI (propidium idodide) was added to the cell suspension and kept 10 min in dark. After 10 min sample was analyze using flow cytometer.

4.2.11 Statistical analysis

All data that showed in the experiment are expressed as the mean± standard error of mean (SEM). Statistical analysis was performed following unpaired student *t* test.

4. 3. Results

4.3.1 Ag-NPs inhibits cell growth in human colorectal cancer (Caco-2) cells

The effect of Brassica Ag-NPs on the inhibition of Caco-2 cell growth was investigated using trypan blue exclusion method. Hence, Brassica Ag-NPs were exposed to Caco-2 cells in four different concentration (1µg/mL, 5µg/mL, 10 µg/mL and 20 µg/mL) for 12 h and 48 h and results showed cell viability was decreased significantly at $p < 0.05$ in a dose dependent manner for both of the 12 h and 48 treatment. Fig. 4.1a and 4.1b showed the percentage of cell viability for the concentration of 1µg/mL, 5µg/mL, 10 µg/mL and 20 µg/mL is 82%, 66%, 19%, 12% and 81%, 66%, 44%, 17% for 12 h and 48 h exposure of Ag-NPs. However, there is no significant difference on cell viability was not found in the treatment group of 5 µg/mL and 10 µg/mL within 12 h and 48 h exposure period. Therefore, further experiment was designated to use 3 different concentrations (1µg/mL, 5µg/mL, 10 µg/mL) as treatment for 12 h incubation with treatment.

4.3.2 Effects of Brassica Ag-NPs on membrane integrity on Caco-2 cells

LDH leakage in the culture medium is one of the indicators of cell membrane disruption and subsequently cell death. In this study to check the cell membrane integrity LDH activity was measured using a non-radioactive assay kit. After exposure of Brassica

Ag-NP at a concentration of 1µg/mL, 5µg/mL and 10 µg/mL in to the Caco-2 cells, LDH activity was remarkably increased significantly at $p < 0.05$ in a dose dependent manner compared with control group for 12 h exposure period (Fig. 4.2).

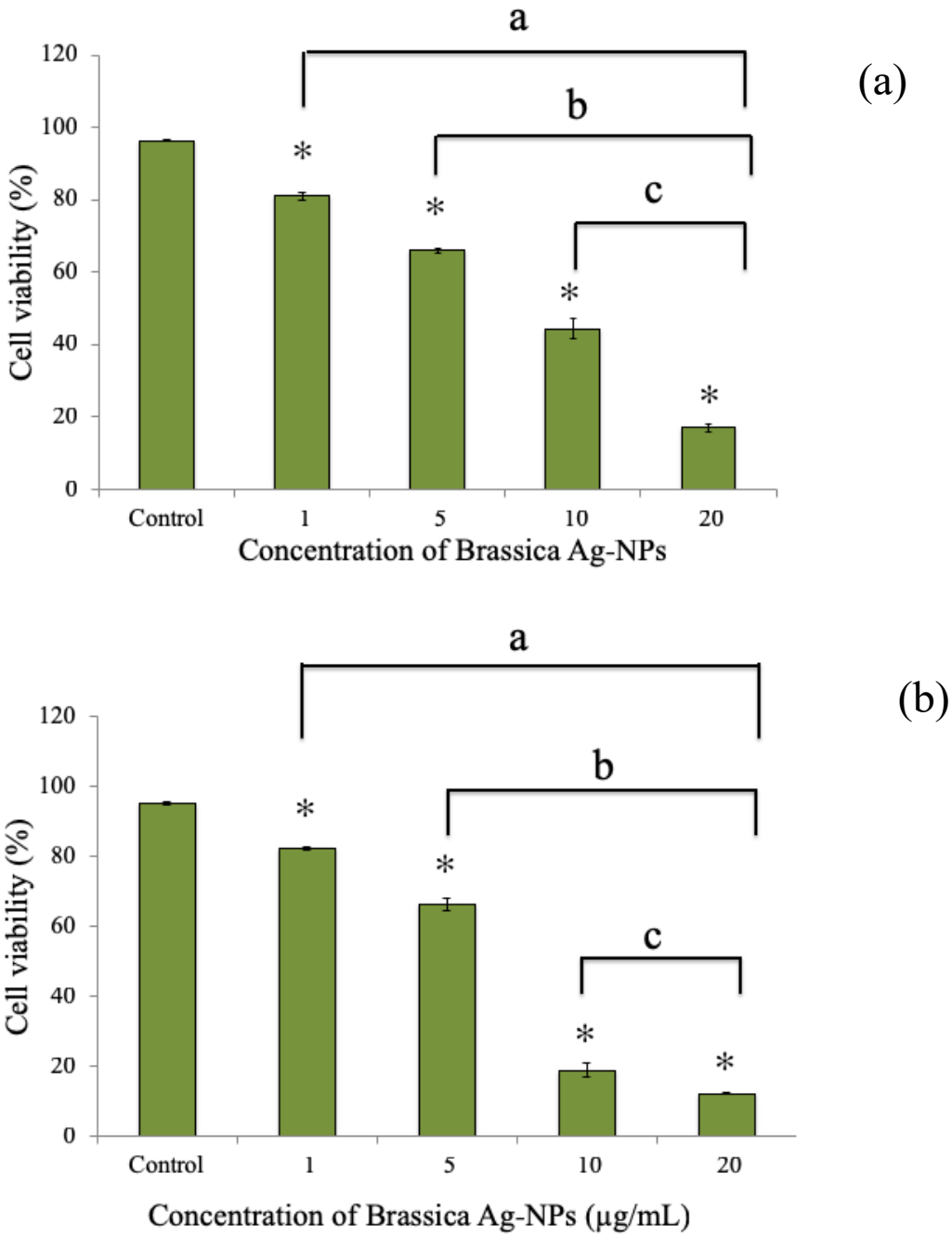

Fig. 4.1 Cell viability of Caco-2 cells after treatment with Brassica Ag-NPs for (a)12 h and (b) 48 h measured by trypan blue staining method. Error bar indicate mean ± SEM (n-3). Asterisk, a, b and c indicate significant at $p<0.05$ compared to control group

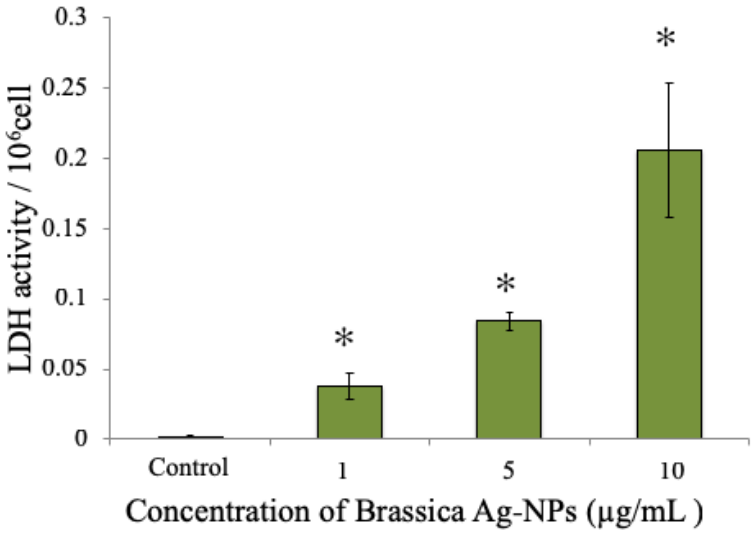

Fig. 4.2 LDH activity of Caco-2 cells after treatment with Brassica Ag-NPs for 12 h measured by nonradioactive assay kit. Error bar indicate mean ± SEM (n-3). Asterisk, and a indicate significant at $p<0.05$ compared to control group

4.3.3. Effects of Brassica Ag-NPs on intracellular level of GSH

Glutathione (GSH) is an antioxidant strictly maintains the intracellular antioxidant defense system. Intracellular reduction of GSH level indicates the anomaly in cellular oxidative homeostasis. Therefore, in this study GSH level was measured in Caco-2 cells upon exposure to 1 µg/mL, 5 µg/mL and 10 µg/mL of Brassica Ag-NPs for 12 h depicts a significant reduction of GSH level in Caco-2 cells at a concentration of 5 µg/mL and 10 µg/mL after 12 h exposure of Brassica Ag-NPs. Though Intracellular GSH level is also decreased for all of the treatment groups but at the concentration of 1 µg/mL change is not significant compared with control group. But for the concentration of 5µg/mL and 10 µg/mL of Brassica Ag-NPs GSH level decreased significantly at $p < 0.05$ (Fig 4.3).

4.3.4 Effects of Brassica Ag-NPs on genomic DNA

Status of genomic DNA was investigated following the agarose gel electrophoresis assay after the exposure of Brassica Ag-NPs for 12h. With the 12 h exposure of Brassica Ag-NPs at a concentration of 1µg/mL, 5µg/mL and 10 µg/mL the gel analysis showed the decrease of intact DNA and also increase of. Fig 4.5 showed a significant increasing trend of DNA smearing for the concentration of 5µg/mL and 10 µg/mL of Brassica Ag-NPs at $p < 0.05$.

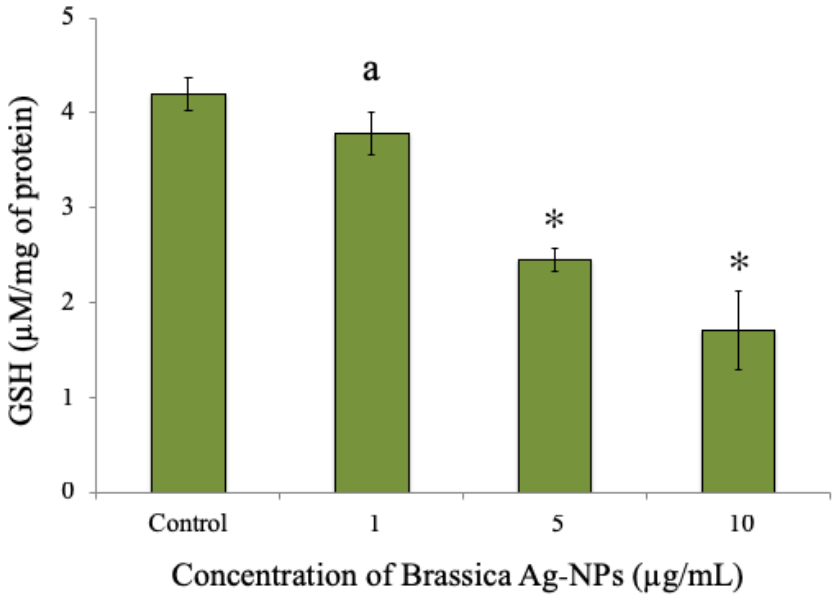

Fig. 4.3 Intracellular GSH level in Caco-2 cells after treatment with Brassica Ag-NPs for 12 h measured via DTNB assay. Error bar indicate mean ± SEM (n-3). Asterisk, and a indicate significant at $p<0.05$ compared to control group

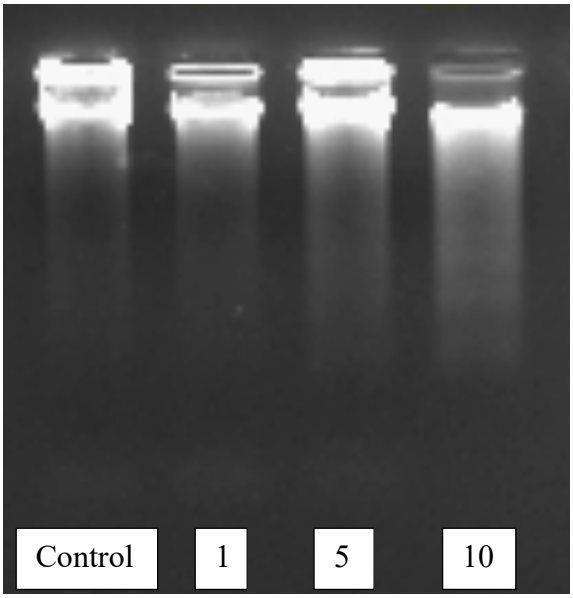

Fig. 4.4 Agarose gel electrophoresis of genomic DNA extracted from Caco-2 cells after treatment with Brassica Ag-NPs for 12 h.

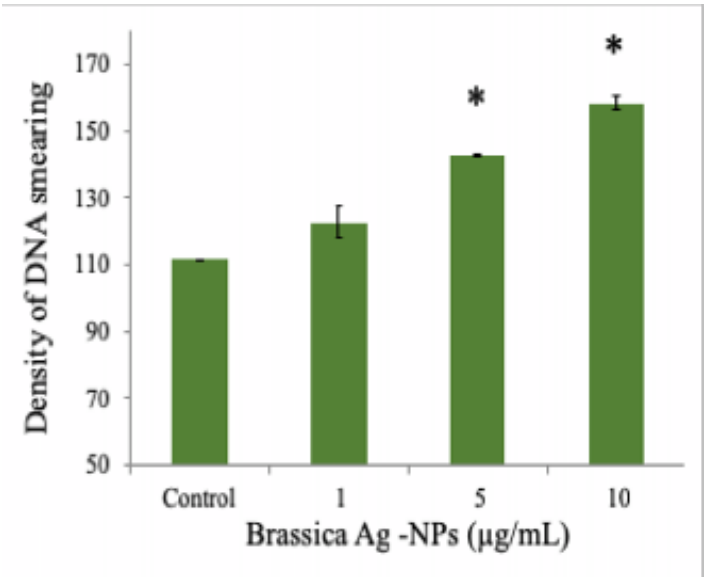

Fig. 4.5 Agarose gel electrophoresis of genomic DNA extracted from Caco-2 cells after treatment with Brassica Ag-NPs for 12 h. DNA smearing intensity for damage detection. Error bar indicate mean ± SEM (n-3). Asterisk indicate significant at $p<0.05$ compared to control group

4.3.5 Effects of Brassica Ag-NPs on the regulation of autophagy related factors in Caco-2 cells through western blotting

In this study we analyzed the expression of key factors for possible elucidation of autophagy mechanism by western blot method. Results showed with the three different concentration of Brassica Ag-NPs (1, 5, and 10 µg/mL) protein showed different expressions. Expression of p53 increase significantly compared with control group for the treatment group of 5 and 10 µg/mL. of expression occurred. Down regulated significantly the contents of autophagy related proteins; p53 (fig. 4.7), mTOR and Akt (fig. 4.8), Beclin 1 and LC3 (fig 4.6). Expression of mTOR and Akt downregulated for all of the treatment group compared with control group. Though expression of NFkB decreased significantly for all of the treatment group but expression of IkB α increase only for the treatment group of 10 µg/mL. Finally, expression of Beclin 1 increased for all of the treatment group but significant increasing tendency found in 5 and 10 µg/mL in LC3-II protein.

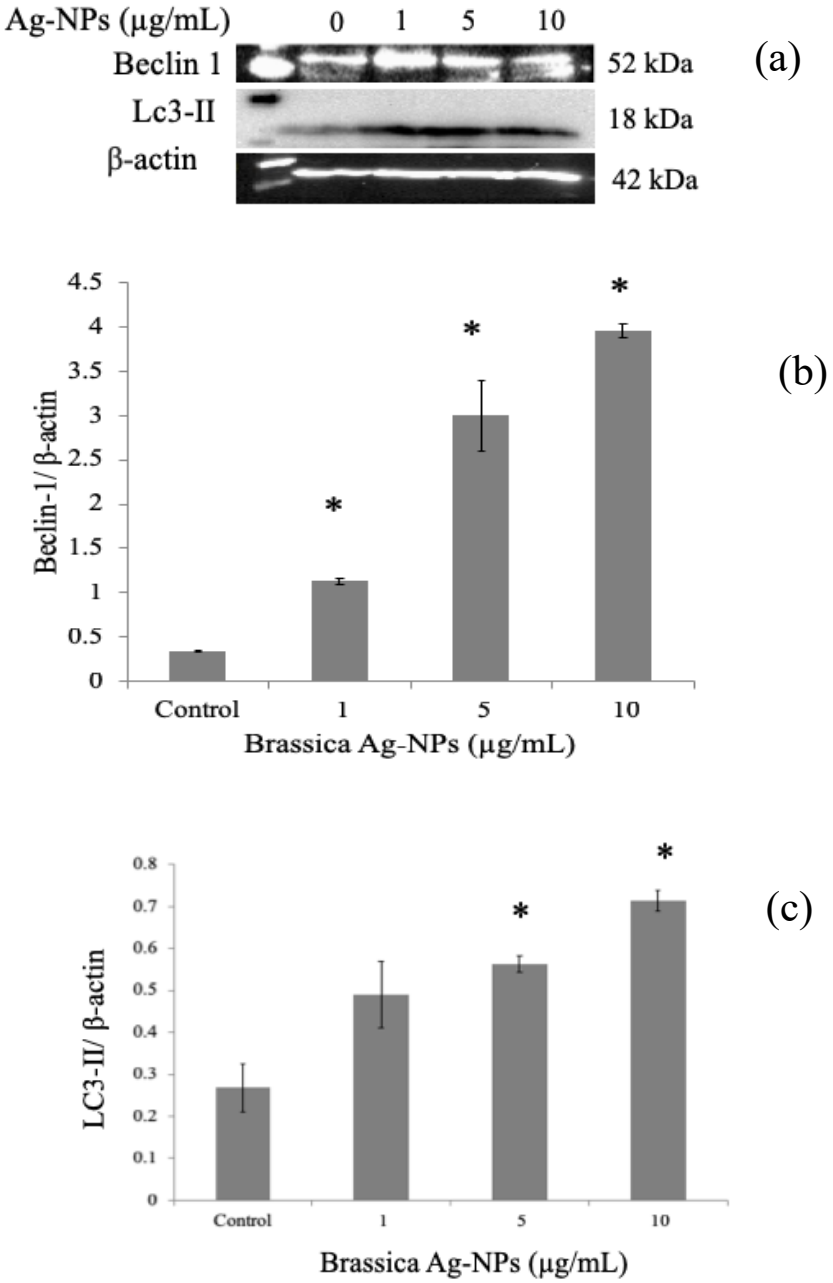

Fig. 4.6 Western blot analysis for protein expression after being exposed to Brassica Ag-NPs for 12 h. (a) Immunoblotting for without and with treatment (b) and (c) are relative density of Beclin 1 and LC3-II to β- actin. Error bar indicate mean ± SEM (n-3). Asterisk indicate significant at $p<0.05$ compared to control group

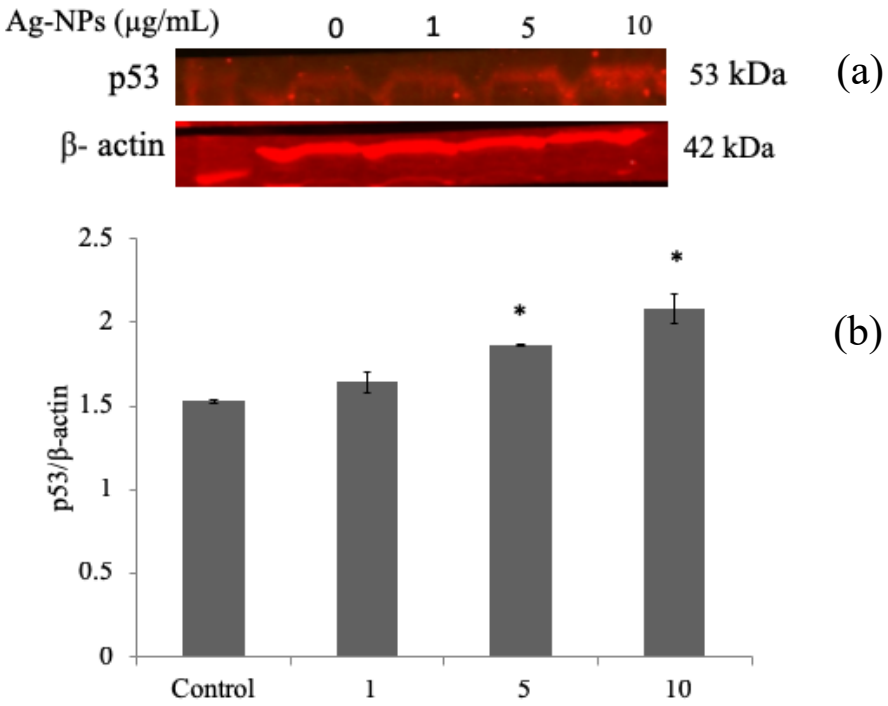

Fig. 4.7 Western blot analysis for protein expression after being exposed to Brassica Ag-NPs for 12 h. (a) Immunoblotting for without and with treatment (b) relative density of p53 to β- actin. Error bar indicate mean ± SEM (n-3). Asterisk indicate significant at $p<0.05$ compared to control

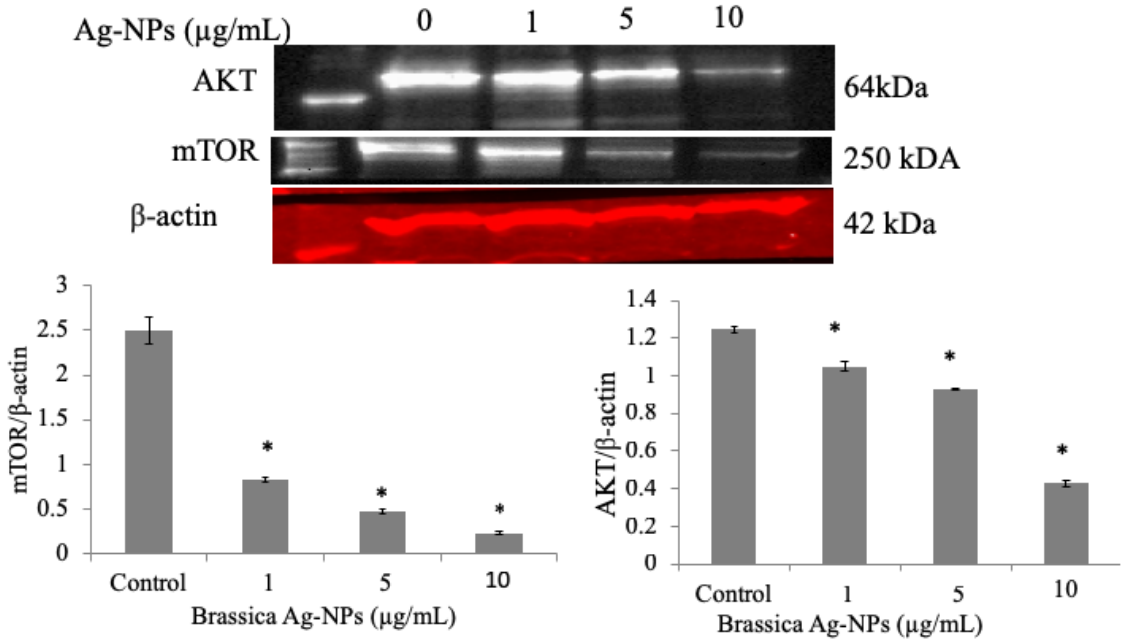

Fig. 4.8 Western blot analysis for protein expression after being exposed to Brassica Ag-NPs for 1 h. (a) Immunoblotting for without and with treatment. Relative density of (b) mTOR and (c) Akt to β- actin. Error bar indicate mean ± SEM (n-3). Asterisk indicate significant at $p<0.05$ compared to control group

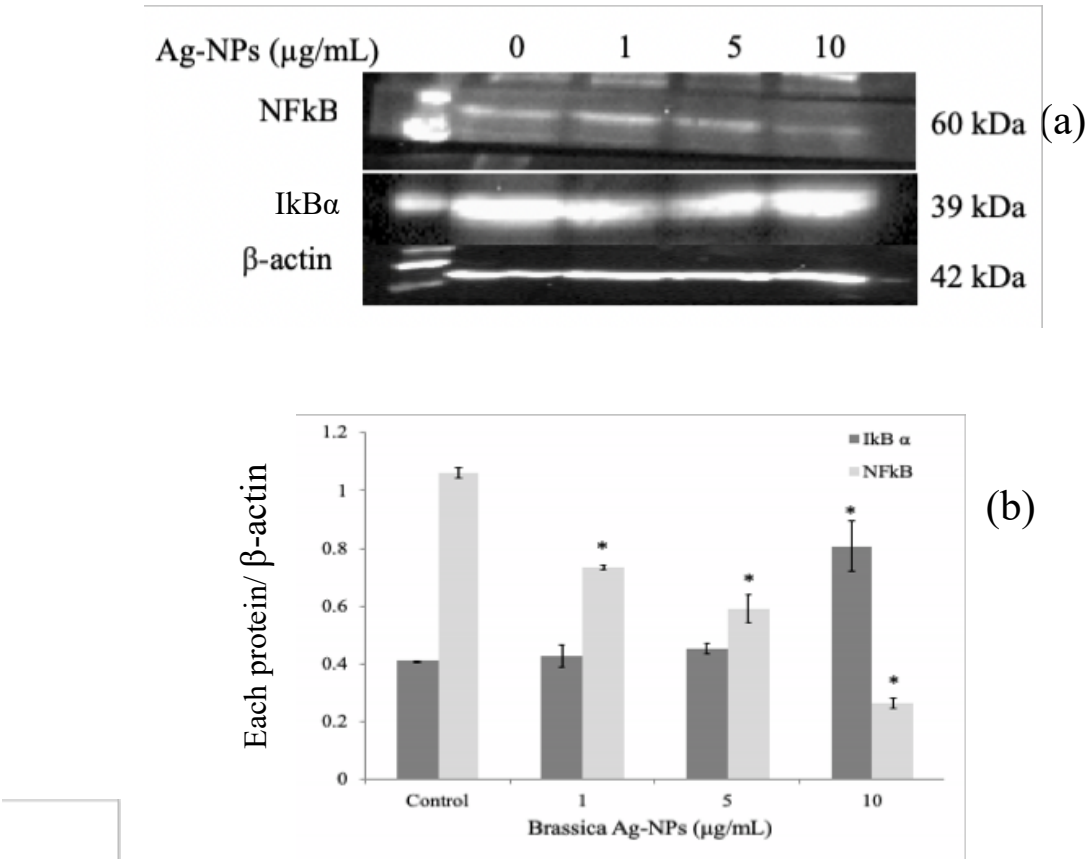

Fig. 4.9 Western blot analysis for protein expression after being exposed to Brassica Ag-NPs for 1 h. (a) Immunoblotting for without and with treatment. Relative density of (b) NFkB and IkB α to β- actin. Error bar indicate mean ± SEM (n-3). Asterisk indicate significant at $p<0.05$ compared to control

4.3.6 Flow cytometry assay

Flow cytometry was carried out after 12 incubation of Caco-2 cells with and without Brassica Ag-NPs. Results of flow cytometry was measured counting the abundance of cells in the provided quadrate. Four quadrates are responsible for four phenomena. Upper left and lower left represent necrosis and viable whereas, upper right and lower right represent late apoptosis and early apoptosis. But in our study with 12 h incubation of Brassica Ag-NPs in different doses no apoptotic or necrotic cells was detected significantly.

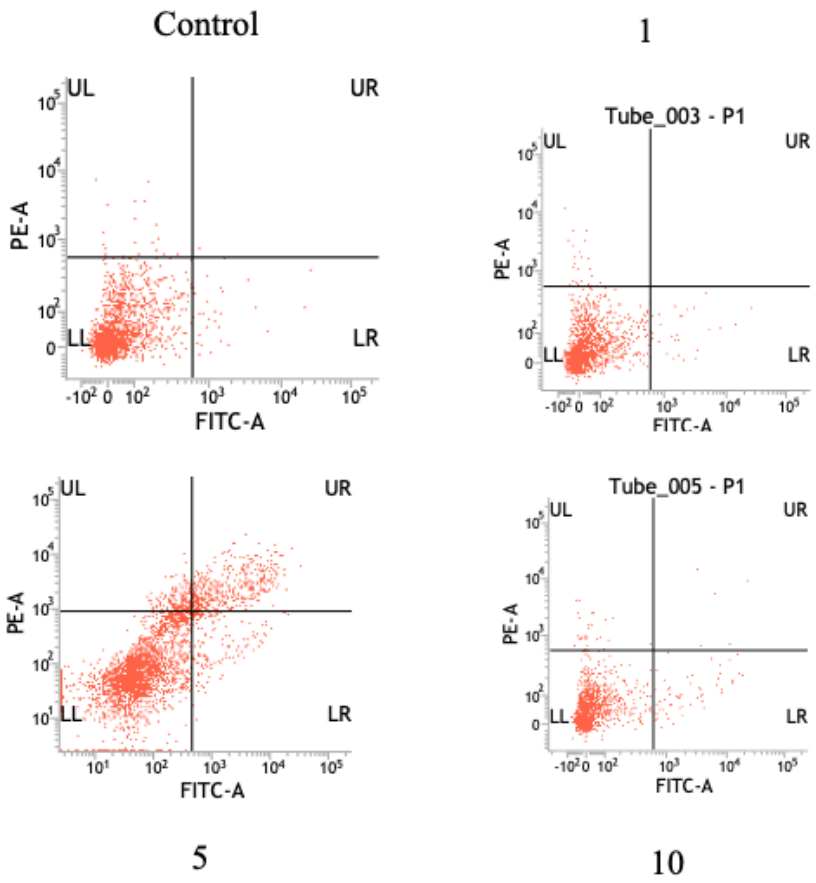

Fig. 4.9 Flow cytometry of Caco-2 cells after 12 h exposure of Brassica Ag-NPs. Four quadrate refers different types of cell death. LL- Live cell, LR- early apoptosis, UL- necrosis, UR- late apoptosis

5. Discussion

In our present study we showed that *Brassica rapa* var. *nipposinica/japonica* leaf extract mediated Ag-NPs (Brassica Ag-NPs) induced autophagy in colorectal cancer cells which is the cell death promoting activity of our synthesized NPs. At first Ag-NPs was

synthesized using *Brassica rapa* var. *nipposinica/ japonica* leaf extract where $AgNO_3$ act as a precursor and leaf extract as a reducing and capping agent.

After successful synthesis, particles were characterized following well-known techniques; UV-Vis. Spectroscopy, EDX, FESEM, XRD, TEM and FT-IR. Results showed that particles are nano sized spherical shaped face centered cubic structured. Synthesis and characterization of Brassica Ag-NPs was elaborately described in Chapter-2. Therefore, to assess the effect of Brassica Ag-NPs on colorectal cancer cells, Brassica Ag-NPs was expoused to Caco-2 cells using 3 different concentration (1, 5 and 10 µg/mL) for 12 h and 48 h.

Autophagy progression consists of four different stages: initiation, autophagosome formation (nucleation, elongation and completion), maturation, and degradation, which ultimately consequences breakdown of cytoplasmic material; lysosome. (kang et al., 2011). Hence, theoretically an excessive level of autophagy can promote cell death, due to the overconsumption of critical cellular organelles/ components. This phenomenon is established as ATG-dependent or type II- programmed cell death (Zou et al., 2012). Results of current study could be concluded as 'Brassica Ag-NPs induced autophagic or type II cell death in Caco-2 cells'.

Firstly, effect of Brassica Ag-NPs on the expression of Beclin 1 and LC3-II in Caco-2 cells supports the formation of autophagy. Beclin 1 is a selective central role-playing autophagy protein and light chain 3 (LC3 is the mammalian ortholog of yeast Atg8) act sequentially during the nucleation and expansion of the autophagosomal membrane. The upregulation of Beclin 1 converts soluble form of LC3-I into lipidated and autophagosome associated form LC3-II. This event is strongly supported by the results from our current study. Brassica Ag-NPs showed an upregulation expression of Beclin 1 which converts soluble LC3-I in to lipidated and autophagosome associated form LC3-II. Therefore, expression of LC3-II is also upregulated. This conversion supports the formation of autophagosome and subsequently autophagy. Hence, Brassica Ag-NPs activated the process of autophagy through Beclin 1 in Caco-2 cells.

Secondly expression of p53, Akt and mTOR confirmed excessive formation of autophagy. p53 is generally recognized as a pro-autophagic factor in a transcription-dependent manner (Maiuri et al., 2010). Autophagic flux is stimulate by multiple p53 target genes, which often results in the downregulation of the central mammalian target of rapamycin (mTOR); mTOR function as a negative regulator of autophagy (Feng et al., 2005). In our study we also found an expression of upregulation of p53 and downregulation of mTOR with the exposure of Brassica Ag-NPs in Caco-2 cells; indicating p53 activates the

AMP responsive protein kinase (AMPK), a positive regulator of autophagy through transcriptional regulation of Sestrins 1 and 2 (Tang et al., 2015). Therefore, activation of AMPK shut down the activity of mTOR. On the other hand, the activity of mTOR can be positively regulated by the protein kinase Akt by the phosphorylation and inhibition of TSC2 and PRAS40 (A well- established Akt substrate within the mTOR complex). Thus, inhibition of Akt decreases the expression of mTOR and ultimately promote autophagy (Guertin et al., 2007). Consistence with this hypothesis, treatment with Brassica Ag-NPs decreased the expression of Akt in Caco-2 cells. Finally, upregulation of p53 and downregulation of Akt and mTOR is indicated that Brassica Ag-NPs induced autophagy is indeed via inhibition of mTOR through p53-Akt-mTOR pathway.

Thirdly, inhibition of NFkB signaling pathway can negatively regulate autophagy in some specific cells *in vitro* (Criollo et al., 2012). The nuclear factor κB (NF-κB) family is a transcription factors, existing in almost all cells which is widely involved in several functions such as immunity, inflammation, and stress response. In normal condition once cellular function activate then the protein IkB degrade, subsequently NFkB translocate to the neucleus and binds with DNA in its specific binding sites, that stimulate transcriptional activity of the respective genes in controlling different cellular responses (Schlottmann et al., 2008). Therefore, upregulation of the protein IkB and downregulation of the protein NFkB results inhibition of cellular transcriptional activity, consequences disruption of genomic DNA in Caco-2 cells; suggesting the promotion of autophagy in Caco-2 cells.

However, the role of autophagy is controversial in the consideration of cell survival and cell death. Still very little is known about the interaction between these two cellular processes in respect of tumor growth in response to anticancer agents (Eisenberg-Lerner et al., 2009).In autophagic cell death, apoptosis can also be induced; where ROS inhibits the autophagy related pro survival factors such as mTOR and Akt in the downstream of the pI3k/mTOR, Akt signaling pathway (Roy et al., 2014). Therefore, unfortunately in flowcytometry involvement of apoptosis or necrosis was not detected in Caco-2 cells for the exposure of Brassica Ag-NPs. This result further confirmed by the expression of Bax and cleaved caspase 3. Where no change for the expression of Bax and cleaved caspase 3 in the treated and untreated group; indicate less possibility of the involvement of apoptosis in this study.

In addition, in order to maintain the cellular homeostasis, intracellular free radicals and ROS is produced consistently which is subsequently neutralized by antioxidant defense systems such as GSH, GPX, superoxide dismutase, vitamins and flavonoids (Urso and Clarson, 2003). Therefore, disruption of the intracellular oxidative homeostasis leads to the

increase level of stress marker such LDH and even cell death indicating; the involvement of apoptosis or sometimes necrosis. Therefore, significant decrease of cell viability along with severe dose dependent increase of LDH activity in the culture medium is an indication of disruption of cell membrane integrity; suggested that Brassica Ag-NPs can promote cell death in Caco-2 cells in a dose dependent manner. Furthermore, we examined possible oxidative stress in Caco-2 cells by determining the GSH. Our results demonstrate significant decrease of GSH level in Caco-2 cells with the exposure of Brassica Ag-NPs for both of the 12 h and 48 h treatment (fig); suggested Brassica Ag-NPs accelerate ROS or intracellular free radicals in Caco-2 cells leads to impede antioxidant defense system.

In summery Brassica Ag-NPs can induce autophagy in Caco-2 cells via Beclin 1 mediated pathway which could be accelerate through p53/Akt/mTOR and NFkB. For establishment of cell death mechanism involvement of apoptosis and necrosis is recognized specifically. Therefore, the cell death occur in Caco-2 cells for the exposure of Brassica Ag-NPs could be explained as type-II or autophagic cell death. But further study could be held to find out the mechanism that is also involved in the regulation of autophagic cell death.

Conclusion

In conclusion, we have presented the evidence that Brassica Ag-NPs induces autophagy in colorectal cancer cell. Autophagy process initiated by Beclin-1, which further trigger following p53/Akt/ mTOR signaling pathway. Finally, NFkB also accelerate autophagy resulting disruption of genomic DNA. Therefore, *Brassica rapa* var. *nipposinica/japonica* leaf extract mediated Ag-NPs induced autophagy regulated type II cell death in colorectal cancer cell where involvement of apoptosis or necrosis is not recognised. This finding might be a new insight for the therapeutic agent of colorectal cancer.

Reference

Akter, M., Rahman, M.M., Ullah, A.K.M.A., Sikder, M.T., Hosokawa, T., Takeshi, S., Masaaki, K., 2018. Brassica rapa var. japonica leaf extract mediated green synthesis of silver nanoparticles and evaluation of their stability, cytotoxicity and antibacterial activity. J. Inorganic Organometallic Polymers Mater. 28, 1483-1493

Axe, E.L., Walker, S.A., Manifava, M., Chandra, P., Roderick, H.L, Habermann, A., Griffiths, G., Ktistakis, N.T., 2008. Autophagosome formation from membrane compartments enriched in phosphatidylinositol 3-phosphate and dynamically connected to the endoplasmic reticulum. J. Cell Biol. 182, 685–701

Buttacavoli, M., Albanese, N.N., Cara, G.D., Alduina, R., Faleri, C., Gallo, M., 2018. Anticancer activity of biogenerated silver nanoparticles: an integrated proteomic investigation. Oncotarget. 9, 9685-9705

Conde, J., Doria, G., Baptista, P., 2012. Noble metal nanoparticles applications in cancer. J Drug Deliv. 2012,751075. https://doi.org/10.1155/2012/751075.

Corcelle, E.A., Puustinen, P., Jaattela, M., 2009. Apoptosis and autophagy: Targeting autophagy signaling in cancer cells – 'trick or treats'? FEBS Journal. 276, 6084-6094

Criollo, A., Chereau, F., Malik, S.A., Niso-Santano, M., Marino, G., Galluzzi, L., 2012. Autophagy is required for the activation of NFkappaB. Cell Cycle. 11,194–9

Feng, Z., Zhang, H., Levine, A.J., Jin, S., The coordinate regulation of the p53 and mTOR pathways in cells. 2005, Proc. Natl. Acad. Sci. U.S.A. 102, 8204- 8209.

Herrero, P.E., Medarde, F.A., 2015. Advanced targeted therapies in cancer: Drug nanocarriers, the future of chemotherapy. Eur J Pharm Biopharm. 93, 52–79

Hulkoti, N.I., Taranath, T.C., 2014. Biosynthesis of nanoparticles using microbes- a review. Colloids Surf B Biointerfaces. 121, 474–83

Hu, Z., Zhong, Z., Huang, S., Wen, H., Chen, X., Chu, H., Li, Q., Sun, C.H., 2016. Decreased expression of Beclin-1 is significantly associated with a poor prognosis in oral tongue squamous cell carcinoma. Molecular medicine reports. 14, 1567-1573

Eisenberg-Lerner, A., Bialik, S., Simon, H.U., Kimchi, A., 2009. Life and death partners: apoptosis, autophagy and the cross-talk between them. Cell Death and Differentiation 16, 966–975

Ishida, A.E., Ohmichi, M., Mabuchi, S., 2004. Inhibition of Phosphorylation of a Forkhead Transcription Factor Sensitizes Human Ovarial Cancer Cells to Cisplatin. Endocrinology. 145: 2014-2022

Kabeya, Y., Kamada, Y., Baba, M., Takikawa, H., Sasaki, M., Ohsumi, Y., 2005. Atg17 functions in cooperation with Atg1 and Atg13 in yeast autophagy. Mol. Biol. Cell. 16, 2544–2553

Kanmani, P., Lim, S.T., 2013. Synthesis and characterization of pullulan- mediated silver nanoparticles and its antimicrobial activities. Carbohydr Polym. 97, 421–8

Kang, R., Zeh, H.J., Lotze, M.T., Tang, D, 2011. The Beclin 1 network regulates autophagy and apoptosis. Cell Death Differ. 18, 571–580

Liang, X.H., Jackson, S., Seaman, M., Brown, K., Kempkes, B., Hibshoosh, H., 1999. Levine B. Induction of autophagy and inhibition of tumorigenesis by beclin 1. Nature 402, 672-6

Liu, W., Mu, R., Nie, F.F., Yang, Y. Wang, J., Dai, Q.S., Lu, N., Qi, Q., Rong, J.J., Hu, R., Wang, X.T.,You, Q.D., Guo, Q.L.,2009. MAC related mitochondrial pathway in oroxylin A induces apoptosis in human hepatocellular carcinoma HepG2 cells**.** Cancer Letters. 284, 198–207

Mattos, S.F., Villalonga, P., Clardy, J., Lam, E.W.F., 2008. Foxo 3a mediates the cytotoxic effects of Cisplatin in colon cancer cells. Mol Cancer Ther. 7, 3237-3246

Maiuri, M.C., Galluzzi, L., Morselli, E., Kepp, O., Malik, S.A., Kroemer, G., 2010. Autophagy regulation by p53, Curr. Opin. Cell Biol. 22, 181–185.

Mizushima, N., Yoshimori, T., Ohsumi, Y., 2011. The role of Atg proteins in autophagosome formation. Annu. Rev. Cell Dev. Biol. 27, 107–132

Poulose, S., Panda, T., Nair, P.P., Théodore, T., 2014. Biosynthesis of silver nanoparticles. J Nanosci Nanotechnol. 14, 2038–49

Rahman, M.M., Uson-Lopez, R., Sikder, M.T., Tan, G., Hosokawa, T., Saito, T., 2018. Kurasaki M. Ameliorative effects of selenium on arenic-induced cytotoxicity in PC12 cells via modulating autophagy/apoptosis. Chemosphere. 196, 453-466

Rajawat, Y.S., Bossis, I., 2008. Autophagy in aging and in neurodegenerative disorders. Neurobiol Aging. 7, 46-61

Rohatgi, R.A., ShawLeslie, M., 2016. An autophagy-independent function of Beclin 1 in cancer. Molecular& Cellular Oncology. 3, https://doi.org/10.1080/23723556.2015.1030539

Roy, R., Singh, S.K., Chauhand, L.K.S., Das, M., Tripathi, A., Dwivedi, P.D., 2014. Zinc oxide nanoparticles induce apoptosis by enhancement of autophagy via PI3K/ Akt/mTOR inhibition. Toxicol. Lett. 227, 29e40.

Russo, M., Meli, A., Sutera, A., Gallo, G., Chillura, Martino., Lo, Meo. P., Noto, R., 2016. Photosynthesized silver– polyaminocyclodextrin nanocomposites as promising antibacterial agents with improved activity. RSC Adv. 6,40090-40096

Schlottmann, S., Buback, F., Stahl, B., Meierhenrich, R., Walter, P., Georgieff, M., 2008. Prolonged classical NF-kappaB activation prevents autophagy upon E. coli stimulation in vitro: a potential resolving mechanism of inflammation. Mediators Inflamm. 2008, 725854, doi: 10.1155/2008/725854

Tang, J., Jiehui Di, J., Cao, H., Bai, J., Zheng, J., 2015. p53-mediated autophagic regulation: A prospective strategy for cancer therapy. Cancer letters. 363, 101-107

Guertin, D.A., Sabatini, D.M., 2007. Defining the role of mTOR in cancer. Cancer Cell. 12, 9–22

Urso, M.L., Clarkson, P.M., 2003. Oxidative stress, exercise, and antioxidant supplementation. Toxicology. 189, 41-54.

Wirawan, E., Lippens, S., Vanden, Berghe. T., Romagnoli, A., Fimia, G.M., Piacentini, M., Vandenabeele, P., 2012. Beclin1: a role in membrane dynamics and beyond. Autophagy. 8,6-17

Zou, M., Lu, N., Hu, C., LW, Sun, Y., Wang, X., You, Q., Gu, C., Xi, Tao., Guo, Q., 2012. Beclin 1- mediated autophagy in hepatocellular carcinoma cells: implication in anticancer efficiency of oroxylin A via inhibition of mTor signaling. cell signal. 24, 1722-1724

Inhibition of mTor suppress cell growth and induces catabolic process including autophagy Ravikumar, B., S Sarkar, S., Davies, J.E.,M. Futter, M Garcia,-A Arenciba et al., physiolpgical reviews 90 (4) 2010, 1383-1435

Chapter 5 General conclusion

5.1 General conclusion

This research has been carried out with some specific objectives majorly green synthesis of Ag-NPs and exploration of their biomedical applications and the underlying mechanism. Recently, NPs are widely used in several sectors such as in human health appliances, industrial fields, medical applications, biomedical fields, engineering, electronics, and environmental studies. Among all of the nanoparticles, Ag-NPs is being one of the most demandable material due to its enormous applications in versatile sectors. Now-a-days it has become a lucrative material in consumer products. At the same time conventional method of Ag-NPs synthesis is a concern of increasing environmental pollution. Already enormous study on the cytotoxic effect of Ag-NPs has been carried out *in vitro* and *in vivo*. Thus, green synthesis of Ag-NPs could be an alternative to overcome the emerging situation and researchers are now concern to have alternative synthesis processes such as biosynthesis, phyto-synthesis, and so on. Therefore, in Chapter-1 we briefly explained applications, some physiochemical parameters responsible for the induction of toxicity and related toxicological aspects with mechanistic insights in different cell lines and also in animal model. We also discussed how green synthesis of NPs is being an important issue. Hence, in Chapter-2, we discussed briefly about our synthesized green Ag-NPs using *Brassica rapa* var. *nipposiinica* / *japonica* leaf extract. In this process, leaf extract act as a reducing and capping agent and $AgNO_3$ act as a precursor. This method is highly cost effective, easy, and most importantly environmental friendly. After successful synthesis of the green Ag-NPs, characterization of the particle was carried out following sophisticated techniques such as UV- Vis. spectroscopy, EDX, XRD, FESEM, TEM, FT-IR and atomic absorption spectrophotometry (AAS) analyses. Characterizations confirmed the Brassica Ag-NPs are face centered cubic structured along with nanosized spherical in shape. On the basis of the EDX analysis we assumed the particle might be coated with biomolecules which was subsequently ensured by FT-IR analysis. FT-IR confirmed the presence of some functional groups which matched with the Brassica leaf biomass and functional groups might represent amino acid, alkaloid and flavonoids in the Brassica Ag-NPs. Amino acid might be responsible to be acted as a reducing agent and capping agent. After synthesis and characterization of newly synthesized Brassica ag-NPs, cytotoxicity and antibacterial activity was evaluated. To assess the cytotoxicity of Brassica Ag-NPs, PC-12 cells were used as a model cell line and result showed that with the comparison of commercial Ag-NPs, Brassica Ag-NPs is less toxic at a concentration of 1 µg/mL and 3 µg/mL. In addition, we assessed antibacterial activity of Brassica Ag-NPs using *E. coli* and *Enterobacter* sp. and

result showed high antibacterial activity of Brassica Ag-NPs compared with other green synthesized Ag-NPs. Thus, *Brassica rapa* var. *nipposinica* leaf extract mediated green synthesized Ag-NPs showed less cytotoxicity compared with commercially available Ag-NPs and higher antibacterial activity compared with other green synthesized Ag-NPs.

Synthesis process might have some influence on the property of the synthesized NPs. Therefore, in Chapter 3, we discussed the effect of temperature on encapsulation of Ag-NPs using green synthesis method. In this study, we synthesized Ag-NPs using *Brassica rapa* var. *nipposinica* leaf extract following the method discussed in chapter-2 but in different synthesis temperature conditions. During synthesis we controlled four different temperatures such as room temperature (25°C), 60°C, 80°C, and 100°C. After synthesis we characterized the particles with UV- vis. sprectroscopy, XRD, TEM and DLS analyses. The aggregation and encapsulation of the synthesized Ag-NPs were visualized from the TEM images. The particles synthesized at room temperature (25 °C) showed a value of about 10-20 nm. However, at 60 °C temperature synthesized Ag-NPs showed a higher value than the 25 °C synthesized Ag-NPs. An intense look on the figure indicates that an aggregation of Ag-NPs was found in this case. When the temperature was increased to 80 °C, particles were found to be formed with a lower size than 60°C. An intense look again demonstrates that particles were starting to be encapsulated and at 100 °C almost all of the particles were encapsulated which hampered the aggregation and ultimately reduced the size of the particles. Therefore, the adopted techniques clearly demonstrate that synthesis temperature affects the size and encapsulation of Ag-NPs. Thus, it can be concluded that *Brassica rapa* var. *nipposinica* leaf extract mediated green synthesis of Ag-NPs might be a potential alternative approach which is cost effective, environmentally friendly, and less toxic with highly antibacterial activity where *Brassica rapa* var. *nipposinica* leaf extract plays the crucial role for the promising properties of presently synthesized Ag-NPs. Finally, in Chapter 3, we assessed the anticancer effect of Brassica Ag-NPs on human colorectal cancer cells (Caco-2). To find out whether Brassica Ag-NPs can induce autophagic cell death in Caco-2 cells, Brassica Ag-NPs was exposed to Caco- cells in three different concentrations (1, 5 and 10 μg/mL) for 12 h. After 12 h exposure of Brassica Ag-NPs, cell viability of Caco-2 cells was decreased in a concentration dependent manner. Then LDH activity in the culture medium confirmed disruption of membrane integrity of Caco-2 cells. Subsequent degradation of GSH and DNA damage indicated the generation of intracellular ROS. Hence, upregulation of Beclin 1 and LC3 -II is an indication of autophagy in Caco-2 cells. This process further stimulates via p53 mediated pathway. In addition, downregulation of Akt inhibit the activation of mTOR; resulted promotion of autophagy in

Caco-2 cells. Finally, upregulation of IkB suppress the expression of NFkB which lead to blockage the transcription process of DNA. Thus, downregulation of NFkB also keep vital role in autophagy promotion. Therefore, massive autophagy turned cells in to the autophagic or type-II cell death. Involvement of apoptosis in this study was not found. Therefore, our finding suggests Beclin 1 mediated type II cell death in Colorectal cells where involvement of apoptosis or necrosis is was not detected. Finally, this finding might be a new insight for the therapeutic agent of colorectal cancer.

In conclusion, in this research Ag-NPs was synthesized using *Brassica rapa* var. *nipposinica/ japonica* leaf extract where leaf extract act as reducing and capping agent. Various well stablished characterization techniques confirmed that synthesized particles are phase centered cubic structured crystalline phase. Further study revealed less cytotoxic effect of Brassica Ag-NPs on PC12 cells with potential antibacterial activity against *E. coli* and *Enterobacter* sp. Finally, Brassica Ag-NPs induced autophagic cell death in Caco-2 cells which might be a novel insight for the therapeutic agent of colorectal cancer.